

A STOCHASTIC LIVE LOAD MODEL FOR BUILDINGS

by

Jong-Cherng Peir

B.S., National Taiwan University
(1963)

M.S., The Ohio State University
(1967)

SUBMITTED IN PARTIAL FULFILLMENT
OF THE REQUIREMENTS FOR THE DEGREE OF
DOCTOR OF PHILOSOPHY

AT THE
MASSACHUSETTS INSTITUTE OF TECHNOLOGY

(FEBRUARY, 1972)

Signature of Author

Signature Redacted

Department of Civil Engineering
September 30, 1971

Signature Redacted

Certified by

Thesis Supervisor

Signature Redacted

Accepted by

Chairman, Departmental Committee on Graduate
Students of the Department of Civil Engineering

Archives



A STOCHASTIC LIVE LOAD MODEL FOR BUILDINGS

by

Jong-Cherng Peir

Submitted to the Department of Civil Engineering on September 30, 1971, in partial requirements for the degree of Doctor of Philosophy.

ABSTRACT

The stochastic modeling of live loads on buildings is presented in this work. It contains two parts; the modeling of the sustained load and the modeling of transient live loads. The model of the sustained load treats the load intensity as a random function varying continuously in space and varying in time at discrete, random points associated with changes in occupancy. The spatial treatment includes continuously decaying correlation and the influence of floor-to-floor and building-to-building effects. Inclusion of influence surfaces permits treatment of a variety of structural load effects (column or footing load, moment, shear etc.). Analysis of the model produces, first, the approximate distributions, means and variances and covariance of the load effects at arbitrary points in time. Second, the approximate distributions of lifetime maximum sustained load effects are provided. These models are fit to office load survey data provided by G.R. Mitchell of BRS, Garston, England, and relatively dependable results are therefore obtained.

The second part deals with the modeling of the load effect caused by the occurrence in time and in space of transient live loads. The distribution of the maximum "extraordinary" load in time interval t is obtained. Reasonable numerical estimates of parameters are substituted to yield specific results, but data on this kind of load is virtually nonexistent. It is anticipated that the analytical models will stimulate collection of appropriate data in future surveys.

Analysis is presented of the design load effects when the sustained load acts simultaneously with the randomly arriving transient load.

Thesis Supervisor: C. Allin Cornell
Title: Associate Professor of
Civil Engineering

ACKNOWLEDGEMENTS

The author wishes to express his sincere gratitude to Prof. C. Allin Cornell for his inspiration of the author's interest in this area and for his suggestion about the general approach used in this work.

Also, the author wishes to thank Prof. Erik H. Vanmarcke for his constant criticisms and suggestions and Prof. Mike B. Godfrey for his help in estimating the parameters.

The data kindly furnished by Mr. G.R. Mitchell, BRS, Garston, England is particularly appreciated. Reliable parameter estimates would have been impossible without the results of this thorough load survey.

The financial aid from the Department of Civil Engineering, the Ford Foundation and the National Science Foundation (Grant No. K-25510) is acknowledged.

The excellent typing by Miss Ann Preston is appreciated.

Finally the author wishes to thank his wife Mei Li for her patience and her constant encouragement.

TABLE OF CONTENTS

| | |
|---|----|
| Title Page | 1 |
| Abstract | 2 |
| Acknowledgement | 3 |
| Table of Contents | 4 |
| CHAPTER I: INTRODUCTION | 7 |
| I-0. Introduction | 7 |
| I-1 Literature Review | 8 |
| I-2 General Behavior of the Live Load | 11 |
| I-3 Stationary Process | 14 |
| I-4 Arbitrary-point-in-time Load Versus Maximum Lifetime Sustained Load | 16 |
| I-5 Design Load Versus Performance Load | 17 |
| I-6 Load Intensity, Total Load, Unit Load, Load Effect, EUDL | 18 |
| CHAPTER II: ORDINARY (SUSTAINED) LOAD | 20 |
| II-0 Introduction | 20 |
| II-1 Load Model | 21 |
| II-1a Model Description | 21 |
| II-1b Moments of Total and Unit Load | 25 |
| II-2 Comparison of Different Load Models with Existing Data | 39 |
| II-3 Influence Surface | 45 |
| II-4 Arbitrary-point-in-time Load | 49 |

| | | |
|--|---|-----|
| II-5 | Maximum Lifetime Sustained Load | 53 |
| II-5a | Introduction | 53 |
| II-5b | Probability Distribution of the Maximum Lifetime Sustained Load for a Single Area | 54 |
| II-5c | Probability Distribution of the Maximum Lifetime Sustained Load for Multiple Loadings | 60 |
| II-5d | Probability Distribution of the Maximum Lifetime Sustained Load Effect | 74 |
| CHAPTER III: EXTRAORDINARY (TRANSIENT) LOAD MODEL | | 78 |
| III-0 | Introduction | 78 |
| III-1 | Load Model for a Particular Event | 80 |
| III-2 | Maximum Extraordinary Load | 85 |
| III-3 | Example: The Extraordinary Load for a Column | 90 |
| III-3a | Exact Solution | 90 |
| III-3b | Approximate Solution | 92 |
| CHAPTER IV: LOAD COMBINATION, DESIGN LOAD AND PERFORMANCE LOAD | | 95 |
| IV-0 | Introduction | 95 |
| IV-1 | Load Combination for the Design Load | 96 |
| IV-1a | Combination 1 | 98 |
| IV-1b | Combination 2 | 100 |
| IV-2 | Load Combination for Performance Load | 102 |

| | | |
|-------------|--|-----|
| IV-3 | Load Pattern | 103 |
| IV-4 | Design Load and Performance Load | 106 |
| IV-4a | EUDL for Axial Load | 107 |
| IV-4b | EUDL for Beam Moment | 108 |
| IV-4c | EUDL for Shear in Beams | 116 |
| CHAPTER V: | DISCUSSION AND SUGGESTIONS | 119 |
| V-0 | Introduction | 119 |
| V-1 | Sensitivity Analysis | 120 |
| V-2 | Live Load Reduction Factor | 129 |
| V-3 | Means, Variances of Design Load | 130 |
| V-4 | Load Concentration Factor | 131 |
| V-5 | Coefficient of Variation of the Sustained Load Versus EUDL | 134 |
| CHAPTER VI: | CONCLUSIONS AND SUGGESTIONS | 135 |
| VI-1 | Conclusions | 135 |
| VI-2 | Suggestions | 138 |
| Figures | | 139 |
| References | | 181 |
| Biography | | 184 |
| Appendices | | 185 |

CHAPTER I

Introduction

I-0: Introduction

With the development of probability codes^{(1),(2)} it becomes more and more urgent that a better knowledge about the live load should be developed in order to achieve a safe and economic design. We are looking not only for the value of the design load but also for probabilistic descriptions of the time-dependent characteristics of live loads. A number of studies have been made of live loads. It is the purpose of this work to summarize the previous results, and develop a new theory to predict the design live load for different probability levels. A set of the most recent field data⁽³⁾ will be used to verify the assumptions and to estimate the parameters.

Some general points are discussed in Chapter I. A brief introduction about the past studies is presented in Section I-1. The nature of the live load is discussed in Section I-2 with the definition of the different kind of loads. The remaining sections include different assumptions and definitions which are important to the following chapters.

I-1: Literature Review

The study of live loads includes two different parts; data collection and theoretical modeling. The first part can be dated back to the 19th century when Stoney⁽⁴⁾ studied packed crowd loads in 1869. Through the past hundred years numerous works have been done in this area. Researchers measured the live load in the buildings and analyzed the data to come up with suggestions for design live loads and their reduction factors. The second part, analytical modeling, has, on the other hand, been studied by comparatively few. Not until recent years have people started building statistical and probabilistic load models. With the accumulation of knowledge the model becomes closer and closer to the real phenomenon of the live load. As a result a few building codes have already adopted their work as the basis for certain aspects of the design live load. It is believed that in the near future more and more building codes will follow this trend and adopt design live loads on a more rational basis.

Several important works will be mentioned below. Dunham⁽⁵⁾ studied the survey data from two federal buildings in Washington, D.C. and derived the live load reduction factor which is still used in this country after more than twenty years. Horne⁽⁶⁾ presented a theoretical model by

assuming independence of the load on different areas. The standard deviation he got is inversely proportional to the square root of the area. This conclusion led to the form of the live load reduction factor adopted in the Mexican and the new Canadian building code. Rosenblueth⁽⁷⁾ introduced influence surface into his model. Jauffred⁽⁸⁾ collected data from Mexican apartments and offices and related them to Horne's model. Fader⁽⁹⁾ considered spatial correlation among live loads. Karman⁽¹⁰⁾ studied the load data from 183 apartments and introduced the idea of the random changes of occupancies. Bryson and Gross⁽¹¹⁾ of National Bureau of Standard surveyed two federal buildings and used statistical methods to analyze the data. Their work will be continued and more data will be collected in the near future. Corotis⁽¹²⁾ and Hasofer⁽¹³⁾ were extending sustained live load modeling capabilities. Mitchell and Woodgate⁽³⁾ have conducted the most extensive field survey to date. For office use it covered $1\frac{3}{4}$ million square feet with 32 buildings and over 100 occupying organizations. They also presented their data in such a way that it can be relatively easily used for statistical analysis.

A more complete review of the literature is not necessary here owing to the very thorough survey in Heaney's recent thesis⁽¹⁴⁾. He has tabulated and summarized virtually

all the work related to live load study. In addition to the references in his list, there are also the recent reference by Borges⁽¹⁵⁾ who provides an excellent review, and compares Mitchell's and Karman's work, plotting their data on extreme value probability papers.

Even though it is conceptually a simple operation to measure the live load content in a building, many researchers nevertheless have encountered the difficulties of how to present the data and how to include the transient, extraordinary loads that might occur during the lifetime of the building. Therefore there are many weaknesses in the above mentioned work. For example there are relatively arbitrarily applied load to reflect the concentration of people (Mitchell and Woodgate), mixed room sizes (Karman, and Bryson and Gross), etc. Heaney made a detailed discussion about this problem which should be considered for any new load survey work.

I-2: General Behavior of the Live Load

As shown in Fig. I-1a the average load (or the total load) on any area (or room) can be plotted along time axis. The load can be decomposed into two parts. One is the ordinary load (Fig. I-1b) which exists on the floor for a fairly long time until a change occurs. The ordinary load itself consists of furniture, safes, file cabinets, printing machines etc. as well as the normal working personnel. The other is the extraordinary load (Fig. I-1c). This kind of load occurs relatively rarely but with a relatively high intensity. It typically has the characteristics of localized concentration in space and short temporal duration. It may be caused, for example, by people coming into the building during a special occasion such as an "open house". The people will concentrate in those organizations that have the "open house" or in those areas that are open to the public. This event in general will last only a few hours. Another occasion that will cause the extraordinary load is the remodelling of rooms. It may happen that furniture from different rooms will be moved to one particular room and cause a heavy load concentration.

Let us examine the ordinary load more closely. The load keeps fairly constant until an abrupt change occurs, e.g., at point A and B (Fig. I-1b). The reason may be

due to the change of the occupancy. The new tenant may have a higher (or lower) average load. It may also be caused by the rearrangement of the floor space. An office room may be converted to a storage room or vice versa and the average load may change drastically.

Even though the average load in any room under the same occupant probably has only a small fluctuation in time, there may be a definite trend. The load can be expected to increase with time due to the addition of new furniture or the accumulation of files etc. However the magnitude of the increase is probably small as compared to the variation from occupant to occupant of the basic load itself.

The ordinary load can be further divided into two groups: the load due to normal working personnel (plus some expected number of visitors) and the rest of the load. The latter group is defined as long-term sustained load as opposed to the normal personnel load. The sustained load is shown in Fig. I-1d and the personnel load is shown in Fig. I-1e on a finer scale. The total length of time that the personnel load presents is much shorter than that of the sustained load. Hence the question arises whether the personnel load should be treated the same as the sustained load in considering the long-term effect. Karman⁽¹⁰⁾ discussed this problem and concluded that the load, acting at least 5% of the

operational time of the building may be considered permanent.
This is to justify that the combination of the above two
loads will be used to produce the long-term effect.

I-3: Stationary Process

The basic information we are seeking is a description of the probabilistic behavior of the load* through the lifetime of the building on any area (Fig. I-1d,e). Direct empirical observation would require the continuous monitoring of the loads on many rooms throughout this whole period. This procedure is both expensive and impractical. Another way to derive the information makes use of the assumption that the process is stationary both in time and in space. This implies: (i) that for any area the probability distributions of the loads at two points on the time axis are identical, (ii) that for any time point the loads on any two areas (of common characteristics) have identical probability distributions, and (iii) that these two distributions (one with respect to time, the other with respect to space) are identical.

As shown in Fig. I-2 the figure represents three different bays (or rooms) with the same area but different load history. The load survey conducted at a particular time t_0 is the measurement of the average load on the

* Either the total load or, equivalent, the load per unit area (i.e., the spatial average load)

different bays. It results in reporting the frequency distribution of the average load along the cross-section t_0 and not the frequency distribution along the time axis. The two distributions may not be the same for an arbitrary process. But, once we make the assumption that the process is stationary, the above two distributions will be the same. This stationary assumption (due originally apparently to Karman but adopted independently by Mitchell⁽¹⁶⁾) permits customary multi-room load survey data to be used to infer behavior-in-time of an individual room.

I-4: Arbitrary-point-in-time Load versus Maximum Lifetime Sustained Load

The arbitrary-point-in-time load is the load which exists at any particular time, t_0 . Its probability distribution (called the marginal or the one-dimensional distribution of the process) is the same as the result from any load survey. By the assumption of the stationary process this probability distribution is identical at any time. The maximum lifetime sustained load is the maximum (sustained) load that should be expected, under a certain probability level, during the lifetime of the structure. Its probability distribution can be visualized by assuming that we have the load histories of n areas and that we pick the peak sustained load from each history. The frequency distribution of those n loads is the frequency distribution of the maximum lifetime sustained load.

I-5: Design Load versus Performance Load

In the practice of the structural design the engineer has to consider not only safety but also serviceability. He has to design the structure to be safe enough to withstand without failure the anticipated maximum load applied during the lifetime of the building. He has also to design the structure strong and rigid enough to maintain the normal service of the building. There should be few sustained cracks or excessive deflections that mar the appearance or function. Therefore two different load criteria have to be chosen. The load used for the purpose of safety is defined as the design load. The other load to be used for serviceability purposes is defined as the performance load. The former will be associated generally with maximum-in-time loads that have very small probability of being exceeded; the latter will usually be sustained loads with relatively less conservative probability levels.

I-6: Load Intensity, Total Load, Unit Load, Load Effect,
EUDL

Several terms will be used quite frequently in the following chapters. They will be defined here:

Load Intensity: The value of the load per unit area on a differential area, in pounds per square foot.

Total Load: The sum or the integration of the load intensity over any finite area, in pounds.

Unit Load (average load): Total load on an area divided by its contributing area, a spatial average load, in pounds per square foot.

Load Effect: The structural effect produced by the load, such as moment, shear, deflection etc. For linear behavior this is an integration of the product of the load intensity and an influence surface.

EUDL (Equivalent Uniformly Distributed Load): This is the value of the uniformly distributed load (in pounds per square foot) that will produce the same specific load effect as that produced by the actual

load intensity on the floor. For the same floor area, the EUDL will have a different value for different load effects.

CHAPTER II

Ordinary (Sustained) Load Model

II-0: Introduction

The ordinary load which was defined in Chapter I will be studied in this chapter. A load model will be proposed in Section II-1 and compared with data in Section II-2. The influence surface will be discussed in Section II-3 because it will be used throughout this work for both the design load and the performance load. The arbitrary-point-in-time load will be discussed in Section II-4. This load forms part of the performance load. In the last section a method to derive the probability distribution of the maximum lifetime sustained load will be introduced. This load will form a part of the design load.

II-1: Load Model

II-1a: Model Description:

The load intensity at any location follows a stochastic process. This process will be modeled in this section. The model proposed below can be considered as an extension of the work done by others. Horne⁽⁶⁾ apparently was the first to start the theoretical modeling of random floor loads. He assumed spatial independence, but ignored time influence. Hasofer⁽¹³⁾ constructed a more refined, but similar model. Rosenblueth⁽⁷⁾ used the influence surface in his work. Fader⁽¹⁹⁾ and Corotis⁽¹²⁾ introduced various correlation factors.

A correlative load model is proposed here to represent the load in the building at an arbitrary point in time.

$$w(x,y) = m + \gamma_{bld} + \gamma_{flr} + \epsilon(x,y) \quad (II-1-1)$$

where $w(x,y)$ is the load intensity at any particular horizontal location (x,y) of a particular building and floor. m is the "grand mean" of the live loads for the case under investigation, i.e., office occupancy. γ_{bld} , γ_{flr} and $\epsilon(x,y)$ are zero mean independent random variables. γ_{bld} represents building effects, γ_{flr} represents floor effects

and $\epsilon(x,y)$ represents load intensity variation spatially on a given floor of a given building. This last term is a random spatial function with non-zero spatial correlation.

$$\text{cov}[\epsilon(x_0,y_0), \epsilon(x_1,y_1)] \neq 0$$

Then

$$E[w(x,y)] = m \quad (\text{II-1-2})$$

$$\text{Var}[w(x,y)] = \sigma_{\text{bld}}^2 + \sigma_{\text{flr}}^2 + \sigma_{\epsilon}^2 \quad (\text{II-1-3})$$

and for two loads on the same floor at locations (x_0,y_0) and (x_1,y_1) (Fig. II-1)

$$\begin{aligned} \text{cov}[w(x_0,y_0), w(x_1,y_1)] &= E[w(x_0,y_0) w(x_1,y_1)] \\ &\quad - E[w(x_0,y_0)]E[w(x_1,y_1)] \\ &= \sigma_{\text{bld}}^2 + \sigma_{\text{flr}}^2 + \text{cov}[\epsilon(x_0,y_0), \epsilon(x_1,y_1)] \end{aligned}$$

(II-1-4)

(Load on different floors will be discussed in Section II-1b)

m is the "grand mean" of the live load which should be the (ensemble) mean of the (spatial) average loads of all buildings. As discussed below there is a systematic difference in the average load for different types of buildings;

therefore proper sampling techniques must be used to avoid a biased estimation of m .

The random building effect, γ_{bld} , represents the variation from office building to office building of the average (over the total buildings) load. This variation could in principle be in part systematic. The data from Mitchell and Woodgate⁽³⁾, for example, show that the mean loads are 14.6 psf and 10.42 psf respectively for the "trade union" group and "the trading A" group. The same explanation holds for the floor effect, γ_{flr} . It represents the variation from floor to floor within a given building of the average (over the total floor) load. Bryson and Gross⁽¹¹⁾ found that within the NBS Administration Building the average loads on the floor 1, 5 and 9 were 5.9 psf, 10.2 psf and 12.7 psf respectively. The cause is apparently that organizations arrange their floor spaces in such a way that different functions and types of users occupy different floors, e.g., an executive floor, a storage floor, a typist and clerical floor etc. Even if it is an office space, the ground floor is typically used differently from upper floors⁽³⁾.

If enough information were available, the means and the variances of γ_{bld} and γ_{flr} could be estimated as functions of the type of building or floor occupancy, floor number, etc. However at the design stage the engineer usually does not know who is going to occupy the floor of a

building or how it will be used, nor does he want to restrict their future use by designing for other than a very general office occupancy. If the model is to be used to determine code specified loadings, then it is describing loads over the population of future buildings and floors to which the code will be applied. Under all such circumstances it is appropriate to treat γ_{bld} and γ_{flr} as zero mean random terms. That these variables are modeled in a simple, independent additive way implies that no complex interactions are hypothesized between floor and building effects, e.g., within-building, floor-to-floor variability is the same for "light" as for "heavy" buildings, and the average load on one total floor is not influenced by its being adjacent to another floor which is heavier (or lighter) than a typical floor in the building. These simplifying assumptions can be dropped if future data prove it necessary. Assigning γ_{bld} and γ_{flr} each a zero mean implies that it is assumed that proper sampling and averaging has been done. (e.g., if the model and subsequent code is to be applied to offices on all floor levels, the sample should contain a proper mix of floor levels, and should not be dominated by, say, ground floors.) For these reasons in this work only single global variances for those two zero mean random terms need be used, and treatment of systematic distinctions between building types, floor numbers etc. will not be discussed further.

The randomness of the stochastic process $\epsilon(x,y)$ represents the uncertainty involved in predicting the floor loading over a particular floor. $\epsilon(x_0,y_0)$ and $\epsilon(x_1,y_1)$ corresponding to two different locations are in general correlated. If the load intensity is higher than average at a particular location then it is likely that the load at a nearby point is high also, i.e., there exists a positive correlation. It is anticipated that the correlation will decrease with the distance between the locations considered. This will be verified later.

II-1b: Moments of Total and Unit Loads

The model of the load intensity $w(x,y)$ above is needed in order to be able to deduce the characteristics of total loads (or unit loads) and of various load effects. Most data are available in terms of unit loads. Therefore these data will be used to deduce estimates of the parameters of the load intensity process. It is necessary therefore to establish the relationships between the moments and parameters of unit loads and those of the load intensity process.

Let $L(A)$ be the total load over a rectangular area A (equal to $a \times b$) on the same floor, then

$$L(A) = \int_0^a \int_0^b w(x,y) dx dy = A\gamma_{b1d} + A\gamma_{f1r} + \int_0^a \int_0^b \varepsilon(x,y) dx dy$$

the mean and the variance of $L(A)$ are given by (see Appendix A):

$$E[L(A)] = \int_0^a \int_0^b E[w(x,y)] dx dy = \int_0^a \int_0^b m dx dy = mA \quad (\text{II-1-5})$$

$$\text{Var}[L(A)] = \int_0^a \int_0^a \int_0^b \int_0^b \text{cov}[w(x_0, y_0), w(x_1, y_1)] dx_0 dx_1 dy_0 dy_1 \quad (\text{II-1-6})$$

Substitute Eq. (II-1-4) into the equation above

$$\text{Var}[L(A)] = \int_0^a \int_0^a \int_0^b \int_0^b \{ \sigma_{b1d}^2 + \sigma_{f1r}^2 + \text{cov}[\varepsilon(x_0, y_0), \varepsilon(x_1, y_1)] \} dx_0 dx_1 dy_0 dy_1 \quad (\text{II-1-7})$$

Three different functional forms of covariance functions were examined by Hauser⁽¹⁷⁾. One is a discrete parameter model

and the other two are continuous. The first one is not preferred because the areas that can be considered are limited to certain discrete values. One continuous model was derived from a first-order autoregressive process⁽¹⁸⁾ where the parameter was spatial distance. The covariance function for such processes will be:

$$\begin{aligned} \text{cov}[\varepsilon(x_0, y_0), \varepsilon(x_1, y_1)] &= \sigma_{\text{sp}}^2 \rho(r) \\ &= \sigma_{\text{sp}}^2 e^{-r/d'} \end{aligned}$$

where d' is a constant and r is the horizontal distance between two points (x_0, y_0) and (x_1, y_1)

$$r = \sqrt{(x_0 - x_1)^2 + (y_0 - y_1)^2}$$

The other form, which will be used here, is a slight modification of the above formula. It uses r^2 to replace r , i.e.,

$$\text{cov}[\varepsilon(x_0, y_0), \varepsilon(x_1, y_1)] = \sigma_{\text{sp}}^2 e^{-r^2/d} \quad (\text{II-1-8})$$

When fit to the same data, both formulae lead to approximately the same results⁽¹⁷⁾. However the second is more convenient because the spatial variables on two perpendicular directions, X and Y, can be uncoupled.

$$\begin{aligned} \text{cov}[\varepsilon(x_0, y_0), \varepsilon(x_1, y_1)] &= \sigma_{sp}^2 e^{-[(x_0-x_1)^2 + (y_0-y_1)^2]/d} \\ &= \sigma_{sp}^2 e^{-(x_0-x_1)^2/d} e^{-(y_0-y_1)^2/d} \end{aligned}$$

and the subsequent integration (e.g., Eq. (II-1-7)) will be greatly simplified. Substitute Eq. (II-1-8) into Eq. (II-1-4) and Eq. (II-1-7).

$$\text{cov}[w(x_0, y_0), w(x_1, y_1)] = \sigma_{bld}^2 + \sigma_{flr}^2 + \sigma_{sp}^2 e^{-r^2/d} \quad (\text{II-1-9})$$

for two points (x_0, y_0) and (x_1, y_1) on the same floor.

$$\begin{aligned} \text{Var}[L(A)] &= \int_0^a \int_0^a \int_0^b \int_0^b (\sigma_{bld}^2 + \sigma_{flr}^2 + \sigma_{sp}^2 e^{-r^2/d}) \\ &\quad dx_0 dx_1 dy_0 dy_1 \quad (\text{II-1-10}) \end{aligned}$$

When two points (x_0, y_0) and (x_2, y_2) are located on different floors (Fig. II-1) we shall introduce a new factor ρ_m which represents the correlation coefficient between the load intensities on two different floors, i.e.

$$\text{cov}[\varepsilon(x_0, y_0), \varepsilon(x_2, y_2)] = \rho_m \sigma_{sp}^2 e^{-r^2/d} \quad (\text{II-1-11})$$

This correlation represents what Mitchell⁽¹⁶⁾ has referred to as the "stacking effect". Areas immediately above or below one another apparently have some tendency to be used in a similar manner (e.g., cabinets may be next to interior rather than exterior walls.) The value of the decay parameters d in Eq. (II-1-11) is taken equal to that in the same-floor case for simplicity only. (Note that there is some potential inconsistency in saying that the γ_{flr} terms represent floor average loads when they are assumed independent and when at the same time $\epsilon(x_0, y_0)$ and $\epsilon(x_2, y_2)$ are assumed correlated. The last assumption in fact implies some correlation between floor averages. Hence the γ_{flr} terms do not strictly represent floor average deviations. The decay in correlation, as controlled by parameters d and ρ_m , is, however, estimated from data to be so rapid that the correlation between the $\epsilon(x, y)$ processes on two different floors does not cause substantial correlation among total or unit loads on areas as large as typical total floor areas. It is therefore justified practically speaking to think of the γ_{flr} terms as representing the deviations in floor averages. In fact, should future data analysis show substantially more correlation in these floor averages, it can be included by relaxing the independence assumption on the γ_{flr} terms.)

Following the same derivation as Eq. (II-1-4), we have

$$\text{cov}[w(x_0, y_0), w(x_2, y_2)] = \sigma_{b1d}^2 + \rho_m \sigma_{sp}^2 e^{-r^2/d} \quad (\text{II-1-12})$$

A priori, it is anticipated this "stacking correlation" will decay with m , the number of floors separating the two locations. Three different forms of ρ_m will be examined later in order to fit the available data.

$$(i) \quad \rho_m = h^m \quad (h < 1)$$

This is the formula derived directly from the simplest, first-order autoregressive process with a discrete parameter, namely story number.

$$(ii) \quad \rho_m = \text{constant, independent of } m.$$

$$(iii) \quad \rho_m = f(m), \text{ a general function of } m.$$

To gain insight into the proposed model and to fit its parameters to commonly available data, let us now determine the dependence of the mean and variance of the total load and unit load as functions of the floor area and of the number of floors involved. First, consider a square area $A(a=b=\sqrt{A})$ on a single floor (Eq. (II-1-5) and Eq. (II-1-10)).

$$E[L(A)] = \int_0^{\sqrt{A}} \int_0^{\sqrt{A}} m dx dy = mA$$

$$\text{Var}[L(A)] = \int_0^{\sqrt{A}} \int_0^{\sqrt{A}} \int_0^{\sqrt{A}} \int_0^{\sqrt{A}} (\sigma_{bld}^2 + \sigma_{flr}^2 + \sigma_{sp}^2 e^{-r^2/d})$$

$$dx_0 dx_1 dy_0 dy_1$$

$$= \iiint_0^{\sqrt{A}} (\sigma_{bld}^2 + \sigma_{flr}^2) dx_0 dx_1 dy_0 dy_1$$

$$+ \iiint_0^{\sqrt{A}} \sigma_{sp}^2 e^{-[(x_0-x_1)^2 + (y_0-y_1)^2]/d} dx_0 dx_1 dy_0 dy_1$$

$$= (\sigma_{bld}^2 + \sigma_{flr}^2) A^2 + \sigma_{sp}^2 \iint_0^{\sqrt{A}} e^{-(x_0-x_1)^2/d} dx_0 dx_1^*$$

$$\iint_0^{\sqrt{A}} e^{-(y_0-y_1)^2/d} dy_0 dy_1$$

$$= (\sigma_{bld}^2 + \sigma_{flr}^2) A^2 + \sigma_{sp}^2 \left[\iint_0^{\sqrt{A}} e^{-(x_0-x_1)^2/d} dx_0 dx_1 \right]^2$$

$$= (\sigma_{bld}^2 + \sigma_{flr}^2) A^2 + \sigma_{sp}^2 \pi d A [\operatorname{erf}(\sqrt{\frac{A}{d}}) - \sqrt{\frac{d}{A\pi}} (1 - e^{-A/d})]^2$$

where $\operatorname{erf}(\)$ is the error function⁽¹⁹⁾,⁽¹⁷⁾

$$\operatorname{erf}\left(\frac{u}{\sqrt{2}}\right) = 2 \int_0^u \frac{1}{\sqrt{2\pi}} e^{-t^2/2} dt$$

Let us define the unit load or the spatial average of the load intensity as:

$$U(A) = L(A)/A = \gamma_{bld} + \gamma_{flr} + \frac{1}{A} \iint_0^{\sqrt{A}} \varepsilon(x,y) dx dy$$

Its mean and variance will be

$$E[U(A)] = E\left[\frac{L(A)}{A}\right] = \frac{mA}{A} = m \quad (\text{II-1-13})$$

$$\begin{aligned} \operatorname{Var}[U(A)] &= \operatorname{Var}\left[\frac{U(A)}{A}\right] = \frac{\operatorname{Var}[L(A)]}{A^2} \\ &= \sigma_{bld}^2 + \sigma_{flr}^2 + \sigma_{sp}^2 \left(\frac{\pi d}{A}\right) [\operatorname{erf}\left(\sqrt{\frac{A}{d}}\right) \\ &\quad - \sqrt{\frac{d}{\pi A}} (1 - e^{-A/d})]^2 \end{aligned} \quad (\text{II-1-14})$$

Let

$$K(A) = \sigma_{sp}^2 \pi d [\operatorname{erf} \sqrt{\frac{A}{d}} - \sqrt{\frac{d}{\pi A}} (1 - e^{-A/d})]^2 \quad (\text{II-1-15})$$

Then

$$\operatorname{Var}[U(A)] = \sigma_{bld}^2 + \sigma_{flr}^2 + \frac{K(A)}{A} \quad (\text{II-1-16})$$

It is apparent that when the area A is sufficiently large compared to d, $\frac{K(A)}{A}$ approaches zero and $\operatorname{Var}[U(A)]$ approaches a constant value, $\sigma_{bld}^2 + \sigma_{flr}^2$. Therefore if $A/d \geq \sim 30$ * $[\sigma_{sp}^2 / (\sigma_{bld}^2 + \sigma_{flr}^2)]$,

$$\operatorname{Var}[U(A)] \cong \sigma_{bld}^2 + \sigma_{flr}^2 \quad (\text{II-1-17})$$

As discussed above this is apparently the case for A = total floor area, when U(A) is simply the average floor load. For intermediate-sized areas the last two terms in the parenthesis of Eq. (II-1-15) are small compared to the first term and therefore can be neglected. The first term can be further simplified since

$$\operatorname{erf}(\sqrt{\frac{A}{d}}) \cong 1$$

for intermediate area, say $\sqrt{\frac{A}{d}} \geq 4$. Hence

$$\operatorname{Var}[U(A)] = \sigma_{bld}^2 + \sigma_{flr}^2 + \sigma_{sp}^2 \frac{K(A)}{A} \cong \sigma_{bld}^2 + \sigma_{flr}^2 + \sigma_{sp}^2 \frac{\pi d}{A} \quad (\text{II-1-18})$$

Note that the dependence of the last term on A is the same as that found for the total variance versus A when one adopts the "independence model" used by Horne⁽⁶⁾ and Rosenblueth⁽⁷⁾.

For small areas ($A \leq \sim 10d$) all terms are important.

The "nominal column load" will be considered next. This load is defined as the sum of all loads on the conventionally considered tributary area of the column. This is not the real column axial force because owing to the static indeterminacy of a typical structure on the conventional tributary area only part of the load on the conventional tributary area will transfer to the column and the rest will transfer to other surrounding columns. Similarly a portion of the loads on the tributary areas of these columns will be transferred to the column in question. Let $L(A_n)$ be the total nominal column load from n floors. Each floor has equal area A. Consider the two floor case first (Fig. II-2):

$$L(A_2) = \int_0^a \int_0^b w(x,y) dx dy + \int_0^c \int_0^d w(u,v) du dv$$

where $w(x,y)$ and $w(u,v)$ are load intensities on the different coordinate axis (x,y) and (u,v) shown in Fig. II-2.

Then (see Appendix A)

$$E[L(A_2)] = \int_0^a \int_0^b m dx dy + \int_0^c \int_0^d m du dv$$

$$\begin{aligned} \text{Var}[L(A_2)] &= \int_0^a \int_0^b \int_0^a \int_0^b \text{cov}[w(x_0, y_0), w(x_1, y_1)] dx_0 dx_1 dy_0 dy_1 \\ &+ 2 \int_0^a \int_0^b \int_0^c \int_0^d \text{cov}[w(x, y), w(u, v)] dx dy du dv \\ &+ \int_0^c \int_0^c \int_0^d \int_0^d \text{cov}[w(u_0, v_0), w(u_1, v_1)] du_0 du_1 dv_0 dv_1 \end{aligned}$$

Assume that two floor plans are identical, i.e. $a = c$ and $b = d$, and substitute Eq. (II-1-9) and Eq. (II-1-12) into the above equations:

$$E[L(A_2)] = 2Am$$

$$\begin{aligned} \text{Var}[L(A_2)] &= 2[(\sigma_{b1d}^2 + \sigma_{f1r}^2)A^2 + \int_0^a \int_0^a \int_0^b \int_0^b \sigma_{sp}^2 e^{-r^2/d} \\ &dx_0 dx_1 dy_0 dy_1] + 2[\sigma_{b1d}^2 A^2 + \rho_1 \int_0^a \int_0^a \int_0^b \int_0^b \sigma_{sp}^2 e^{-r^2/d} \\ &dx du dy dv] \\ &= 2(\sigma_{b1d}^2 + \sigma_{f1r}^2)A^2 + 2AK(A) + 2\sigma_{b1d}^2 A^2 + 2\rho_1 AK(A) \end{aligned}$$

These formulas are very easy to extend to n floors.

$$E[L(A_n)] = nAm$$

$$\begin{aligned} \text{Var}[L(A_n)] = & n(\sigma_{\text{bld}}^2 + \sigma_{\text{flr}}^2)A^2 + nAK(A) + n(n-1)\sigma_{\text{bld}}^2A^2 \\ & + \sum_{m=1}^{n-1} 2(n-m)\rho_m AK(A) \end{aligned} \quad (\text{II-1-19})$$

In terms of unit load:

$$U(A_n) = \frac{L(A_n)}{nA}$$

$$E[U(A_n)] = E\left[\frac{L(A_n)}{nA}\right] = \frac{nAm}{nA} = m$$

$$\begin{aligned} \text{Var}[U(A_n)] = & \text{Var}\left[\frac{L(A_n)}{nA}\right] = \frac{\text{Var}[L(A_n)]}{n^2A^2} \\ = & \sigma_{\text{bld}}^2 + \frac{\sigma_{\text{flr}}^2}{n} + \frac{K(A)}{nA} + \frac{1}{n^2} \sum_{m=1}^{n-1} 2(n-m)\rho_m \frac{K(A)}{A} \end{aligned} \quad (\text{II-1-20})$$

In order to determine their characteristics and to facilitate parameter estimation, we next examine different forms of ρ_m :

$$(i) \quad \rho_m = h^m \quad h < 1$$

then

$$\lim_{n \rightarrow \infty} \text{Var}[U(A_n)] \cong \sigma_{bld}^2 \quad (II-1-21)$$

In this case all the column variances will converge to the same limit independent of the area A on each floor.

$$(ii) \quad \rho_m = \text{constant} = \rho_c$$

then

$$\lim_{n \rightarrow \infty} \text{Var}[U(A_n)] \cong \sigma_{bld}^2 + \rho_c \frac{K(A)}{A}$$

Since $\frac{K(A)}{A}$ is different for different areas, the column load in this case will approach different limits for different areas (unless $\rho_c = 0$).

$$(iii) \quad \rho_m = f(m), \text{ a general function of } m$$

The values of ρ_m can be estimated individually, sequentially, i.e., use the available data for $\text{Var}[U(A_n)]$ versus A and n to estimate ρ_1 first and then ρ_2 etc. Inspection of Eq. (II-1-20) reveals that for fixed A the variance of $U(A_n)$

will have one term independent of ρ_m that will decay like $1/n$, and a second term which will depend on the form of ρ_m . Assuming, following a priori judgement, that ρ_m is a positive, decaying function of m , the forms of decay of $\text{Var}[U(A_n)]$ versus n possible are restricted to those between $1/n$ and those independent of n . If another form is observed in the data, it implies that ρ_m does not conform to this a priori assumption. This phenomenon was in fact observed in the data to be considered.

II-2: Comparison of different load models with existing data

There are some load survey data sets available but only Mitchell and Woodgate⁽³⁾ present the data in such a way that it can be readily adopted for this study. (A brief description of their work is presented in Appendix B). Therefore their results will be used to estimate all the parameters introduced in the previous section. When new data becomes available it can be used in the manner to be demonstrated to re-estimate the parameters and to check further whether the model assumptions are appropriate.

Two sets of the reduced data from the report of Mitchell and Woodgate⁽³⁾,⁽²⁰⁾ are particularly useful in estimating the value of second-moment parameters*:

(i) The coefficient of variation, $\frac{\sqrt{\text{Var}[U(A)]}}{m}$, versus the area (Fig. II-3) which can be used to estimate three parameters; $\sigma_{bld}^2 + \sigma_{flr}^2$; σ_{sp}^2 and d . (Fig. (II-3) is a slight modification of the original data. See Appendix C).

(ii) The column load data (Fig. II-4) which can be used to estimate the remaining two parameters; ρ_m and σ_{bld}^2 .

The detailed estimation will be demonstrated step

* Other, more direct schemes of parameter estimation are possible if one has access to the raw data

by step below.

(i) From Eq. (II-1-17) the variance of the unit load on an area on a single floor will approach $(\sigma_{bld}^2 + \sigma_{flr}^2)$ as the area becomes large. Therefore estimate the value of $(\sigma_{bld}^2 + \sigma_{flr}^2)$ by the variance of the largest area reported (see Table B in Appendix C).

$$\sigma_{bld}^2 + \sigma_{flr}^2 = 20.25* (lb/ft^2)^2 \quad (II-2-1)$$

(ii) Eq. (II-1-18) could be used to get an estimate of the value of the product of σ_{sp}^2 and d in the range of the intermediate area; then Eq. (II-1-14) and a small area could be used to solve for the individual values of σ_{sp}^2 and d. In short the data is fit at two points. Unfortunately no pairs of values can fit the data from Mitchell and Woodgate⁽³⁾ consistently at all points. An alternative is to find the value of σ_{sp}^2 and d which will produce a minimum sum† of the squared error (SSE) of the standard

*The units will be in feet and pounds throughout this work.

†The sum is taken here over the nine data points (A value) shown in Fig. II-3. This choice may put undue emphasis on the smaller areas owing to the particular choices of A adopted by Mitchell and Woodgate. Weighted least squares could also be used.

deviation. The results are plotted in Fig. II-5, where the integer d value giving the minimum SSE for each of a set of σ_{sp}^2 values is shown. Also shown are several d values for $\sigma_{sp}^2 = 260$. The minimum square error is at

$$\sigma_{sp}^2 = 260 \text{ (lb/ft}^2\text{)}^2$$

$$d = 9 \text{ ft}^2 \quad (\text{II-2-2})$$

Notice that we use the minimum SSE of the standard deviation and not that of the variance because the latter will place too much emphasis on the small areas where the variance is high. With above parameters the results are plotted in Fig. II-3. The fits obtained by two other sets of parameters are shown by dotted lines.

(iii) Use the column load data to find the form of ρ_m and the values of parameters.

The column data show a rather unusual trend. The variance drops from 1 story to 2 stories by about 48% then stays constant up to 7 to 9 stories. Beyond that the variance increases again. It is not clear why the tail went upward. One possible explanation is that the sample of taller buildings was too small for the statistics to be meaningful. This part (more than 8 stories, except A = 624

where $n = 8$ is not considered) will be neglected from subsequent consideration.

From the figure of the column load data where each curve approaches a different limit it is clear that $\rho_m = h^m$ can not fit the data (see eq. (II-1-21)). The second form $\rho_m = \rho_c$ will be examined first. Again, there is no feasible way to estimate the parameter separately. Least square fitting was used again. The following values given the best fit (Fig. II-6).

$$\sigma_{bld}^2 = 3$$

$$\rho_c = 0.7 \quad (II-2-3)$$

Next consider that ρ_m is an arbitrary function of m so that the model will fit the data completely. As discussed before the data shows the following trend;

$$\text{Var}[U(A_n)] \approx 0.52 \text{Var}[U(A_1)] \text{ for } n \geq 2 \quad (II-2-4)$$

Substituting Eq. (II-1-16) and Eq. (II-1-20) into the above equation

$$\sigma_{bld}^2 + \frac{\sigma_{flr}^2}{n} + \frac{K(A)}{nA} + \frac{1}{n^2} \sum_{m=1}^{n-1} 2(n-m)\rho_m \frac{K(A)}{A} = 0.52 \left(\sigma_{bld}^2 + \sigma_{flr}^2 + \frac{K(A)}{A} \right) \quad (II-2-5)$$

Use the values of the parameters found from previous fitting, i.e.

$$\sigma_{sp}^2 = 260$$

$$d = 9$$

$$\sigma_{bld}^2 + \sigma_{flr}^2 = 20.25$$

$$\sigma_{bld}^2 = 3$$

then solve the value of ρ_m sequentially from Eq. (II-2-5).

Consider $A = 336$ first. The results are shown in Table (II-1)

Table II-1

| | | | | | |
|----------|-------|------|-------|-------|-------|
| n | 2 | 3 | 4 | 5 | 6 |
| m | 1 | 2 | 3 | 4 | 5 |
| ρ_m | -0.08 | 1.44 | 0.942 | 0.931 | 0.932 |

The results show that any floor is practically uncorrelated with its adjacent floor but highly correlated with the rest of the building. (Note that $\rho_m > 1$ is, of course, impossible. The value $\rho_2 = 1.44$ is merely the solution from Eq. (II-2-5).) There is, as yet, no reasonable explanation for this conclusion. Similar results were found for

A = 151 and 624 also. (A similar pattern with respect to ρ_1 and ρ_2 will also emerge if σ_{b1d}^2 is changed from the value found in the previous fitting.)

Another way to investigate the model is to assume ρ_m equals a constant, ρ_c , and then choose ρ_c so that the model fits the data for a chosen value of n. This implies finding for some n the value of ρ_c that will satisfy Eq. (II-2-5). The results are shown in Table II-2 for several values of n with A = 336. The value of ρ_c (=0.7) obtained above

Table II-2

| n | 2 | 3 | 4 | 5 | 6 | 7 |
|----------|-------|-------|-------|-------|-------|-------|
| ρ_c | -0.08 | 0.427 | 0.597 | 0.682 | 0.732 | 0.769 |

fits the results in Table II-2 except when n = 2. Therefore the values in Eq. (II-2-3) will be used in the remainder of this work.

One way to improve the fit to the column load is to include the correlation between two σ_{flr} 's. This may in fact exist. However, at the present stage we would like to keep the model as simple as possible. Any improvement can be introduced when new data becomes available. Estimating correlation among the σ_{flr} variables could best be done by looking directly at the correlation within a building of pairs of average floor loads spaced m floors apart.

II-3: Influence Surface

In structural design it is not the load itself but different load effects, such as axial load, shear, moment etc., which are the factors used for the design of an individual member. It is therefore necessary to transform the load into the load effect in the process of the design. The first step will transform the load from the floor to the surrounding frame. Assuming linear behavior of the structural system, there are several methods available (such as Navier or Levy type solutions⁽²¹⁾) to represent the behavior of the floor slab. For most purposes, however, it is believed that a simplified influence surface^{(22),(23),(12)} is the most suitable procedure. Even though this method is approximate it has the advantage of simplicity. All the related equations will be greatly simplified, e.g., the use of a three-degree polynomial to replace an infinite series. This method will be explained below.

An influence surface is the two-dimension extension of the principle of influence lines. The ordinate $I(x,y)$ of the influence surface at any point (x,y) is the influence on some desired load effect due to a unit load at (x,y) . The Muller-Breslau principle states that an influence line (or surface) for a given load effect may be constructed by removing the constraint associated with that load effect and introducing a corresponding unit displacement. The deflected

shape of a beam without distributed load is governed by:

$$y^{iv} = 0$$

a fourth order differential equation. Its general solution is a three-degree polynomial. There are four degrees of freedom involved which can be solved by introducing four boundary conditions. Following Ayer and Cornell's⁽²³⁾ assumption simplified influence surface may be obtained by multiplying appropriate influence lines. This is not an exact solution for a flat plate but is probably as accurate as is the representation of the real structure by a flat plate.

As an example consider the axial load on a typical interior column (Fig. II-7). The influence line along the X-X axis approximately equals the influence line for a two span fix end beam (Fig. II-8) which can be constructed by assuming a unit vertical displacement at the middle support. The deflected shape of the beam is the influence line. Due to the assumed symmetry only one span will be considered. Four boundary conditions must be satisfied, i.e. zero slope at both ends, zero displacement at one end and unit displacement at the other. The above constraints lead to the following equation (Fig. II-9):

$$z = 3x^2 - 2x^3 \quad 0 \leq x \leq 1$$

where

z = deflection of the beam

x = relative location of the beam ($0 \leq x \leq 1$)

The influence line along Y-Y direction is the same. The influence surface for a bay is approximately the product of the two influence lines^{(23), (12)}, i.e. (Fig. II-10)

$$I(x,y) = (3x^2 - 2x^3)(3y^2 - 2y^3) \quad 0 \leq x \leq 1, \quad 0 \leq y \leq 1$$

A five bay six story frame is selected for the illustration purpose in this work (Fig. II-11). For any particular force resultant of interest the influence line along the frame was constructed by a readily available program called "STRUDL II"⁽²⁴⁾. A unit deformation corresponding to the force resultant of interest was the input and the displacements and rotations for all joints were the output. The influence line can be constructed accordingly. Along the direction perpendicular to the frame it is assumed that only two adjacent spans contribute. Consistent with the assumption of behavior approximately like continuous one-way slabs, the influence line perpendicular to the frame will be assumed the same as that of the axial load (Fig. II-9). This implies that the loads on the slab are transformed to the frame first like a column load and then produce the

influence to the load effect interested as if they were concentrated loads on the frame. Part of the influence surface for the moment at mid-span of beam A-B is shown in Fig. II-12.

The influence surface will be used throughout this work. It will not be mentioned explicitly but whenever we encounter load effect it should be understood that the influence surface as described above has been used.

II-4: Arbitrary-Point-in-Time Load:

The previous two sections dealt with the first and second-order moments of the unit load, $U(t)$. Next we consider the shape of the (marginal) probability distribution of $U(t)$, that is the PDF of the unit load that exists at a point t along the time axis (Fig. II-13). The load comes from two different sources: in part from the personnel in the office and in part from the sustained load (See chapter I). Due to the different characteristics of these loads they will be treated separately. The sustained load in a particular office will change from time to time, i.e., it is a stochastic process, but under the assumption that the process is stationary in time, the marginal or one-dimensional probability distribution will be the same along time axis, i.e.

$$f_{U(t)}(u) = f_U(u) \quad \text{for all } t$$

where $f_{U(t)}(u)$ is the PDF of the unit load $U(t)$ as discussed above. Assuming stationarity in space and time, most histogram results of the load survey conducted by many researchers (3), (8), (11) can be interpreted as belonging to this category.

The probability distribution of the unit load for different areas can be obtained directly from load surveys

(under the stationary assumption described in Chapter I). The report of Mitchell and Woodgate⁽³⁾ is most useful in this regard because they presented the data in such a way that it can be adopted for such statistical analysis directly. As discussed in Appendix B the only discrepancy is that their report includes both normal working people load and allowances for loads attributed to transient concentration of people, in addition to the directly observed or sustained load results. Owing to the data recording technique, there is no economical way to separate the latter loads from the total load reported. Therefore the data will be used as it is with the understanding that there are some additional non-observed "loads" contained in it. The subsequent analysis will at a minimum demonstrate how the model and such data can be analyzed. At best, the additional loads may have had little influence on means, variances and histograms. This is a stronger possibility for the smaller areas (see Mitchell and Woodgate⁽³⁾, Table 8).

The sample frequency distributions for different areas are plotted in Fig. II-14. The distributions are highly skewed to right when the area is small. The skewness gradually diminishes as the area becomes large. All the distributions can be approximately fitted by different gamma distributions (Appendix D). It is anticipated that this conclusion will remain true for other sources of data as

well. It is therefore assumed in this work that the (marginal or one-dimensional) probability distribution for the unit load $U(t)$ from any area is gamma. The mean and the variance are given by Eq. (II-1-13) and Eq. (II-1-14). k and λ of the gamma distribution can be derived as:

$$k = \frac{m^2}{\sigma^2} \quad (\text{II-4-1})$$

$$\lambda = \frac{m}{\sigma^2}$$

where

m = mean of the unit load = $E[U(t)]$

σ^2 = variance of the unit load = $\text{Var}[U(t)]$

with the value of k and λ known the gamma distribution is completely defined. The load associated with any desired probability level can be derived easily⁽²⁵⁾.

The load at any arbitrary-point-in-time contributed by the normal occupants varies widely but its intensity, with high probability, is very small as compared to those from stationary load⁽¹⁴⁾. Some researchers^{(3), (11)} included the personnel load in their survey but they did not treat it exactly as an arbitrary-point-in-time load. They asked about the normal working people in the room, which is sort of an average people load, instead of recording the number of people

they saw at the time of survey. Besides they did not report the people load separately and there is no information about its probability distribution. For this reason the personnel load will be treated deterministically. Its assumed value is set equal to the expected (average) value, which is estimated to be about 1.5 psf (2 persons/200 ft²).

Alternatively the above two loads, stationary and personnel load, can be lumped together as Mitchell and Karman did. However, due to their different stochastic properties, we think it is more appropriate to separate them. We also suggest that any new load survey should think about this problem and collect more pertinent data.

II-5: Maximum Lifetime Sustained Load

II-5a: Introduction

The maximum lifetime sustained load is the maximum sustained load during the lifetime of the building. The purpose of this section is to derive its probability distribution. Karman⁽¹⁰⁾ Mitchell⁽¹⁶⁾ and Meaney⁽¹⁴⁾ used a fixed number of changes of occupants to find the distribution of the maximum load, but considered only simple unit loads on areas in conjunction with these time changes. The logical extension, which will be discussed in the following sections, is the combination of the above idea with the more complete sustained load model from Section II-1a.

The general behavior of live loads was discussed in Chapter I. Certain simplifications must be made for rigorous theoretical consideration to be tractable. Therefore it is assumed that the load is constant under the same occupant until either a change of occupants or a rearrangement of the furniture by the same owner occurs (Fig. II-15). The small fluctuation during that period will be neglected. A more complicated model can include the presumed trend in this variation. As shown in Fig. II-16 the load might be increased linearly with time since the last changes. Then the maximum load during an interval is

$$L = L_0 + \theta s_0$$

The magnitude of the load L will not be independent of the time to the last occurrence. If, as previous authors have implicitly done, we assume changes take place at regular time intervals, s_0 , then our interest is only in the random variable $Y = Y_0 + \theta s_0$, and the analysis is unchanged, provided information can be obtained about the random variables Y_0 and θ . If, on the other hand, load changes are assumed (as will be done here) to take place at random points in time, the time intervals S_0 will be random. In this case the important load magnitudes, $Y = Y_0 + \theta S_0$, and the number (and times) of load occurrence will not be stochastically independent. The analysis of such a model becomes much less tractable than that which follows. Therefore the simplified model (Fig. II-15) will be used in this work. The second model may have to be considered if there is any new data in the future to show strongly that the load increase under the same occupant is significant.

II-5b: Probability Distribution of the Maximum Lifetime Sustained Load for a Single Area

Let

$$z = \max_{0 \leq \tau \leq t} L(\tau)$$

where $L(\tau)$ is the total load at any time τ , then

$$F_z(\alpha) = P[z \leq \alpha] = P[L(0) < \alpha] P[\text{no up-crossing of } \alpha \text{ from } 0 \text{ to } t]$$

(II-5-1)

The first term $P[L(0) < \alpha]$, which equals the CDF of $L(t)$ at α or $F_{L(t)}(\alpha)$, can be calculated from the results of the previous section. In order to evaluate the second term the results of the survey about the change of occupants must be examined. Mitchell and Woodgate⁽³⁾ used a clever way to sample the period between the change of occupants by searching through the telephone directories. The results are plotted in Fig. II-17. As shown in the figure an exponential function fits the data approximately*, which suggests that the occupants changes follow a Poisson Occurance model⁽²⁵⁾ with mean rate ν . Under this assumption (and assuming independence of the individual load values), the up-crossings are approximately a Poisson process with random selection⁽²⁵⁾. Then the probability of no up-crossing in 0 to t is:

$$P[\text{no up-crossing of } \alpha \text{ from } 0 \text{ to } t] = e^{-\nu \alpha t} \quad (\text{II-5-2})$$

* Relatively short occupancy times (0 to 2 years) may have been missed by this data collection scheme. Also if load changes are assumed to occur with same occupant re-arrangements as well as with occupancy changes, the short duration interval (0 to 2 years) will be represented.

where v_α is the average rate of up-crossings of threshold level α . The approximation arises from the lack of strict independence of the up-crossing event. (There can not be two in a row for example.) The dependence is weak if the crossings are relatively rare, i.e., if the threshold is not too low, ignore this dependence. Eq. (II-5-2) is exact under the Poisson occurrence assumption. If the load changes do not follow Poisson occurrence, Eq. (II-5-2) still holds for high load levels, i.e., if α is high and the expected number of crossings is much less than one in 0 to t. Then

$$\begin{aligned}
 &P[\text{no up-crossing of } \alpha \text{ from } 0 \text{ to } t] \\
 &= 1 - P[1 \text{ up-crossing}] - P[\text{more than } 1 \text{ up-crossing}]
 \end{aligned}$$

If $P[\text{more than } 1 \text{ up-crossing}]$ is much less than $P[1 \text{ up-crossing}]$, then

$$\begin{aligned}
 &P[\text{no up-crossing of } \alpha \text{ from } 0 \text{ to } t] \\
 &\cong 1 - P[1 \text{ up-crossing}]
 \end{aligned}$$

On the other hand,

$$\begin{aligned}
 \text{mean number of up-crossing} &= v_\alpha t = 1 * P[1 \text{ up-crossing}] \\
 &+ 2 * P[2 \text{ up-crossings}] + 3 * P[3 \text{ up-crossings}] + \dots
 \end{aligned}$$

If the events are rare, then

$$\sum_{i=2}^{\infty} i \cdot P[i \text{ up-crossing}] \ll P[1 \text{ up-crossing}]$$

therefore

$$\text{mean number of up-crossing} \cong P[1 \text{ up-crossing}]$$

and thus

$$\begin{aligned} P[\text{no up-crossing of } \alpha \text{ from } 0 \text{ to } t] &\cong 1 - \text{mean} \\ &\quad \text{number of up-crossing} \\ &= 1 - v_{\alpha} t \cong e^{-v_{\alpha} t} \end{aligned}$$

for $v_{\alpha} t \ll 1$

The next step is to find v_{α} , the mean rate of up-crossings. Consider an infinitesimal time interval Δt . Under the Poisson process assumptions, the probability that more than two load changes occur in Δt is assumed zero (strictly speaking it is a smaller order than the probability of 1 change). Therefore the probability of more than two up-crossings is also zero:

$$P[n \text{ up-crossings in } \Delta t] = 0 \quad \text{for } n \geq 2$$

v_{α} is the (expected) rate of up-crossings and the expected number of the up-crossing in Δt will therefore be:

$$v_{\alpha} \Delta t = E[\text{number of up-crossings in } \Delta t]$$

$$= \sum_{n=0}^{\infty} n * P[n \text{ up-crossings in } \Delta t]$$

$$\cong P[1 \text{ up-crossing in } \Delta t]$$

An up-crossing will happen when the load at the beginning of Δt is smaller than α and larger than α after Δt (Fig. II-18).

Hence

$$v_{\alpha} \Delta t = P[1 \text{ up-crossing in } \Delta t]$$

$$= P[\{L(t+\Delta t) \geq \alpha\} \cap \{L(t) < \alpha\}]$$

It is useful here to anticipate a more general development which will be discussed next, to follow the following lines of development. Since $L(t)$ changes value only at changes in occupant we can write

$$v_{\alpha} \Delta t = P[(\text{there is a change of the occupant in } \Delta t) \cap$$

$$\{L(t+\Delta t) \geq \alpha\} \cap \{L(t) < \alpha\}]$$

$$= P[\text{There is a change of the occupant in } \Delta t]^*$$

$$P[\{L(t+\Delta t) \geq \alpha\} \cap \{L(t) < \alpha\} \mid (\text{There is a change of occupant in } \Delta t)] \quad (\text{II-5-4})$$

Now⁽²⁵⁾

$$P[\text{There is a change of the occupant in } \Delta t] = \nu \Delta t \quad (\text{II-5-5})$$

where ν = average rate of the changes of a single occupant. Given that there is an occupant change in the time interval, $L(t+\Delta t)$ and $L(t)$ are two (assumed independent) random variables with the same CDF, $F_{L(t)}$. Therefore

$$P[\{L(t+\Delta t) \geq \alpha\} \cap \{L(t) < \alpha\} \mid (\text{There is a change of occupant})] \\ = [1 - F_{L(t)}(\alpha)] F_{L(t)}(\alpha) \quad (\text{II-5-6})$$

Substituting Eq. (II-5-5) and Eq. (II-5-6) into Eq. (II-5-4):

$$\nu_{\alpha} \Delta t = \nu \Delta t [1 - F_{L(t)}(\alpha)] F_{L(t)}(\alpha)$$

Since ν_{α} is independent of time, the mean number of occurrences in 0 to t reduced to simply

$$v_{\alpha} t = \int_0^t v_{\alpha} \Delta t = vt[1-F_{L(t)}(\alpha)]F_{L(t)}(\alpha) \quad (\text{II-5-7})$$

Combining Eq. (II-5-1), Eq. (II-5-2) and Eq. (II-5-7) we obtain

$$\begin{aligned} F_z(\alpha) &= F_{L(t)}(\alpha) \exp[-v_{\alpha} t] \\ &= F_{L(t)}(\alpha) \exp\{-vt[1-F_{L(t)}(\alpha)]F_{L(t)}(\alpha)\} \quad (\text{II-5-8}) \end{aligned}$$

If we have interest in only the higher loads, then

$$F_{L(t)}(\alpha) \cong 1$$

and

$$1-F_z(\alpha) \cong 1-\exp\{-vt[1-F_{L(t)}(\alpha)]\} \cong vt[1-F_{L(t)}(\alpha)] \quad (\text{II-5-9})$$

This is of the same form that Karman⁽¹⁰⁾ obtained for higher loads when he derived the maximum load by assuming a fixed number, n , of load changes; in Eq. (II-5-9) the expected number of load changes, vt , takes the place of his n .

II-5c: Probability Distribution of the Maximum Lifetime Sustained Load for Multiple Loadings

Consider again the load on a column pictured in Fig.

II-19, and recognize that there are time variations in the floor loads. Let

$$F(t) = \sum_{i=1}^n L_i(t)$$

be the sum of n total loads at time t . Note the difference in character of any $L_i(t)$ and $F(t)$. The latter has a higher mean rate of jumps and the relative magnitude of the fluctuations to the mean load is small. (Note the vertical scale change in Fig. II-19.) The same model will obviously also treat different occupants on the same floor or any mixture of number of occupants and number of floors.

Define the maximum column load as

$$Z_n = \max_{0 \leq \tau \leq t} F(\tau)$$

Following the same derivation as in the previous section:

$$P[Z_n \leq \alpha] = P[F(0) < \alpha] P[\text{no up-crossing of } \alpha \text{ from } 0 \text{ to } t]$$

and

$$P[\text{no up-crossing of } \alpha \text{ from } 0 \text{ to } t] = e^{-v_\alpha t} \quad (\text{II-5-10})$$

We have already demonstrated that the reason why the load will jump from below α to above α is due to the load changes.

There are n different loads in this case. Each load may in general have different probability distribution or different occupancy change rates v_i and therefore different associated rates of up-crossing, $(v_\alpha)_i$. Let

$(v_\alpha)_i$ = average rate of up-crossing of α -threshold due to a change in the i th load (or occupant)

then

$$P[\text{no up-crossing of } \alpha \text{ from } 0 \text{ to } t \text{ due to } i\text{th load changes}] = e^{-(v_\alpha)_i t} \quad (\text{II-5-11})$$

Consider Eq. (II-5-10).

$$P[\text{no up-crossing of } \alpha \text{ from } 0 \text{ to } t] = P[(\text{no up-crossing of } \alpha \text{ from } 0 \text{ to } t \text{ due to 1st load})U \\ (\text{no up-crossing of } \alpha \text{ from } 0 \text{ to } t \text{ due to 2nd load})U \\ \vdots \\ (\text{no up-crossing of } \alpha \text{ from } 0 \text{ to } t \text{ due to } n\text{th load})]$$

Assume that (consistent with Poisson occurrences) no two load changes occur at the same time and that the load changes by different occupants are independent of each other, then all events in the above equation are independent. Then

$$\begin{aligned}
& P[\text{no up-crossing of } \alpha \text{ from } 0 \text{ to } t] \\
& = P[\text{no up-crossing of } \alpha \text{ from } 0 \text{ to } t \text{ due to 1st load}] * \\
& \quad P[\text{no up-crossing of } \alpha \text{ from } 0 \text{ to } t \text{ due to 2nd load}] * \\
& \quad \quad \quad \vdots \\
& \quad \quad \quad P[\text{no up-crossing of } \alpha \text{ from } 0 \text{ to } t \text{ due to nth load}] \\
& = e^{-(v_\alpha)_1 t} e^{-(v_\alpha)_2 t} \dots e^{-(v_\alpha)_n t} \\
& = e^{-[(v_\alpha)_1 + (v_\alpha)_2 + \dots + (v_\alpha)_n] t} \tag{II-5-12}
\end{aligned}$$

Comparing with Eq. (II-5-10),

$$\begin{aligned}
v_\alpha & = (v_\alpha)_1 + (v_\alpha)_2 + (v_\alpha)_3 + \dots + (v_\alpha)_n \\
& = \sum_{i=1}^n (v_\alpha)_i \tag{II-5-13}
\end{aligned}$$

Again, following the same derivation as in previous sections up to Eq. (II-5-4),

$$\begin{aligned}
(v_\alpha)_j \Delta t & = P[\text{There is a change of the } j\text{th occupant in } \Delta t] * \\
& \quad P[\{F(t+\Delta t) \geq \alpha \cap F(t) < \alpha\} | (\text{There is a change of the} \\
& \quad \quad \quad j\text{th occupant in } \Delta t)] \tag{II-5-14}
\end{aligned}$$

Now

$$P[\text{There is a change of the } j\text{th occupant in } \Delta t] = v_j \Delta t \quad (\text{II-5-15})$$

in which v_j is the mean rate of occupancy changes in the j th floor (or area). And

$$P[\{F(t+\Delta t) \geq \alpha \cap F(t) < \alpha\} | (\text{There is a change of the } j\text{th occupant in } \Delta t)]$$

$$= \int_0^\alpha P[F(t+\Delta t) \geq \alpha | F(t) = x] f_F(t)(x) dx \quad (\text{II-5-16})$$

where $f_F(t)(x)$ is the PDF of the total load $F(t)$. Substituting Eq. (II-5-15) and Eq. (II-5-16) into Eq. (II-5-14),

$$\begin{aligned} (v_\alpha)_j \Delta t &= v_j \Delta t \int_0^\alpha P[F(t+\Delta t) \geq \alpha | F(t) = x] f_F(t)(x) dx \\ &= v_j \Delta t \int_0^\alpha P[\{F(t+\Delta t) - F(t)\} \geq \alpha - x | F(t) = x] f_F(t)(x) dx \end{aligned} \quad (\text{II-5-17})$$

Since the j th load changes, then

$$\begin{aligned} F(t+\Delta t) - F(t) &= \left\{ \sum_{\substack{i=1 \\ i \neq j}}^n L_i(t) \right\} + L_j(t+\Delta t) - \sum_{i=1}^n L_i(t) \\ &= L_j(t+\Delta t) - L_j(t) \end{aligned} \quad (\text{II-5-18})$$

Substituting Eq. (II-5-18) into Eq. (II-5-17),

$$(v_\alpha)_j \Delta t = v_j \Delta t \int_0^\alpha P[\{L_j(t+\Delta t) - L_j(t)\} \geq \alpha - x | F(t) = x] f_F(t)(x) dx$$

(II-5-19)

Let W_j equal the random change in load on the j th floor when a new load replaces an old one.

$$W_j = L_j(t+\Delta t) - L_j(t) \quad (II-5-20)$$

Assume as before that the new load is independent of the old one and that they have identical (γ) probability distribution. Then the distribution of W_j can be derived from elementary probability theory. The mean of W is

$$E[W_j] = m_{W_j} = m_{L_j} - m_{L_j} = 0$$

$$\text{Var}[W_j] = \sigma_{L_j}^2 + \sigma_{L_j}^2 = 2\sigma_{L_j}^2$$

The correlation between W_j and $F(t)$ will be examined next. W_j and $F(t)$ are not strictly independent, because they both are functions of the random variable $L_j(t)$. But their covariance is

$$\begin{aligned}
\text{cov}[W_j, F(t)] &= E[(W_j - m_{W_j})(F(t) - m_{F(t)})] \\
&= E[W_j F(t)] - m_{W_j} m_{F(t)} \\
&= E[\{L_j(t+\Delta t) - L_j(t)\} F(t)] \\
&= E[L_j(t+\Delta t) F(t)] - E[L_j(t) F(t)] \\
&= E[L_j(t+\Delta t) \sum_{i=1}^n L_i(t)] - E[L_j(t) \sum_{i=1}^n L_i(t)]
\end{aligned}$$

Ignoring, for this argument, the correlation among floor loads

$$\text{cov}[W_j, F(t)] = \sum_i m_{L_i} m_{L_j} - \left(\sum_{i=j} m_{L_i} m_{L_j} + E[L_j^2] \right) = -\sigma_{L_j}^2$$

The correlation coefficient between W_i and $F(t)$ is

$$\frac{\text{cov}[W_j, F(t)]}{\sigma_{W_j} \sigma_{F(t)}} = \frac{-\sigma_{L_j}^2}{\sqrt{2} \sigma_{L_j} \sigma_{F(t)}}$$

The absolute value of the correlation coefficient is down to 0.707 even if only a single floor, when $\sigma_{F(t)} = \sigma_{W_j}$. But, this case will be handled by the method described in Section II-5b rather than the method above. For more floors it will

fall off with the rate between $1/\sqrt{n}$ and $1/n$. Therefore the worst case we have is when $n = 2$ and the correlation coefficient equal to $0.707/\sqrt{2} = 0.5$. (Note that the above argument applies only to the case where all L_i 's are of the same order of magnitude. The case where one load dominates will be discussed later). The conclusion is that W_j and $F(t)$ are not highly correlated, therefore they will be assumed independent.* The conditional probability in Eq. (II-5-19) can then be replaced by a marginal value.

$$\begin{aligned}
 P[\{L_j(t+\Delta t) - L_j(t)\} \geq \alpha - x | F(t) = x] &= P[L_j(t+\Delta t) - L_j(t) \geq \alpha - x] \\
 &= 1 - F_{W_j}(\alpha - x)
 \end{aligned}$$

where $F_{W_j}(x)$ is the CDF of W_j .

If n or A is large $F(t)$ is at least approximately normal. This approximation is also checked numerically in Appendix E and found satisfactory for practical bay sizes. Then

$$f_{F(t)}(x) \cong \frac{1}{\sigma_{F(t)} \sqrt{2\pi}} \exp\left[-\frac{1}{2} \left(\frac{x - m_{F(t)}}{\sigma_{F(t)}}\right)^2\right]$$

*This assumption is checked numerically against an exact result in Appendix E for the special case when the $L_i(t)$'s are independent.

where

$$m_F(t) = \text{mean of } F(t)$$

$$\sigma_F(t) = \text{standard deviation of } F(t)$$

(See, for example, Eq. (II-1-19) for values of two moments for simple nominal column loads.) Substitute into Eq. (II-5-19)

$$(v_\alpha)_j \Delta t = \int_0^\alpha v_j \Delta t [1 - F_{W_j}(\alpha - x)] \frac{1}{\sigma_F(t) \sqrt{2\pi}} \exp\left[-\frac{1}{2} \left(\frac{x - m_F(t)}{\sigma_F(t)}\right)^2\right] dx$$

Since $(v_\alpha)_j$ is independent of t

$$(v_\alpha)_j t = \int_0^t (v_\alpha)_j \Delta t = \int_0^\alpha v_j t [1 - F_{W_j}(\alpha - x)] \frac{1}{\sigma_F(t) \sqrt{2\pi}} \exp\left[-\frac{1}{2} \left(\frac{x - m_F(t)}{\sigma_F(t)}\right)^2\right] dx \quad (\text{II-5-21})$$

All $(v_\alpha)_j$'s can be found from Eq. (II-5-21) and

$$v_\alpha t = \sum_i^n (v_\alpha)_i$$

Then, combining results

$$\begin{aligned}
 F_{Z_n}(\alpha) &= F_{F(t)}(\alpha) \exp[-v_\alpha t] \\
 &= 1 - v_\alpha t && \text{(for large threshold } \alpha) \\
 & && \text{(II-5-22)}
 \end{aligned}$$

If all loads have identical distributions and common v_j 's, then

$$v_j = v \quad \text{for all } j$$

$$(v_\alpha)_i = (v_\alpha)_j \quad \text{for all } i \text{ and } j$$

hence

$$v_\alpha t = n(v_\alpha)_j$$

$$= \int_0^\alpha nvt [1 - F_{W_j}(\alpha - x)] \frac{1}{\sigma_{F(t)} \sqrt{2\pi}} \exp\left[-\frac{1}{2} \left(\frac{x - m_{F(t)}}{\sigma_{F(t)}}\right)^2\right] dx$$

(II-5-23)

Next, the probability distribution of W_j will be derived.

Recall that

$$W_j = L_j(t + \Delta t) - L_j(t)$$

and the probability distribution of $L_j(t)$ is assumed gamma.

Consider the case that the parameter k is integer, then

$$f_{L_j}(t)(x) = \frac{\lambda^k x^{k-1} e^{-\lambda x}}{(k-1)!}$$

The distribution of W_j is obtained by simple convolution⁽²⁵⁾. Several derived distribution of W_j are presented below. The distributions are symmetrical about zero; only the results for positive argument W or $(\alpha-x)$ are shown.

$$F_{W_j}(\alpha-x) = 1 - \frac{1}{2} e^{-\lambda(\alpha-x)} \quad \text{for } k=1$$

$$F_{W_j}(\alpha-x) = 1 - e^{-\lambda(\alpha-x)} \left[\frac{1}{2} + \frac{5}{16} \lambda(\alpha-x) + \frac{1}{16} \lambda^2(\alpha-x)^2 \right] \quad \text{for } k=3$$

$$F_{W_j}(\alpha-x) = 1 - e^{-\lambda(\alpha-x)} \left[\frac{1}{2} + \frac{93}{256} \lambda(\alpha-x) + \frac{29}{256} \lambda^2(\alpha-x)^2 + \frac{7}{384} \lambda^3(\alpha-x)^3 + \frac{1}{1536} \lambda^4(\alpha-x)^4 \right] \quad \text{for } k=5$$

(II-5-24)

Note that $F_{W_j}(\alpha-x)$ is a function of $\lambda(\alpha-x)$ only. It is shown in the Appendix F that we can also use the unit load to replace total load in the Eq. (II-5-21) and Eq. (II-5-22).

There is no guarantee, of course, that the distribution of $L_j(t)$ will have an integer k . In most cases they will

not. There is apparently no closed form solution for $F_{W_j}(\alpha-x)$ when k is not integer. Two approaches can solve this problem; first, solve Eq. (II-5-21) numerically or second, solve Eq. (II-5-21) twice with two integer k and then interpolate the results to the desired k value. e.g., $x(k_{2.6}) = 0.4*x(k_3)+0.6*x(k_2)$ where $x(k_{2.6})$ is the load due to $k = 2.6$, etc.

The second approach is much preferred because of its simplicity and it will be used in this work. Its accuracy will be examined next. Assume an arbitrary case of column load with 150 sq. ft. area and a unit influence surface. The maximum lifetime sustained load corresponding to a probability 0.99 of not being exceeded was calculated from Eq. (II-5-22) for different integer k values. (Note that the values of λ are so chosen that they all have the same mean.) The results are plotted in Fig. II-20. The figures show that the results for any two adjacent k values are so close that simple interpolation will have a high accuracy. The only exception is when k lies between 1 and 2. The gap is larger for smaller n and smaller k . However the interpolation still can be used because the load is higher for smaller k and the error will remain small in percentage basis. Also k is greater than 2 when the area is greater than 150 ft².⁽³⁾ Most cases that we are interested in will have k greater than

2. Another case with a more typical area, 624 ft.², was examined also. The results (Fig. II-21) are the same as the previous one.

A closed form approximation for v_α and hence $F_z(\alpha)$ is derived in Appendix G. The range of its application is rather limited, therefore it will not be discussed here.

The independence between W_j and $F(t)$ will be re-examined. Recall Eq. (II-5-19):

$$(v_\alpha)_j \Delta t = v_j \Delta t \int_0^\alpha P[\{L_j(t+\Delta t) - L_j(t)\} \geq \alpha - x | F(t) = x] f_F(t)(x) dx$$

(II-5-19)

If all $L_j(t)$'s are of the same order of magnitude (like the column axial load where $L_j(t)$ is the contribution due to the j th floor) $W_j = [L_j(t+\Delta t) - L_j(t)]$ and $F(t)$ are approximately independent. This was discussed before. However in a situation where one load component, say $L_i(t)$, dominates, i.e.,

$$\sigma_{L_i}^2(t) \cong \sigma_F^2(t)$$

then the correlation coefficient between W_j and $F(t)$ will be as high as 0.7 and will not fall off with n . The independent assumption is not very appropriate. Let us examine the correlation between $L_i(t)$ and $F(t)$. Since

$$F(t) = \sum_{\substack{j=1 \\ j \neq i}}^n L_j(t) + L_i(t) = (SL)_{n-1} + L_i(t)$$

The correlation coefficient between $F(t)$ and $L_i(t)$ will be

$$\rho_{F(t), L_i(t)} = \frac{\sigma_{L_i(t)}^2 + \rho_{(SL)_{n-1}, L_i(t)} \sigma_{L_i(t)} \sigma_{(SL)_{n-1}}}{\sigma_{F(t)} \sigma_{L_i(t)}}$$

where $\rho_{(SL)_{n-1}, L_i(t)}$ is the correlation coefficient between $(SL)_{n-1}$ and $L_i(t)$. There is no reason to believe that $\rho_{(SL)_{n-1}, L_i(t)}$ will be negative. (The negative correlation coefficient under the linearity assumption means that the larger the $L_i(t)$, the smaller the $(SL)_{n-1}$ and vice versa.) Assume that $\rho_{(SL)_{n-1}, L_i(t)}$ is positive, then

$$\rho_{F(t), L_i(t)} \geq \frac{\sigma_{L_i(t)}^2}{\sigma_{F(t)} \sigma_{L_i(t)}} \cong 1$$

This shows that $F(t)$ and $L_i(t)$ are almost perfectly correlated. Assume that the above relation is true, i.e., $F(t)$ and $L_i(t)$ are perfectly correlated, then

$$\begin{aligned}
P[\{L_i(t+\Delta t) - L_i(t)\} \geq \alpha - x | F(t) = x] &= P[L_i(t+\Delta t) \geq \alpha] \\
&= 1 - F_{L_i}(t)(\alpha)
\end{aligned}$$

Substitute the above equation into Eq. (II-5-19):

$$\begin{aligned}
(v_\alpha)_i \Delta t &= v_i \Delta t \int_0^\alpha [1 - F_{L_i}(t)(\alpha)] f_{F(t)}(x) dx \\
&= v_i \Delta t [1 - F_{L_i}(t)(\alpha)] F_{F(t)}(\alpha)
\end{aligned} \tag{II-5-25}$$

Thus $(v_\alpha)_i$ corresponding to the dominating load $L_i(t)$ can be evaluated from Eq. (II-5-25). The load other than $L_i(t)$ will be treated the same as before. A numerical example will be used to check the above assumptions in Chapter IV.

II-5d: Probability Distribution of the Maximum Lifetime Sustained Load Effect

Let $G(A)$ be the total load effect of any kind from area A , then

$$G(A) = \iint_0^{\sqrt{A}} I(x,y) w(x,y) dx dy \tag{II-5-26}$$

where $w(x,y)$ is defined in Section II-2 and $I(x,y)$ is the coordinate of the influence surface at point (x,y) . Its mean and variance are (see Appendix A):

$$\begin{aligned}
 E[G(A)] &= \iint_0^{\sqrt{A}} E[I(x,y)w(x,y)] dx dy \\
 &= m \iint_0^{\sqrt{A}} I(x,y) dx dy \\
 &= m \cdot V_I \qquad \qquad \qquad (II-5-27)
 \end{aligned}$$

where V_I is the volume enclosed by the influence surface.

$$\begin{aligned}
 \text{Var}[G(A)] &= \iiint_0^{\sqrt{A}} \iiint_0^{\sqrt{A}} I(x,y) I(x_1,y_1) \text{cov}[w(x,y), w(x_1,y_1)] \\
 &\qquad \qquad \qquad dx dx_1 dy dy_1 \qquad \qquad \qquad (II-5-28)
 \end{aligned}$$

This last equation reduces to Rosenblurth's⁽⁷⁾ if the $w(x,y)$ process is assumed to be "white noise", i.e., lacking spatial correlation. The equation is identical to that considered by Fader⁽⁹⁾.

Recall that in Section II-5b and Section II-5c, where we derive the maximum lifetime sustained load, there was no restriction on the total load, $L_i(t)$. If we replace it with total load effect, $G_i(t)$, we will end in the same result as Eq. (II-5-7) and Eq. (II-5-21). That is, for one occupant,

$$v_{\alpha}^t = vt[1-F_{G(t)}(\alpha)]F_{G(t)}(\alpha) \quad (\text{II-5-29})$$

and for several occupants

$$(v_{\alpha})_j^t = \int_0^{\alpha} v_j^t [1-F_{W_j}(\alpha-x)] \frac{1}{\sigma_F(t)\sqrt{2\pi}} \exp\left[-\frac{1}{2}\left(\frac{x-m_F(t)}{\sigma_F(t)}\right)^2\right] dx \quad (\text{II-5-30})$$

where

$$W_j = G_j(t+\Delta t) - G_j(t)$$

$$F(t) = \sum_{i=1}^n G_i(t)$$

and

$$v_{\alpha}^t = \sum_j^n (v_{\alpha})_j^t \quad (\text{II-5-31})$$

This is the equation needed to evaluate the probability

distribution of the maximum lifetime sustained load effect, Eq. (II-5-22). If we make the same assumption that the probability distribution of $G_i(t)$ is gamma, Eq. (II-5-24) can be used in the evaluation of Eq. (II-5-30). This assumption will be adopted in the subsequent chapters.

After the maximum load effect is found for a prescribed probability level, the corresponding EUDL, that will produce the same load effect when it is put on the structure, is equal to the load effect divided by V_I , the volume of influence surface.

The above model can be used in a more general way. For example in a column load case (Fig. II-22) we can assume that each floor has different tenants. The load changes on each floor will be independent of each other. We can also assume that the same tenant occupies both floor A and B. Then the load on those two floors will change simultaneously. Under this circumstance we can combine the load on floors A and B as a single load and proceed as before to find the maximum lifetime sustained load. Any other combination can be treated in the same way. Thus the model can handle cases ranging from a multiple number of tenants on each of a number of floors through a single occupier of all floors.

CHAPTER III

Extraordinary (Transient) Load Model

III-0: Introduction

The general characteristics of extraordinary transient loads were discussed in Chapter 1. We seek in this section the effect of a single event. The load model proposed below can be best thought of by considering the load caused by crowds of people but it is not limited to this source. Any other extraordinary load that has the same characteristics can be represented by this model also. Lacking other information, it will be assumed here to represent all sources of transient loads, including re-modeling loads.

There has been virtually no stochastic modeling of these transient loads in the literature. (See Heaney⁽¹⁴⁾ and Karman⁽¹⁰⁾.) The model proposed here assumes random occurrences in time of events which are characterized in space by randomly located load "cells". This latter aspect of the model is somewhat similar to the sustained load models proposed by Corotis⁽¹²⁾ and independently by Hasofer⁽¹³⁾.

This chapter will develop the model and its analysis. First the random load effect associated with a particular event will be modeled and analyzed. Then, the random occurrence in time of these events will be considered, and the

behavior of their maximum effect will be sought. The combination of this extraordinary load with the ordinary (sustained) load will be treated in Chapter IV.

III-1: Load Model for a Particular Event

A distinguishing characteristic of the behavior of a group of people that get together is that they tend to gather in small groups. The number of groups (or load cells) depends upon the area of the floor and the number of people in the building. Each cell contains an uncertain number of persons which may vary from cell to cell. Therefore the first assumption is that the loads are grouped into N load cells and each cell contains R items (Fig. III-1). Both N and R are random numbers.

Consider a single load cell first. Let

$$S_r = Q_1 + Q_2 + \dots + Q_r \quad (\text{III-1-1})$$

where

Q_i = weight of the i th item, a random variable

S_r = weight of the sum of r items

Assuming that the weights of all items are independent and identically distributed, the probability distribution of S_r can be derived by convolution integration. Let

S = the weight of the sum of R items where R
is a random variable.

Its cumulative distribution will be:

$$P[S \leq s] = F_S(s) = \int_r P[S_r \leq s | R=r] P[R=r] \quad (\text{III-1-2})$$

For situations other than such crowds (e.g. remodeling loads) a cell and its weight S may represent a particular heavy item or a cluster of items.

The area occupied by a load cell is assumed to be small as compared to the whole contributing area. Therefore the change in the value of the influence surface over the area of the cell will be small. This difference will be neglected, i.e., the influence surface will be assumed uniform over a load cell. The load effect, P , due to a load cell is then

$$P = S * I \quad (\text{III-1-3})$$

where I is the value of the influence surface at the center of the load cell.

$$\begin{aligned} P[P \leq p] &= F_P(p) = P[S * I \leq p] \\ &= \int_0^s P[I \leq \frac{p}{s} | S=s] f_S(s) ds \end{aligned}$$

If, at the instant of maximum load effect, the location of a load cell is assumed to be equally likely to occur

at any point over the whole area under consideration, then I , its influence value is a random variable and

$$P\left[I \leq \frac{p}{s} \mid S=s\right] = \frac{\text{area with } I \leq \frac{p}{s}}{\text{total area}} \quad (\text{III-1-4})$$

Let

$$H_m = P_1 + P_2 + \dots + P_m \quad (\text{III-1-5})$$

where H_m is the total load effect of m load cells. Its probability distribution can be derived in the same way as S_r if all P_i 's are assumed independent. Let

H = total load effect due to M load cells
where M is a random number

Then the CDF of H is

$$F_H(h) = P[H \leq h] = \sum_M P[H_M \leq h \mid M=m] P[M=m]$$

= CDF of the extraordinary load effect

Theoretically the probability distribution of the extraordinary load effect H can be derived following the above steps. However there are some difficulties. First

the probability distributions of Q, R and M are not known; second no closed form solution can be obtained because some of the integrations may not be tractable analytically. There are two approaches that can be employed to resolve this problem; one is making some particular distribution assumptions so that all the analytical difficulties can be avoided or solved by numerical integration; the other is an approximate method. The first approach is not preferred because our knowledge about the extraordinary load is so limited that any sophisticated assumption is not justified. Therefore the second approach will be used and is described below.

The only distribution assumption required ultimately is the shape of the distribution of H. It will be demonstrated in the next section by a numerical example that the probability distribution of P is "exponential-like" and that the distribution of H is close to gamma. Therefore H is assumed to be gamma distributed. Only its parameters are now required.

Assuming independence of R and the Q_i , and of S and I, the mean and variance of S and P are⁽²⁵⁾:

$$E[S] = m_Q m_R$$

$$\text{Var}[S] = m_R^2 \sigma_Q^2 + m_Q^2 \sigma_R^2$$

$$E[P] = m_S m_I$$

$$\text{Var}[P] = m_S^2 \sigma_I^2 + m_I^2 \sigma_S^2 + \sigma_I^2 \sigma_S^2$$

Assuming independence of M and the P_i , the equation of H has the same form as that of S and therefore the formulas for the mean and the variance are the same also:

$$E[H] = m_P m_M$$

$$\text{Var}[H] = m_M^2 \sigma_P^2 + m_P^2 \sigma_M^2$$

Once the mean and the variance are known, the gamma distribution of H is completely defined.

In the above derivation only the means and the variances of Q, R and M are used. It is much easier to make a reasonable assumptions or estimations about their two moments than about the complete distributions.

III-2: Maximum Extraordinary Load

The probability distribution of a single occurrence of the extraordinary load is discussed in the previous section. Next we want to find the probability distribution of the maximum extraordinary load. There is as yet no data about the occurrences in time of the extraordinary load available. Assume that they follow a Poisson process with mean rate ν_e , then the CDF of the maximum extraordinary load in the time interval 0 to t is⁽²⁵⁾:

$$F_{L_2|t}(x) = \exp[-\nu_e(1-F_H(x)t)] \quad (\text{III-2-1})$$

where L_2 = the maximum extraordinary load during the period of 0 to t.

If we set t equal to the lifetime of the building, Eq. (III-2-1) gives the CDF of the maximum lifetime extraordinary load.

Because of the short duration and low mean arrival rate of extraordinary events, if there is more than one occupant involved, it is unlikely that they will have transient extraordinary loads at the same time. (Neglecting this possibility is exact if these loads are assumed to be instantaneous.) Assume that the occurrences of the extraordinary loads on the n_0 different occupants are mutually independent with average

rates of occurrence, v_{e_i} , for $i = 1, 2, \dots, n_0$, then

$P[\text{maximum extraordinary load effect from } 0 \text{ to } t \leq x]$

$=P[(\text{maximum extraordinary load effect due to occupant 1 from } 0 \text{ to } t \leq x) \cup$

$(\text{maximum extraordinary load effect due to occupant 2 from } 0 \text{ to } t \leq x) \cup$

\vdots

$(\text{maximum extraordinary load effect due to occupant } n_0 \text{ from } 0 \text{ to } t \leq x)]$

$=P[\text{maximum extraordinary load effect due to occupant 1 from } 0 \text{ to } t \leq x]^*$

$P[\text{maximum extraordinary load effect due to occupant 2 from } 0 \text{ to } t \leq x]^*$

\vdots

$P[\text{maximum extraordinary load effect due to occupant } n_0 \text{ from } 0 \text{ to } t \leq x]$ (III-2-2)

Substitute Eq. (III-2-1) into above equation:

$$\begin{aligned}
F_{L_2|t}^{\text{total}}(x) &= \prod_i^{n_0} F_{L_2|t}^{(i)}(x) \\
&= \prod_i^{n_0} [\exp\{-v_{e_i}(1-F_H^{(i)}(x))t\}] \\
&= \exp[-t \sum_i^{n_0} v_{e_i}(1-F_H^{(i)}(x))] \quad (\text{II-2-3})
\end{aligned}$$

where

$$F_{L_2|t}^{\text{total}}(x) = \text{CDF of the (total) } L_2 \text{ from 0 to } t$$

$$F_{L_2|t}^{(i)} = \text{CDF of } L_2 \text{ from 0 to } t \text{ due to occupant } i \text{ alone}$$

The term "occupant" can be broadly interpreted here. It can represent the personnel of an individual room or a set of rooms (in which case the mean number of load cells, m_M , would be relatively small). On the other hand, each "occupant" might represent a firm occupying several floors and the events their individual open house. Finally the "occupant" might be associated with a building-wide event (opening day, passing parades, etc.), in which m_M , the mean number of load cells, should perhaps be associated with the total (public) area of the building. Finally it might be

important to consider the possibility that all of the various kinds of events can occur (some might be more important for small members and some for larger). Then assuming independence, the CDF, $F_{L_2|t}^{\text{total}}$, of each individual kind of occupant can be found and their product (see the derivation of Eq. (III-2-3)) is the CDF for all types of events. A general equation of the CDF of the maximum load due to q different independent events is:

$$F_{Z_{\max}}(x) = F_{Z_{1 \max}}(x)F_{Z_{2 \max}}(x)\dots F_{Z_{q \max}}(x) \quad (\text{III-2-4})$$

where $F_{Z_{i \max}}(x)$ is the CDF of the maximum load Z_i . (Z_i itself may be a combination of different events like Eq. (III-2-3).)

It is assumed above that the extraordinary load follows Poisson occurrence. This is not appropriate for people load from seasonal parties, e.g., a Christmas party or a birthday party where the event will take place at a fixed interval of time (one year). Under this circumstance the probability distribution of L_2 will be:

$$F_{L_2|t}(x) = [1 - F_H(x)]^{\nu} e^{-\nu t} \quad (\text{III-2-5})$$

Eq. (III-2-5) can be combined with other types of load (Eq. (III-2-1)) as part of Eq. (III-2-4).

III-3: Example: The Extraordinary Load for a Column

The probability distribution of the extraordinary axial load will be determined here to demonstrate the model and to show that the results from the approximate approach are about the same as those from exact numerical integration. Assume that a column with a single floor is considered (Fig. III-1). The exact integration will be discussed in Section III-3a and the approximate approach will be discussed in Section III-3b.

III-3a: Exact Solution

Assume that all Q's (the weight of items) have the same normal distribution and that they are independent of each other with:

$$m_Q = 145 \text{ lbs}$$

$$\sigma_Q = 30 \text{ lbs}$$

Then S_r is also normal.

$$S_r = N(r*145, \sqrt{r}*30)$$

The discrete distribution of R is assumed as shown in Fig. III-2. The CDF of S can be numerically integrated according

to Eq. (III-1-2). The results are shown in Fig. III-3.

The influence surface for a column axial load is shown in Fig. II-10. The results of the numerical integration from Eq. (III-1-4) are shown in Fig. III-4. Assume also that the number of load cells has a Poisson distribution and that the expected number is a function of the area:

$$f_M(m) = P[M=m] = \frac{\lambda_M^m e^{-\lambda_M}}{m!}$$

$$E[M] = \lambda_M = \sqrt{\frac{A-164}{9}} \text{ for } A \geq 200 \quad (\text{III-3-1})$$

The last expression is simply unsubstantiated judgement, but it is designed to reflect the fact that the number of people per square foot will be (on the average) smaller during an extraordinary event in a larger area. The particular numbers were chosen to give an extraordinary event an expected total load per square foot of about 7.25 psf at A=200 and about 3.74 psf at A = 4000.

Consider two cases with different areas, 1208 ft² and 604 ft². The numerical integration results for the CDF of P and H are plotted in Fig. III-5 and Fig. III-6. The probability distribution of P is "exponential-like" and the probability distribution of H is very close to gamma. The

former conclusion is apparently dominated by the character of the distribution of I which is in turn related to the nature of the influence surface. It is anticipated that most other surfaces, which are typically equally or more peaked than that of Fig. II-10, will give a similar conclusion. That V has a gamma distribution would follow directly from the assumption that the P_i 's in $H = \sum_{i=1}^M P_i$ have (common) exponential distributions, if M were not random but deterministic⁽²⁵⁾. The assumed randomness of M makes the gamma distribution only an approximation.

III-3b: Approximate Solution

For the same assumptions as above, the mean and the variance of the weight of a load cell are:

$$E[S] = m_Q m_R = 725 \text{ lbs.}$$

$$\text{Var}[S] = m_R^2 \sigma_Q^2 + m_Q^2 \sigma_R^2 = 46550 \text{ (lbs)}^2$$

The mean and the variance of I can be found analytically or numerically and tabulated for various load effects and aspect ratios a/b.

$$m_I = \frac{1}{ab} \int_0^a \int_0^b I(x,y) dx dy \quad (\text{III-3-2})$$

$$\sigma_I^2 = \frac{1}{ab} \int_0^a \int_0^b I^2(x,y) dx dy - m_I^2 \quad (\text{III-3-3})$$

For this example of the column with the influence surface of Fig. II-10:

$$m_I = 0.254$$

$$\sigma_I^2 = 0.0745$$

for any area A and any aspect ratio. Then

$$E[P] = m_S m_I = 184 \text{ lbs.}$$

$$\text{Var}[P] = m_S^2 \sigma_I^2 + m_I^2 \sigma_S^2 + \sigma_S^2 \sigma_I^2 = 46270 \text{ (lbs)}^2$$

From Eq. (III-3-1) for $A = 604 \text{ ft}^2$

$$E[M] = \lambda_M = 6.99$$

$$\text{Var}[M] = \lambda_M = 6.99$$

and

$$E[H] = m_P m_M = 1288$$

$$\text{Var}[H] = m_M \sigma_P^2 + m_P \sigma_M^2 = 560,000$$

Since the distribution of H is assumed gamma, its parameters can be estimated as:

$$k_H = \frac{m_H^2}{\sigma_H^2} = 2.96$$

$$\lambda_H = \frac{k_H}{m_H} = 0.0023$$

The results are plotted in Fig. III-7, which is almost identical to the curve in Fig. III-6. It is therefore concluded that the assumption of the gamma distribution of H is appropriate. The results for A = 1208 are also plotted in Fig. III-7. Clearly more examples should be considered to confirm this assumption or to determine the range of its validity. On the other hand, given the difficulty of obtaining information on the subject of transient live loads, it may be just as appropriate simply to assume H is gamma distributed as to make and justify the intermediate distribution assumptions on Q, R and M.

CHAPTER IV

Load Combinations, Design Load and Performance Load

IV-0: Introduction

Due to the complexity of the live load it has been decomposed into several components (sustained, normal personnel and extraordinary load). Each component was discussed in a previous chapter. It is the purpose of this chapter to develop logical ways to combine the above load components for various design conditions. Several load combinations will be considered and their probability distributions determined. Throughout this chapter reference will be made to "loads" but one can equally well read "load effect", because they have been assumed in previous chapters to follow the same probability laws (with different parameters).

IV-1: Load Combination for the Design Load

Recall that in Chapter I we discussed three different kinds of loads: extraordinary loads, sustained loads and normal personnel loads (Fig. I-1). The combination of the above loads is shown in Fig. IV-1. For design with respect to safety, it is the maximum of this process that represents the extreme combined load. The direct determination of the distribution of the maximum of the sum of two random processes is a difficult problem. Here we shall assume that this maximum of the total coincides with one or the other of two extreme events defined below and shown in Fig. IV-1.

$$i) \quad L_t = L_1 + L_2 + L_3 \quad (IV-1-1)$$

where

L_t = the total load

L_1 = the maximum lifetime sustained load

L_2 = the maximum extraordinary load during the
period of L_1

L_3 = the arbitrary-point-in-time people load.

$$\text{ii) } L_t = L_3 + L_4 + L_5 \quad (\text{IV-1-2})$$

where

L_t and L_3 are defined above.

L_4 = the maximum extraordinary load during the lifetime of the building

L_5 = the arbitrary-point-in-time sustained load

There is a high probability that one or the other of the above combinations will include the maximum combined load during the lifetime of the building, but this may not always be true. For some load histories a moderate (or less than maximum) stationary load plus a moderate (or less than maximum) extraordinary load will be higher than either of the above load combinations. The probability of such an event causing the maximum combined load will be ignored.

The probability distribution of each of these potential maximum combined loads will be derived below. Several alternative applications are possible. First, consistent with modern "load-factor" and "limit-state" design philosophies, the "design loads" (i.e., the loads associated with selected high probabilities of not being exceeded) for each combination can be computed. These are then treated as two of the

several load combinations that are considered in design. Second, one could use each of these distributions for more complex structural reliability studies involving uncertain resistances, etc. Third, one can estimate the CDF of the maximum combined load by assuming it is the product of the CDF's of each of the two potential maxima⁽²⁵⁾ (i.e., by assuming one or the other causes the maximum combined load and by assuming the two loads are independent.). With this probability distribution of the maximum (combined) live load, one can either set a single "design load" or work with the probability distribution in conjunction with more complex reliability analysis. In this work emphasis will be on the separate treatment of the two loads and their individual design values.

IV-1a: Combination 1: $L_1+L_2+L_3$

The probability distribution of L_2 is derived in previous chapter.

$$F_{L_2|t}(x) = \exp[-v_e(1-F_H(x))t]$$

The probability distribution of T , the duration of the occupant in a building, is exponential with parameter v as

discussed in Section II-5. L_2 is the maximum extraordinary load during the random duration of the maximum sustained load. (Fig. IV-1). Its probability distribution is:

$$\begin{aligned}
 F_{L_2}(x) &= \int_0^{\infty} F_{L_2|t}(x) f_T(t) dt \\
 &= \int_0^{\infty} \exp[-v_e(1-F_H(x))t] v e^{-vt} dt \\
 &= \frac{v}{v+v_e(1-F_H(x))} \qquad \qquad \qquad (IV-1-3)
 \end{aligned}$$

If there is more than one occupant involved, Eq. (III-2-2) should be used instead of Eq. (III-2-1). Then

$$F_{L_2}(x) = \frac{v}{v + \sum_{i=1}^{n_0} [v e_i (1-F_H^{(i)}(x))]} \qquad \qquad \qquad (IV-1-4)$$

The fixed interval event which led to Eq. (III-2-4) will not be considered here because generally a party is held at a particular room where either there are very few items of furniture and equipment or where the furniture has been removed. It is not clear at this time what the interaction will be and what is the influence on the combination of loads.

The probability distribution of L_1 is found in Section II-5. L_3 is assumed as a constant, ℓ_3 , in Section II-4. The probability distribution of the total load, L_t , can be evaluated by a simple straight-forward (but numerical) convolution integration:

$$\begin{aligned}
 F_{L_t}(\ell) &= \int_0^{\ell-\ell_3} F_{L_2}^{\text{total}}(\ell-x-\ell_3) f_{L_1}(x) dx \\
 &= \int_0^{\ell-\ell_3} F_{L_1}(\ell-x-\ell_3) f_{L_2}^{\text{total}}(x) dx \quad (\text{IV-1-5})
 \end{aligned}$$

IV-1b: Combination 2: $L_3+L_4+L_5$

The probability distribution of L_4 is given by Eq. (III-2-1) or Eq. (III-2-2) where t equals the lifetime of the building. L_5 is discussed in Section II-4. The combined load can be obtained by the same way as above.

It should be pointed out that the model can be used to treat a variety of mixtures of conditions. As discussed in Section II-5d the maximum sustained load (or load effects) model can represent a variety of different assumptions about the nature of occupancy (or re-modeling) changes. Similarly,

as discussed in Section III-2, the maximum extraordinary load model can represent a variety of assumptions about the types and combinations of types of "occupants" associated with the events causing extraordinary loads. There is no reason why the "occupants" need be the same in the analyses of the two loads. For example, for a single owner-user building, the sustained loads might change everywhere virtually simultaneously whereas the extraordinary loads might be considered to be those associated with many independent local events associated with individual rooms within the building. The model has all these capabilities. How they should be exercised for any particular building or for a general code study is a difficult question requiring further study.

IV-2: Load Combination for Performance Load

The performance load, L_p , is simply the sum of L_5 and L_3 , the arbitrary-point-in-time sustained load plus the arbitrary-point-in-time people load respectively. Since the second load is assumed constant, ℓ_3 (Section II-4), the probability distribution of the performance load will be virtually the same as the first load (see Section II-4).

$$F_{L_p}(x) = F_{L_5}(x - \ell_3)$$

IV-3: Loading Pattern

No specific loading pattern is assumed in the above derivations. All loadings are modeled as close to reality as possible. L_1 and L_5 are the sustained loads which exist on the building all the time to a greater or lesser extent. Contrary to the conventional, conservative checkerboard loading pattern we load L_1 and L_5 on all floors and bays. Since we integrate over the whole distribution of the load, we have considered all possible combinations of low and high values already, i.e., the distribution of L_t represents the sum of different combinations each weighted by its joint probability. Nothing artificial has entered into this scheme. The extraordinary loads are modeled in the same way, but it results that they will contribute to the distribution of the load effect L_t only when they occur on its positive influence contribution areas. Examine Eq. (III-2-2). For positive x

$$P[\text{maximum extraordinary load due to occupant } i < x] = 1$$

if the i th occupant is located in the negative influence area because it can never produce a load effect greater than zero. This conclusion is in essence saying that we load the extraordinary load in checkerboard pattern (or; in general, on

the positive influence portions of the influence surface). We come to this conclusion through the model itself and not from the reasoning of "conservatism". For example, an influence line for the mid-span moment is shown in Fig. IV-2. Spans 1, 3 and 5 have positive contribution and spans 2 and 4 have negative contribution. The sustained load is applied on all spans. Though the mean of the load effect will be smaller as compared to the checkerboard loading pattern, the variance will be larger because all spans contribute positive variance. Actually it is not immediately clear which approach is more conservative when we compare the performance load, say at 99%. Span 2 and 4 contribute not only to the variance but also to the v_{α} , the average rate of up-crossing of α threshold. The event that the total load effect changes from below α to above α happens in two different ways: the positive load effect changes from a small value to a large one or the negative load effect changes from a large value to a small one. Therefore even though the load effect itself is negative, it will effectively contribute to the maximum lifetime sustained load.

The extraordinary load is applied to all spans also, but spans 2 and 4 contribute nothing to the maximum extraordinary load (i.e., they contribute nothing to the probability of exceeding a given design load). The results will

be the same as if we only load spans 1, 3, and 5. This is the same as if we used the checkerboard loading pattern for extraordinary loads.

IV-4: Design Load and Performance Load

The EUDL for different areas and different floors will be evaluated in this section for different load effects. Under the present code formats this is the design (or performance) load that should be specified for a consistent probability of not being exceeded. The values of the load that will be evaluated in the following sections are the 99% load which implies that there are 1% probability of being exceeded in the lifetime* of the building.

In order to have numerical results for the design load and the performance load we need numerical estimates of all parameters. The values obtained in Section II-2 will be used for sustained loads and the values estimated in Section III-3 will be applied to extraordinary load. We also estimate that v , the expected number of the occupant change, is $\frac{1}{8}$ changes/year and vt equals 8, the total changes during the lifetime of the building. The value of v_e , the average rate of occurrence of the extraordinary load, is set arbitrarily to 1. There are many parameters involved (e.g. v_e , Q , R and M), and the effects of the parameter are not independent of each other, because there is a continuous spectrum of "unusual"

*The lifetime is assumed 64 years. Its sensitivity will be examined.

events. For example, m_M , the expected number of load cells, will be different (smaller) if we set $v_e = 1$ than if we set $v_e = 0.1$ (occurrences/year). We can expect that there are fewer load cells associated with the event which happened, on the average, once a year than that associated with the event which happened, on the average, once in ten years. Therefore we just set the value of one parameter, and estimate the others. Thus, here, extraordinary loads are by definition those which occur once a year on the average.

A sensitivity analysis will be carried out in the next chapter to identify the important parameters and to study the effect of its changes.

IV-4a: EUDL for Axial Load

The EUDL's for two design combinations and performance column load are evaluated. Here, each floor is assumed to be occupied by a different occupant and therefore the change of occupancy on any floor is independent to that of other floors. The extraordinary load is also assumed to take place on each floor independently. The results are plotted in Fig. IV-3, Fig. IV-4, and Fig. IV-5. Since the influence surface for column axial load is assumed independent of the building frames, the results in those figures is suitable

for any frame. The 99% maximum lifetime load is shown in Fig. IV-6 and the design load of different probabilities is plotted in Fig. IV-7.

IV-4b: EUDL for Beam Moment

The influence line for the moment at mid-span RS (Fig. II-11) was constructed by STRUDL II. The joint rotations of the nine most influential spans are tabulated in Table IV-1

Table IV-1 Joint Rotation for the Influence Line
at Mid-span RS

| Joint | Rotation |
|-------|----------|
| J | 0.00183 |
| K | -0.01003 |
| L | 0.01002 |
| M | -0.00186 |
| Q | -0.00419 |
| R | 0.0495 |
| S | -0.0495 |
| T | 0.00409 |
| X | 0.00126 |
| Y | -0.00831 |
| Z | 0.00831 |
| a | -0.00127 |

(The joint displacements are of small order and neglected). The means and the variances of the load effect are tabulated in Table IV-2. It is apparent that the contribution from span RS dominates. Let us check the assumption made in Section II-5c that $F(t)$ and $L_j(t)$ are almost perfectly correlated for this case. Since

$$F(t) = \sum_1^n L_i(t) = \sum_{\substack{i=1 \\ i \neq j}}^n L_i(t) + L_j(t) = (SL)_{n-1} + L_j(t)$$

$$\text{Var}[F(t)] = \text{Var}[(SL)_{n-1}] + \text{Var}[L_j(t)] +$$

$$+ 2\rho_{(SL)_{n-1}, L_j(t)} \sigma_{(SL)_{n-1}} \sigma_{L_j(t)}$$

Therefore

$$\rho_{(SL)_{n-1}, L_j(t)} = \frac{\text{Var}[F(t)] - \text{Var}[(SL)_{n-1}] - \text{Var}[L_j(t)]}{2\sigma_{(SL)_{n-1}} \sigma_{L_j(t)}} = 0.555$$

$$\rho_{F(t), L_j(t)} = \frac{\text{Var}[L_j(t)] + \rho_{(SL)_{n-1}, L_j(t)} \sigma_{(SL)_{n-1}} \sigma_{L_j(t)}}{\sigma_{F(t)} \sigma_{L_j(t)}} = 0.993$$

Its correlation coefficient is as high as .993 so the assumption made before seems justified.

The occupancy pattern is assumed different from that

Table IV-2 Means and Variances of the Moment at
Mid-span RS due to Loads on Other Spans

| Span | Mean | Variance (10 ⁵) | Total Variance (10 ⁵) |
|------|----------------|-----------------------------|-----------------------------------|
| QR | -713.3 | 1.292 | 1.292 |
| ST | -711.9 | 1.288 | 2.802 |
| KL | -266.2 | 0.173 | 3.142 |
| JK | 157.4 | 0.062 | 3.488 |
| LM | 157.7 | 0.062 | 3.846 |
| YZ | -220.6 | 0.119 | 4.241 |
| XY | 127.0 | 0.041 | 4.571 |
| Za | 127.2 | 0.041 | 4.909 |
| RS | 7649.0 | 164.9 | 201.3 |
| | <u>Σ6307.0</u> | | |

of the column load. Here, each single bay is assumed to be occupied by a different tenant. The occupancy change and the extraordinary load from any bay are assumed independent of each other. The 99% design load for combinations 1 and 2 are calculated to be 70 psf and 61 psf respectively. The 99% performance load is 32 psf.

The procedures to find the design and the performance load are the same for the moment as for the column axial load, but there are two additional problems. First, the influence lines for moments depend upon the relative stiffness of the structural frame. We can not possibly make an exhaustive examination of all different frames. Second, the EUDL depends upon the assigned loading pattern. This will be discussed later.

Since the moment is dominated by span RS, it will be helpful to examine the change of the design load etc. due to the change of the influence line which is caused by the change of the frame stiffness. Three different influence lines on a single span were examined (See Fig. IV-8). Beam A shows exactly the same influence line as that from the whole frame. Beam B has a more rigid end while Beam C a more flexible end. It is believed that in a real frame the influence line for span RS will lie between the above two. Means, variances, design loads and performance loads for the above three beams are calculated and tabulated in Table

IV-3. The results for different beams are surprisingly close to each other. Results from different areas are also given in Table IV-3. The same conclusion still holds, i.e., the results are very close to each other for different end conditions.

Next, compare two results; one is calculated by considering the whole frame, the other by considering only the dominating span. In the first case, we considered nine bays and each bay had its own tenant and extraordinary load. In the second case only one bay and one tenant was involved. The EUDL's for the combination 1 of the design load are 70 psf and 57 psf respectively. The difference between the two EUDL design load is due partly to the fact that we use different loading patterns for the two cases. In the first case we load all nine spans uniformly with 70 psf; it will produce the moment at mid-span of RS equal

$$70*6307/11.8 = 37400 \text{ lb-ft}$$

(Note that 6307 (sum of the mean from 9 spans) is the moment produced by a uniform 11.8 psf load (mean sustained load).) In the second case we only load span RS with 57 psf which will produce moment at mid-span equal

$$57*7649/11.8 = 37000 \text{ lb-ft}$$

Table IV-3 EUDL for the Moment at Mid-span due to Different End Rotations

| $\ell = 15 \quad A = 900$ | | | | | | |
|----------------------------|--------|--------------------|--------------|--------------------|---------------|-------------------------|
| Beam | Mean | Variance(10^7) | c.o.v (%) | Design Load (EUDL) | | Performance Load (EUDL) |
| | | | | Combination 1 | Combination 2 | |
| A | 7649.3 | 1.649 | 53 | 57 | 53 | 31 |
| B | 6330.2 | 1.176 | 54 | 59 | 54 | 31.5 |
| C | 8987.4 | 2.215 | 52.5 | 56 | 52 | 31 |
| $\ell = 10 \quad A = 400$ | | | | | | |
| A | 2269.0 | 0.2195 | 65.3 | 80 | 77 | 36.5 |
| B | 1875.6 | 0.1576 | 66.9 | 83 | 80 | 37.5 |
| C | 2662.9 | 0.2924 | 64.2 | 78 | 74 | 36 |
| $\ell = 20 \quad A = 1600$ | | | | | | |
| A | 18152 | 7.406 | 47.4 | 48 | 43 | 28.5 |
| B | 15005 | 5.222 | 48.2 | 49 | 44 | 29.0 |
| C | 21303 | 9.993 | 47 | 47 | 42 | 28.5 |

After translating from EUDL to the load effect, we find that two different considerations give almost the same results. Therefore we can draw the conclusion that in order to find the design load and the performance load for the mid-span moment, only the dominating span need be considered. The corresponding EUDL will depend upon the assumed loading pattern.

As discussed in the previous paragraph the fixed end beam (Beam B in Fig. IV-8) will produce about the same design load etc. as the other two beams. Since Beam B gives about the same results as the whole frame, we can conclude that the design load and the performance load for the mid-span moment of any beam in a structural frame is approximately the same as that of a fixed end beam with the same span and area.

An influence line is also constructed for the mid-span moment on the exterior span TU (Fig. II-11). Only six spans are considered in this case and the results are tabulated in Table IV-4. The design loads are 67 psf and 58 psf for combination 1 and 2 respectively. The performance load is 31 psf. The load effect produced by 67 psf is

$$67 * 6774 / 11.8 = 38400 \text{ lb-ft}$$

which is about the same as before.

In all three cases discussed above, the interior span, the exterior span and a single span fixed end beam, we got

Table IV-4 Means and Variances of the Moment at
Mid-span TU due to Loads on Other Spans

| Span | Mean | Variance (10^5) | Total Variance (10^5) |
|------|----------------|---------------------|---------------------------|
| TU | 7816.0 | 175.2 | 175.2 |
| ST | -725.7 | 1.334 | 179.0 |
| MN | -339.9 | 0.283 | 184.7 |
| LM | 167.9 | 0.071 | 185.6 |
| Za | 132.7 | 0.044 | 186.4 |
| ab | -276.6 | 0.187 | 191.2 |
| | <u>Σ6774.0</u> | | |

the same load effect (mid-span moment) for design, but its EUDL is different due to the loading pattern we chose, i.e., apply the uniform load to all spans or to one span. If we define a different loading pattern in which case we only apply the uniform load to the beam in consideration, then the EUDL will be a function of the span length only and independent of the frame. Even though this is not the traditionally used loading pattern, yet it has the advantage that the EUDL derived from it is independent of the location of the beam. Other loading patterns such as checkerboard or uniform pattern will produce different EUDL for interior span than exterior span. The design load and the performance load under the specified load pattern is given in Fig. IV-9 for different areas.

For negative moment at the end of the beam, the influence from an adjacent span becomes important. Following the conclusion from previous paragraph we can use a two-span fixed-end, continuous beam (Fig. IV-10) to find the design load and the performance load for the negative moment. Results for different areas are plotted in Fig. IV-11.

IV-4c: EUDL for Shear in Beams

The design load, the performance load and the total load effect for shear are computed for four different locations on a beam (Fig. IV-12). The results are tabulated in

Table V-5. As can be expected, the mean load effect decreases to zero as the location moves closer to mid-span. The corresponding c.o.v. and EUDL increase. When the mean load effect becomes zero, both c.o.v. and EUDL approach infinity. The total load effect to be designed for, however, is decreasing with the mean load effect; it does not approach zero, of course, because the variance of the load effect is not zero. The assumed loading pattern, i.e. the entire span loaded uniformly, is apparently not suitable for this case because the EUDL will approach infinity. A different loading pattern has to be developed. (It may not be in EUDL form.) Since the total design load effect can be calculated, the artificial EUDL can easily be obtained once the loading pattern is decided upon.

Table IV-5 Design Load and Performance Load for Shear
at Different Locations on a Beam

| | Mean | Variance (10 ⁵) | c.o.v. (%) | Design Load EUDL (Total Load Effect) | | Performance Load EUDL (Total Load Effect) |
|--------|--------|--------------------------------|---------------|--------------------------------------|-----------------------|--|
| | | | | Combination 1 | Combination 2 | |
| Beam A | 0 | 1.52 | ∞ | ∞ (2295 lb.) | ∞ (2070 lb.) | ∞ (900 lb.) |
| Beam B | 986.1 | 4.11 | 65.0 | 78 psf (6510 lb.) | 75 psf (6270 lb.) | 38 psf (3180 lb.) |
| Beam C | 1239.0 | 5.48 | 59.7 | 80 psf (7350 lb.) | 66 psf (6930 lb.) | 35.5 (3520 lb.) |
| Beam D | 2655.0 | 18.4 | 51.0 | 56 psf (12600 lb.) | 52 psf (11700 lb.) | 31.5 psf (7090 lb.) |

CHAPTER V

Discussion and Applications

V-0: Introduction

Due to the lack of data many parameters in previous chapters were estimated using the incomplete information available or by judgement. Their sensitivity to the final results is studied in Section V-1. The live load reduction factor is discussed in Section V-2. In many probabilistic code formats⁽¹⁾ the analysis requires the mean and the variance of the live load, which are studied in Section V-3. In Section V-4 the load concentration factor, as defined by Mitchell and Woodgate⁽³⁾ are evaluated as a check on the model. Finally the relation between coefficient of variation of the sustained load and the EUDL is discussed in Section V-5.

V-1: Sensitivity Analysis

Different parameters are analyzed below:

- (a) d : the constant in the correlation equation (Eq. II-1-8).

The square root of d is a measure of the "correlation distance". For example, if $r = \sqrt{d}$, then the correlation has decreased to $e^{-1} = 0.368$. An increase in d has the effect of increasing the area over which important local correlation exists, and thus of causing a slower decay in variance with the area. Three curves for different d values are shown in Fig. V-1.

- (b) v : the average rate of change of occupancy.

Increasing v tends to have the effect of increasing the maximum lifetime sustained load because the number of load changes during the lifetime is increased. On the contrary, the maximum extraordinary load during the (random) period associated with the maximum sustained load is likely to decrease because the expected duration of the maximum sustained load decreases. Both effects are small and compensate each other so the resulting change in the design load due to the change of v is practically negligible. This conclusion is supported by the results in Table V-1 where three different values of v are used to find the design load

Table V-1 Design Load for Different Values of v

| Area = 900 | $v = 0.125$ $v_t = 8$ | | $v = 0.1875$ $v_t = 12$ | | $v = 0.25$ $v_t = 16$ | |
|------------------------------------|--------------------------|--------------------|----------------------------|--------------------|--------------------------|--------------------|
| | Design Load (EUDL) | | Design Load (EUDL) | | Design Load (EUDL) | |
| | Combina- tion 1 | Combina- tion 2 | Combina- tion 1 | Combina- tion 2 | Combina- tion 1 | Combina- tion 2 |
| Moment Influence Surface | 60 | 55 | 60 | 55 | 61 | 55 |
| Axial Load Influence Surface | 57 | 52 | 57 | 52 | 57 | 52 |

for two different influence surfaces. (Note that the performance load is independent of v .) The same conclusion was arrived at by Heaney⁽¹⁴⁾ who found that the maximum load was insensitive to n , the total number of load changes.

(c) t : the lifetime of the building

The lifetime, t , of the building was assumed to be 64 years. Following the argument presented in the previous paragraph, it can be expected that the design load will not be sensitive to changes in t . The results, shown in Table V-2, of four different cases examined indicate that the design load does not change much when t varies.

(d) Aspect Ratio: Ratio between the length and the width.

In all previous chapters the area was treated as a square because Mitchell and Woodgate⁽³⁾ established empirically that there was no consistent relationship between the 99% probable loading intensity and the aspect ratio of the area. Its effect on the design load and the performance load will be examined here. The results for the mid-span moment and the axial load corresponding to an area of 576 ft² and 5 different aspect ratios are tabulated in Table V-3. The fact that they are almost identical lends further support to the hypothesis that the aspect ratio does not significantly influence the design load and the performance load. Therefore,

Table V-2 Design Load for Different Lifetimes of Building

Area = 900

| Axial Load Influence Surface | $v_t = 5$ $t = 40$ | $v_t = 8$ $t = 64$ | $v_t = 12$ $t = 96$ | $v_t = 16$ $t = 128$ |
|------------------------------|-----------------------|-----------------------|------------------------|-------------------------|
| Design Load Combination 1 | 55 | 57 | 58 | 59 |
| Design Load Combination 2 | 51 | 52 | 53 | 54 |

Table V-3 Mean, Variance, Design Load and Performance Load for
Different Aspect Ratios

| Aspect Ratio (length/ width) | Mean | Variance 10^6 | c.o.v % | Design Load (EUDL) | | Performance Load (EUDL) |
|------------------------------------|------|--------------------|------------|--------------------|---------------|----------------------------|
| | | | | Combination 1 | Combination 2 | |
| Moment Influence Surface | | | | | | |
| 4(48*12) | 6482 | 14.85 | 59.5 | 71 | 67 | 35.5 |
| 2.25(36*16) | 4862 | 8.613 | 60.4 | 72 | 68 | 36.0 |
| 1(24*24) | 3241 | 3.852 | 60.5 | 72 | 68 | 36.0 |
| 0.444(16*36) | 2161 | 1.653 | 59.5 | 71 | 67 | 35.5 |
| 0.25(12*48) | 1621 | 0.884 | 58.0 | 70 | 67 | 34.5 |
| Axial Load Influence Surface | | | | | | |
| 4(48*12) | 1699 | 0.9057 | 56.0 | 66 | 62 | 34.0 |
| 2.25(36*16) | 1699 | 0.9354 | 56.9 | 67 | 62 | 34.0 |
| 1(24*24) | 1699 | 0.9504 | 57.4 | 67 | 62 | 34.5 |
| 0.444(16*36) | 1699 | 0.9354 | 56.9 | 67 | 62 | 34.0 |
| 0.25(12*48) | 1699 | 0.9507 | 56.0 | 66 | 62 | 34.0 |

the use of a square area in all previous discussions seems justified.

(e) Parameters in the extraordinary load model:

There are five parameters to be determined in the extraordinary load model: m_Q , σ_Q^2 , m_R , σ_R^2 and m_M . All have the same general effect on the final design load, i.e., an increase in the value of the parameter leads to an increase in the design load. First, consider the effect of m_M , the expected number of extraordinary load cells. The assumed value of m_M is (Eq. III-3-1)

$$m_M = E[M] = \sqrt{\frac{A-164}{9}}$$

Table V-4 shows the design loads respectively corresponding to a mean value, m_M , of one half and twice the value given by the above expression. It is apparent that m_M does change the design load. Its influence on small areas is larger than those on large areas.

A change in the mean and the variance of the total load of a load cell has the same effect as that of m_M . This is checked by increasing the value of m_Q and σ_Q^2 simultaneously (increase the value of m_R and σ_R^2 can achieve the same effect). The results are tabulated in Table V-5. It is important to note that the load due to combination 2 controls when the

area is small but the load due to combination 1 controls when the area becomes larger.

Table V-4 Design Load for Different Expected Load Cells

| Axial Load Influence Surface | Area | Design Load (EUDL) | |
|---|------|--------------------|---------------|
| | | Combination 1 | Combination 2 |
| $E[M] = \sqrt{\frac{A-164}{9}}$ | 200 | 99 | 97 |
| | 900 | 57 | 52 |
| | 2500 | 43 | 38 |
| $E[M] = \frac{1}{2} \sqrt{\frac{A-164}{9}}$ | 200 | 88 | 84 |
| | 900 | 50 | 45 |
| | 2500 | 40 | 35 |
| $E[M] = 2 \sqrt{\frac{A-164}{9}}$ | 200 | 117 | 116 |
| | 900 | 68 | 64 |
| | 2500 | 49 | 45 |

Table V-5 Design Load for Different Mean and Variance of a Load Cell

| | Area | Design Load (EUDL) | |
|------------------------------|------|--------------------|---------------|
| | | Combination 1 | Combination 2 |
| Axial Load Influence Surface | | | |
| mQ=145 $\sigma_Q^2=900$ | 200 | 99 | 97 |
| | 900 | 57 | 52 |
| | 1600 | 48 | 43 |
| | 2500 | 43 | 38 |
| mQ=290 $\sigma_Q^2=22500$ | 200 | 160 | 174 |
| | 900 | 80 | 80 |
| | 1600 | 62 | 60 |
| | 2500 | 53 | 50 |
| Moment Influence Surface | | | |
| mQ=145 $\sigma_Q^2=900$ | 200 | 109 | 108 |
| | 900 | 60 | 55 |
| | 1600 | 49 | 44 |
| | 2500 | 44 | 39 |
| mQ=290 $\sigma_Q^2=22500$ | 200 | 178 | 199 |
| | 900 | 86 | 87 |
| | 1600 | 70 | 69 |
| | 2500 | 56 | 53 |

V-2: Live Load Reduction Factor

Traditionally the live load reduction factor is a function of the total area only⁽⁵⁾. However this rule is not confirmed by the results found in the previous chapter. As shown in Fig. IV-3 the load for $A = 200$ and $n=2$ is not equal to that corresponding to $A=400$ and $n=1$. The respective values are 74 psf and 77.5 psf. Similar results are observed for the pair of values $A = 400$ and $n = 4$ and $A = 1600$ and $n = 1$ respectively; two values are 43.5 psf and 48 psf. It appears that the reduction factor is not a function of a single variable, nA , but of two variables, n and A . The design load will decrease with one variable if the other is kept constant. Unfortunately, no simple formula can be found for the live load reduction factor, but one might adopt a conservative approximation if the need for a simple code formula demands it.

V-3: Means and Variances of Design Load

As discussed in Section II-5b the derivation of the maximum sustained load is exact only when the load is high because it only yields the upper tail of the CDF exactly. The complete CDF of the design load cannot be obtained. Of course, there is no way of finding the mean and the variance of a random variable when only the tail portion of the CDF curve is known. The procedure adopted here is to (i) assume the form of the probability distribution of the design load, (ii) determine its parameters by fitting the upper tail, and (iii) derive the mean and the variance. For example, assume that the design load follows Type II Extreme Value distribution⁽²⁵⁾. The 98% and 99% design loads for $A = 200$ are 90.5 psf and 100 psf respectively. The mean and the variance derived from the above values are 55.6 and 153.2 respectively. If, in a probabilistic code, the load used, $m + \beta\sigma$, corresponds closely to the 98% or 99% probability level, then the accuracy would be fairly good. In fact, once the value of β (in $m + \beta\sigma$) is determined in the code, the assumed probability distribution should be so chosen that its $m + \beta\sigma$ falls between 98% and 99% probability level. The mean and the variance corresponding to other areas are plotted in Fig. V-2, again for the Type II Extreme Value distribution.

V-4: Load Concentration Factor

The load concentration factor is defined by Mitchell and Woodgate⁽³⁾ as the ratio between two load effects (corresponding to a given probability level): one is caused by the concentrated loads as they are observed at the time of the load survey, the other by the spatially averaged load. It will be checked in this section how the load concentration factors obtained using the load model (Eq. II-1-1) compare with those observed by Mitchell and Woodgate⁽³⁾.

Due to difficulties encountered in determining and evaluating influence surfaces, only one simple case will be considered, i.e., the slab center moment, M_x of a simply supported flat slab. The influence surface is⁽²¹⁾

$$I(x,y) = \frac{4}{\pi^2} \sum_m \sum_n \frac{\sin \frac{m\pi x}{a} \sin \frac{n\pi y}{a}}{(m^2+n^2)^2} \sin \frac{m\pi}{2} \sin \frac{n\pi}{2} (m^2 + \nu n^2)$$

where ν is the Poisson ratio for the concrete (equal to 0.18).

The mean and the variance can be calculated from Eq.

(II-5-27) and Eq. (II-5-28). To find the load effect corresponding to any probability level we also need the probability distribution. The results given here are based on the assumption that the load effect is gamma distributed. Thus we find the first load effect as discussed in the previous paragraph by the load model. The second load

effect is simply the product of the unit load for any probability level and v_I , the volume enclosed by the influence surface. The ratio of the above two is the load concentration factor.

The results from the above load model and from Mitchell and Woodgate⁽³⁾ are tabulated in V-6. Both results show the same trend, i.e., the load effect will increase when the randomness of the loading is explicitly considered. There are, however, some differences in the percentage of the increase. It will be discussed below.

The distribution of the unit load (or total load) was assumed gamma in section II-4 and was confirmed by Mitchell and Woodgate's data. The distribution of the load effect is assumed gamma also because of the reasoning that the load effect might be considered as the sum of several unit loads multiplied by its influence value. Since the unit load is gamma distributed, the summation is approximately gamma. However, from the results of Table V-6 the gamma distribution predicts the results a little higher for that particular load effect at the particular probability level. Apparently more data are needed about the distribution of the load effect in order to establish its probability distribution, especially at such high levels (99.9%).

V-6 Load Concentration Factors for Slab
Center Moment, (M_x (at 99.9% Probability
Level)).

| | | | | | | |
|------------------------------------|------|------|------|------|------|------|
| Area | 56 | 151 | 336 | 624 | 1197 | 2069 |
| Results from Mitchell and Woodgate | 1.22 | 1.39 | 1.24 | 1.33 | 1.50 | 1.25 |
| Area | | 144 | | 576 | 1156 | |
| Results from Load Model | | 1.65 | | 1.5 | 1.46 | |

V-5: Coefficient of Variation (c.o.v.) of the Sustained Load versus EUDL

There is a close relation between the c.o.v. of the sustained load and the EUDL. As shown in Table IV-3 and Table V-3, when the influence surface and the extraordinary load are known, the EUDL is approximately an increasing function of the c.o.v. of the sustained load. Otherwise, as shown in Table V-5, there can be a large difference between two EUDL's though the c.o.v.'s for the sustained load are the same. This is due to the change in the contribution from the extraordinary load. For a given influence surface and the extraordinary load, the EUDL will be the same if the c.o.v. is the same.

CHAPTER VI

Conclusions and Suggestions

VI-1: Conclusions

- (1) Load models and methods to represent time and space variability of the extreme loads and sustained live loads on office buildings are presented in this work. The results include "design load" values associated with small probability of being exceeded. The models are flexible enough to handle different cases ranging from a multiple number of tenants on each of a number of floors to a single occupier of all floors. Influence surfaces are introduced to produce moments and distributions of structural load effects (e.g. axial forces, shears etc.).
- (2) Owing to observed differences in the nature of the spatial correlation vertically and horizontally, the live load reduction factor is not a function of simply the total area alone, but rather a function of both n , the number of floors, and A , the floor area. Though the difference between two cases with the same area but different combinations of n and A is not very substantial for the particular chosen values of parameters of the extraordinary load and of the occupancy pattern, it

might be expected, however, that, if future data suggest different values for the parameter and different occupancy patterns, the difference may be significant.

- (3) Comparing the design loads from two potentially critical combinations, the load obtained from Combination 2 (extraordinary load control) increases faster with the decrease of the area than that from combination 1 (maximum sustained load control). In some cases the first combination governs for larger areas and the second one governs for small areas. (These combinations are defined on page
- (4) The design load will increase with the lifetime of the building, but the magnitude of the increase is very small. Therefore a rough estimate of the economic lifetime of the building will not introduce a significant error in finding the design load.
- (5) Both the "design load" and the "performance load" are insensitive to the rate of change of occupancy and the aspect ratio of the area.
- (6) The values of the design load and performance load that might be specified in a building code are evaluated for different load effects (moment, shear and axial load) and for different areas (on the same floor or on different floors).

(7) Present load surveys (Mitchell's survey was used here) may provide information adequate to provide reasonable estimates of the parameters of the sustained and maximum sustained load and load effect models. But additional information is needed to estimate parameters and to verify the extraordinary load model. It is believed that providing a tentative model in the absence of data can provide a valuable service to engineers responsible for deciding what information should be collected in a live load survey.

VI-2: Suggestions

- (1) The correlation model (Eq. II-1-1) can be expanded to involve other effects such as the age of the building, the use of the room etc., if future data suggest that those effects are important.
- (2) More extensive work should be done to find a simple systematic way of defining the design load, the loading pattern and the load reduction factor for different load effects.
- (3) More data, to be obtained from load surveys, and improved analytical models are needed in the area of extraordinary loads.

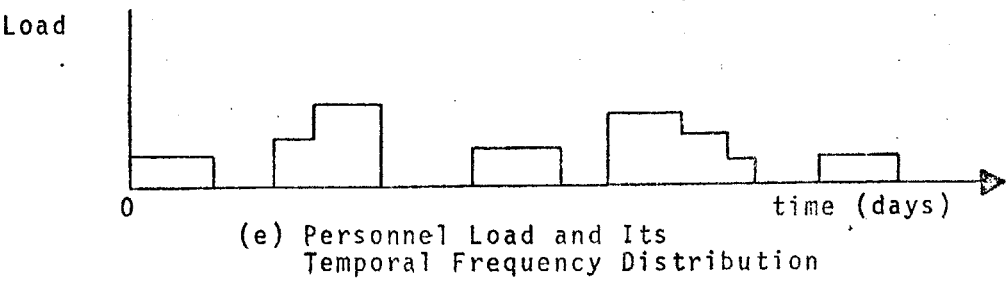
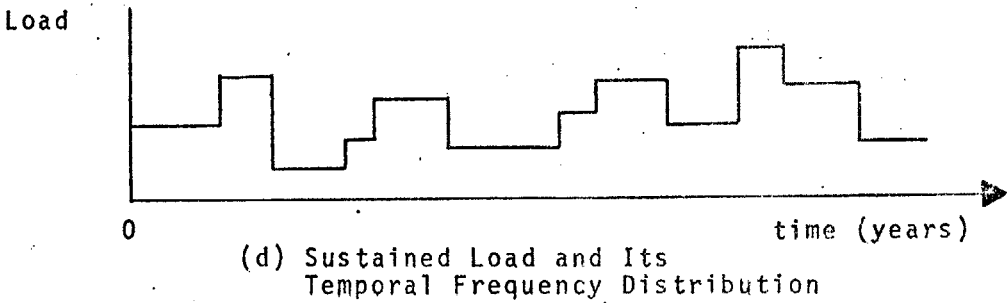
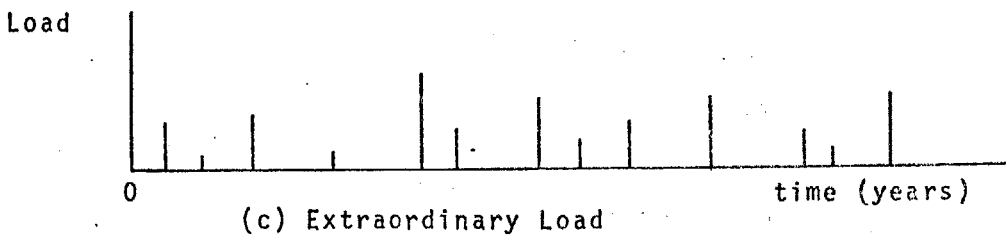
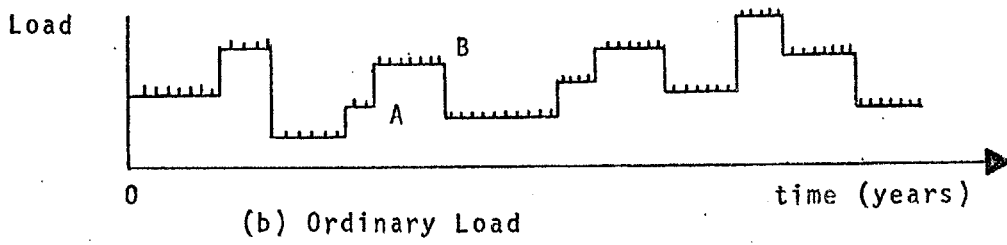
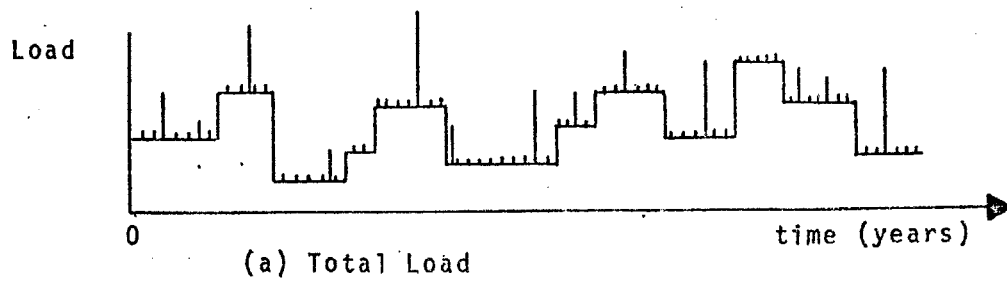


Fig. I-1 Time Histories of Live Loads

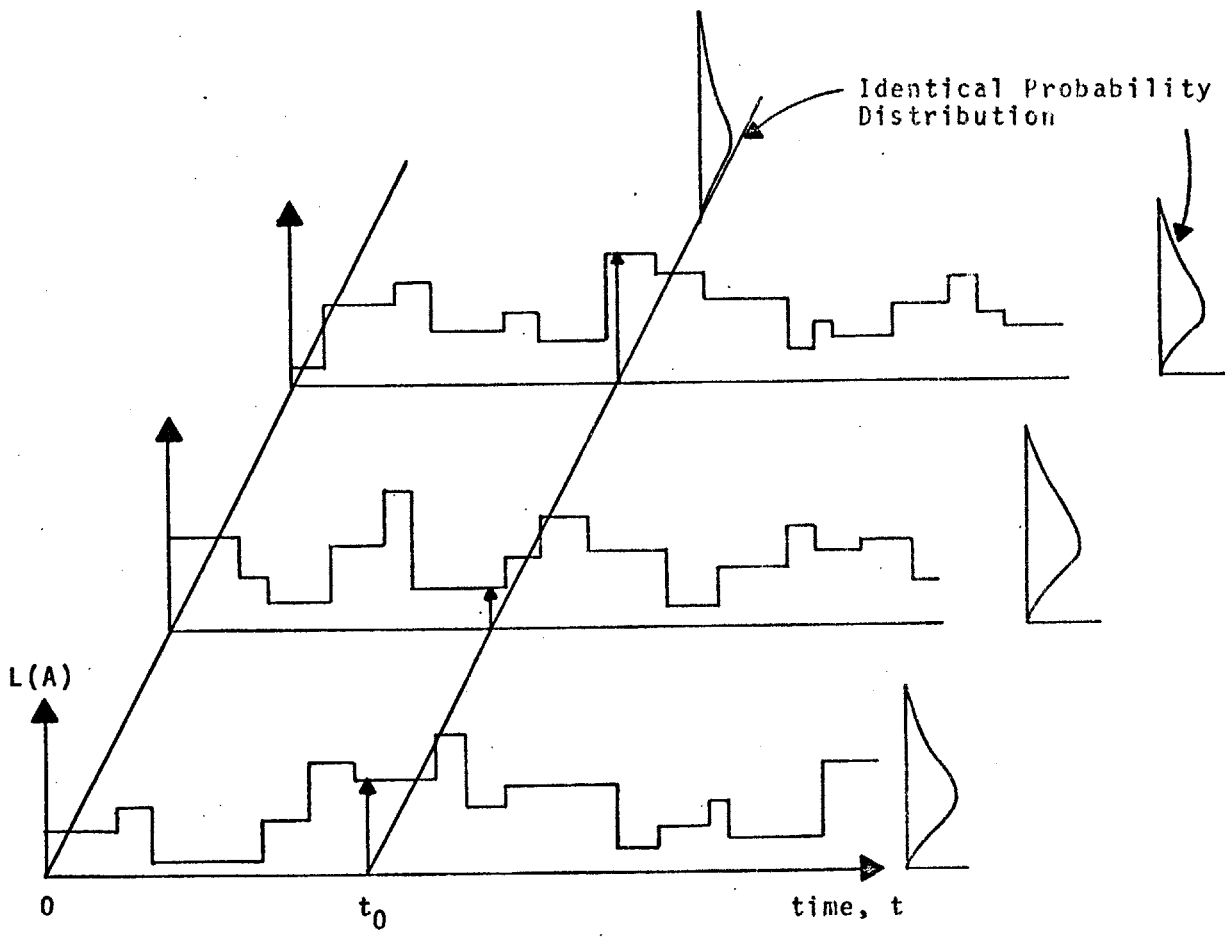


Fig. I-2 Three Different Load Histories and Its Temporal and Spatial Frequency Distribution

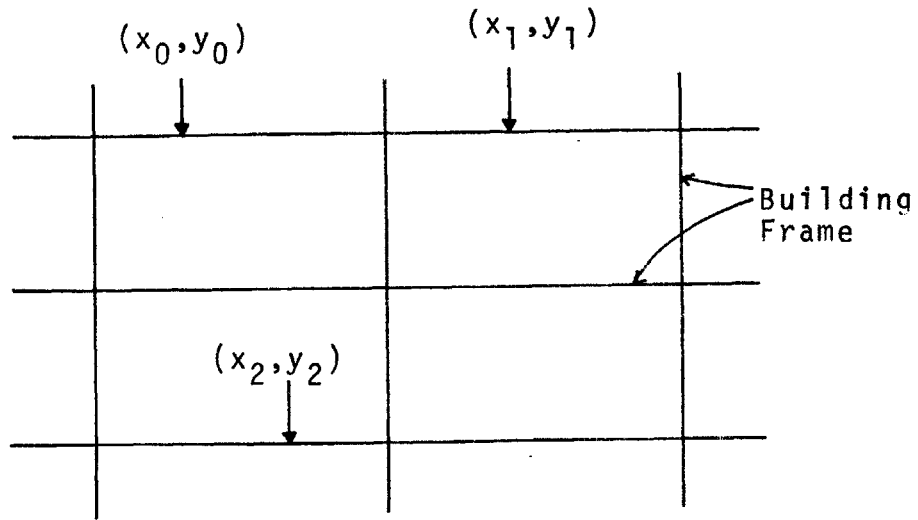


Fig. II-1 Relative Location of Loads in A Building

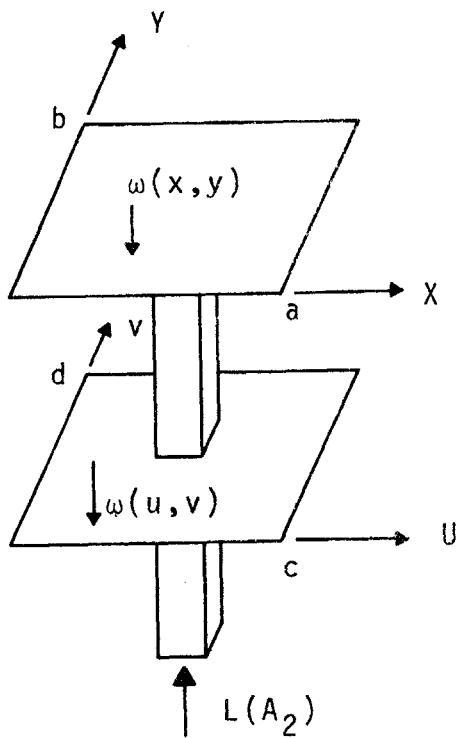


Fig. II-2 Nominal Column Load from Two Floors

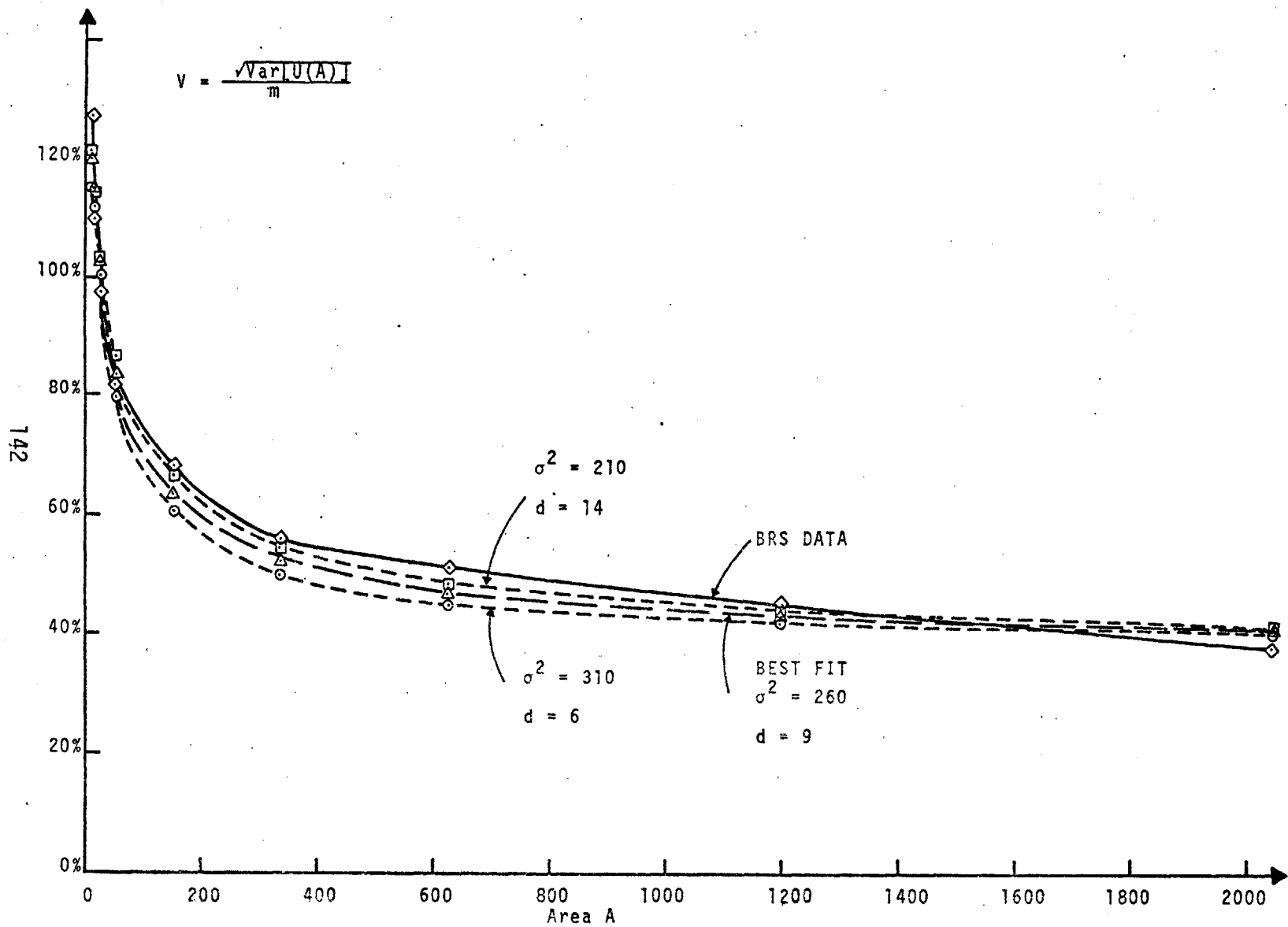


Fig. II-3 Comparison of BRS Data with Different Fittings

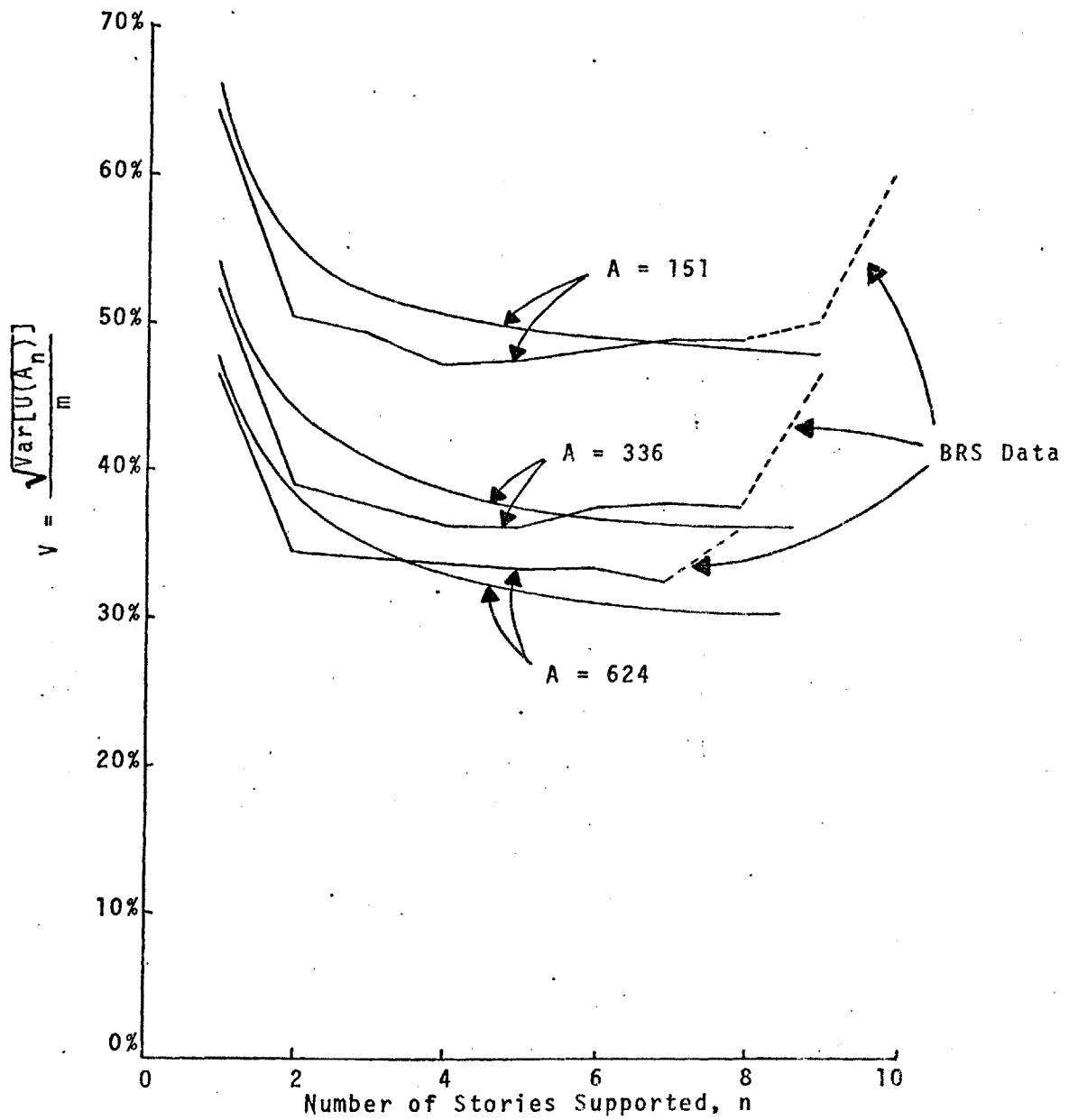


Fig. II-4 Comparison of Column Data with the Model

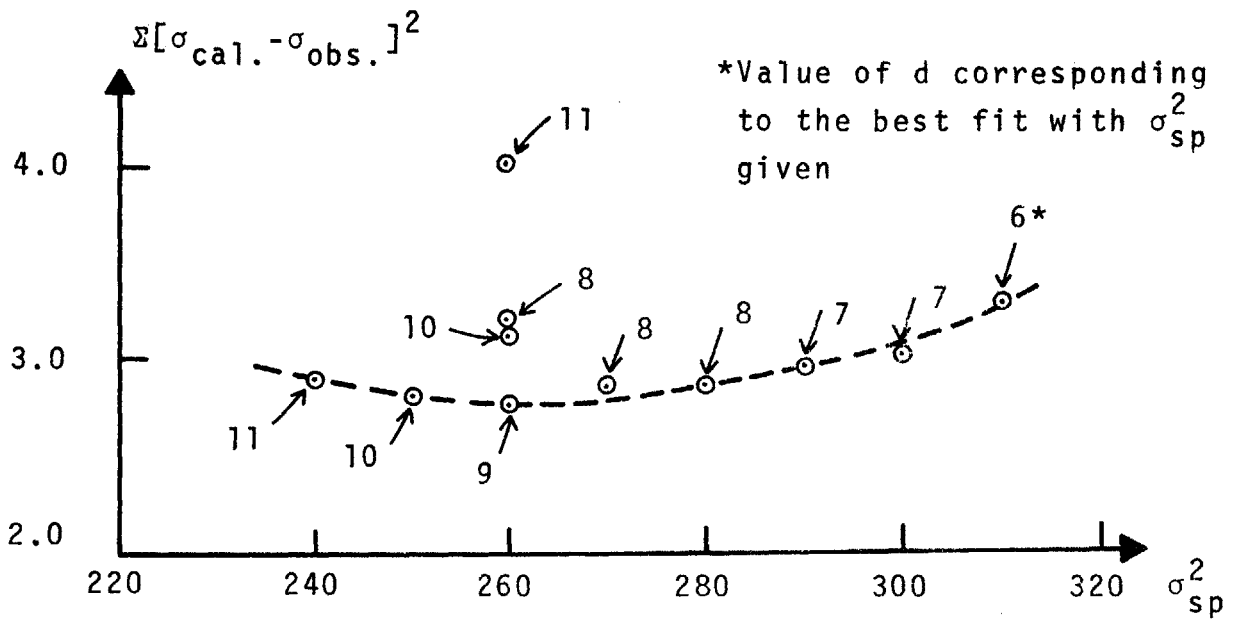


Fig. II-5 Measure of Goodness of Fit for σ_{sp}^2 and d

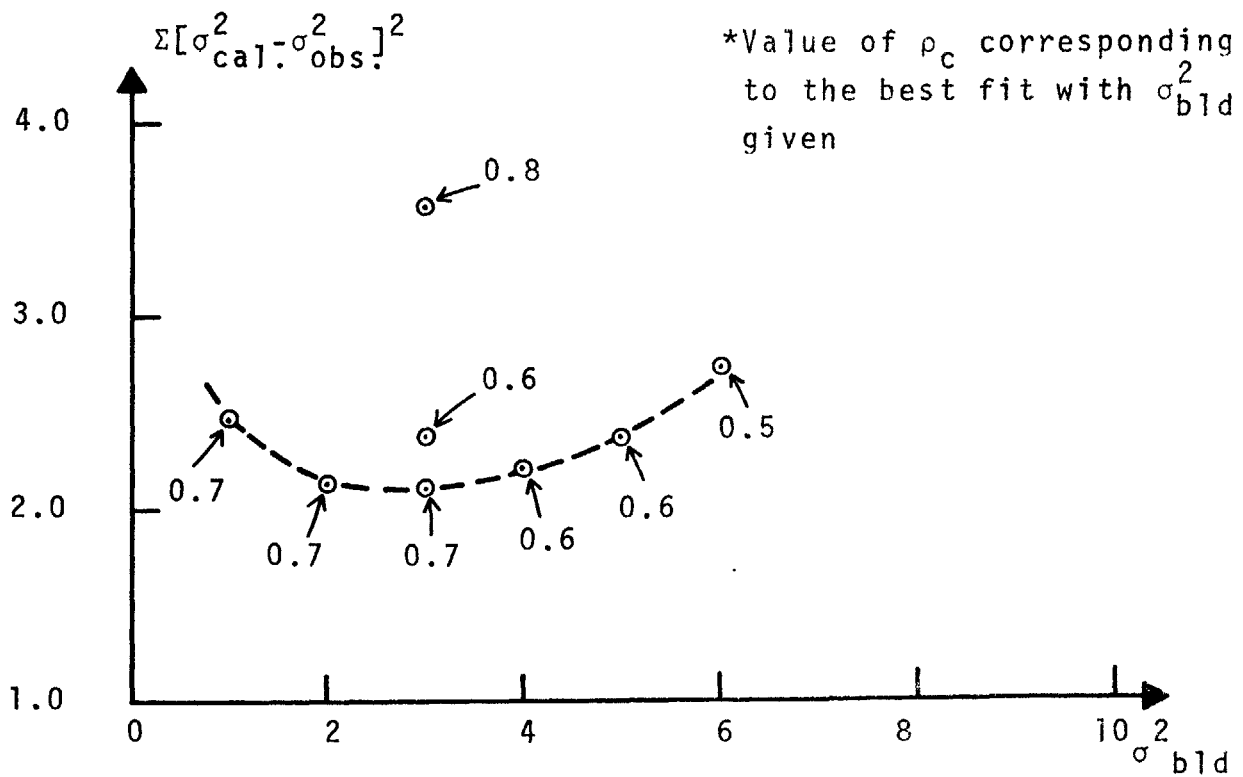


Fig. II-6 Measure of Goodness of Fit for σ_{bld}^2 and ρ_c

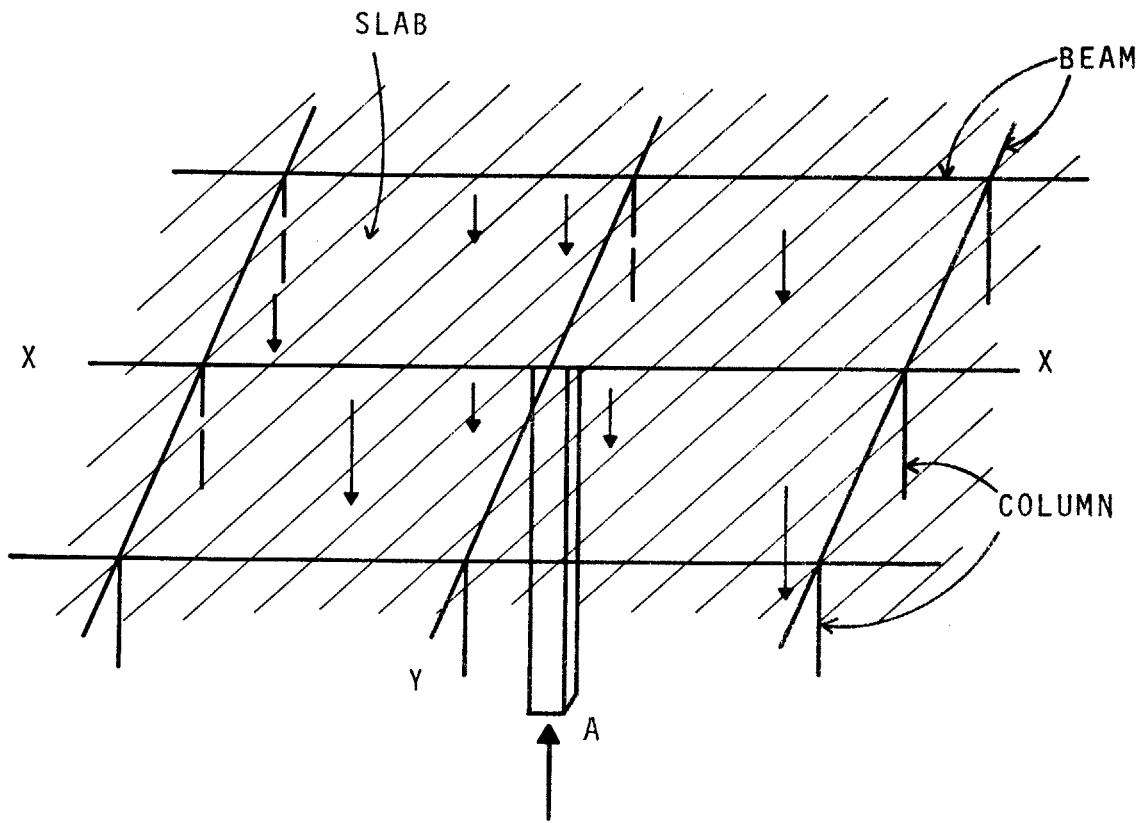


Fig. II-7 A Typical Interior Column



Fig. II-8 A Two-span Fixed End Beam



Fig. II-9 Influence Line for the Vertical Reaction of a Fixed End Beam

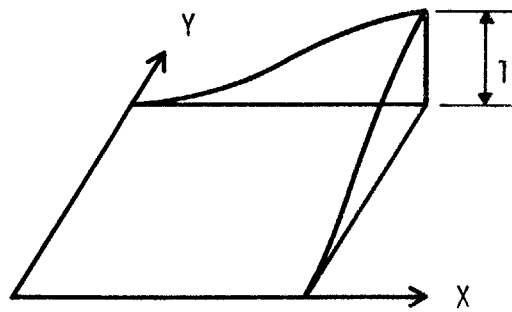
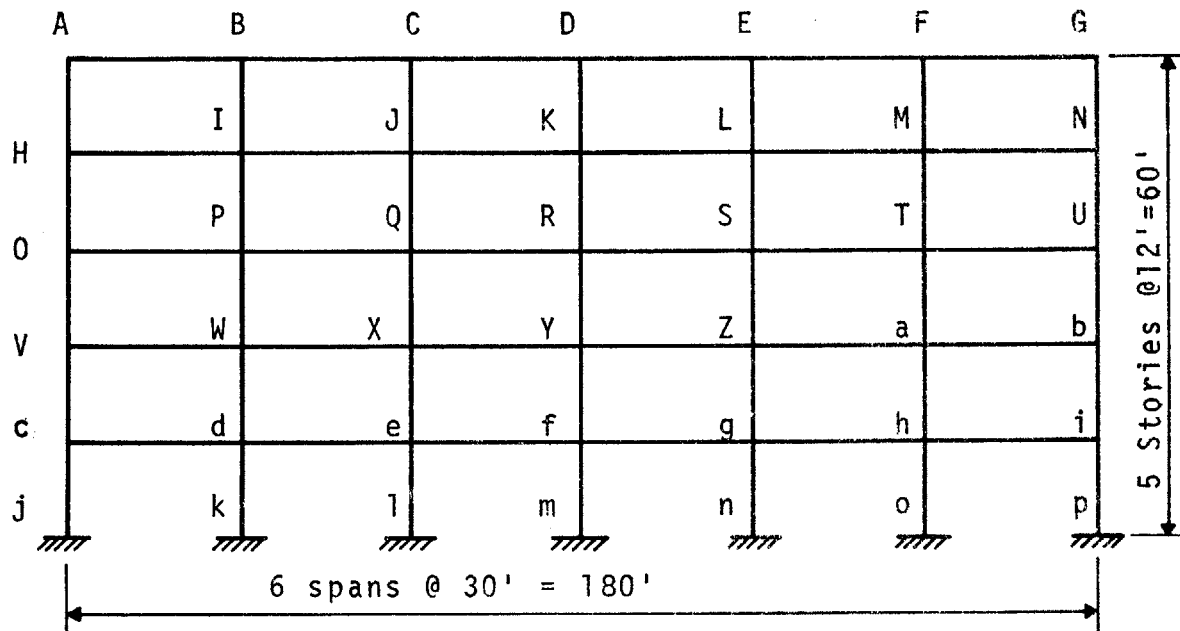


Fig. II-10 Influence Surface for the Axial Load



Members used: All beams: 21 WF 55
 Columns: 1st and 2nd story 14 WF 119
 3rd and 4th story 14 WF 84
 5th story 14 WF 74

Figure II-11 The 6 Bays and 5 Stories Frame Used for Illustration

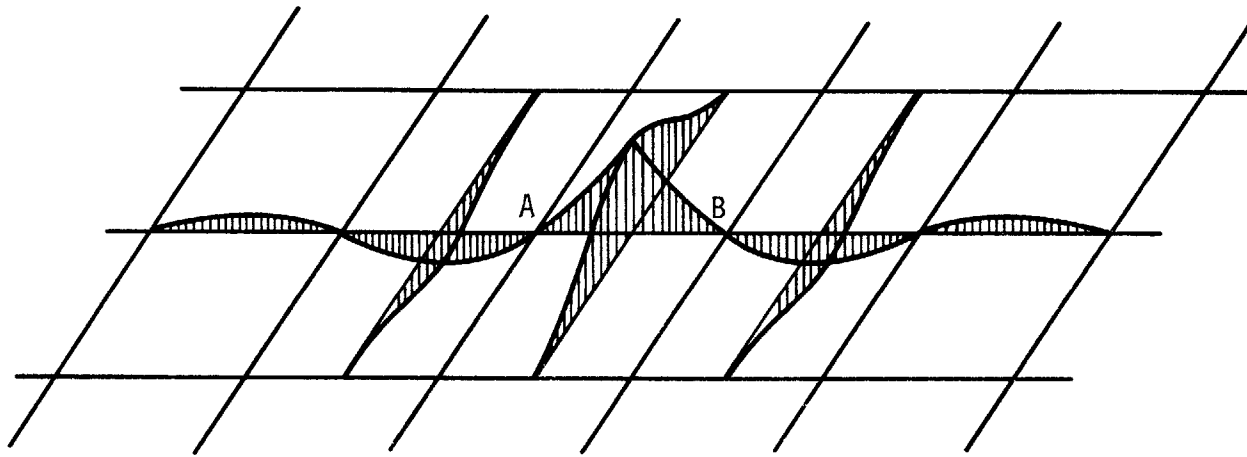


Fig. II-12 Plan View of a Floor Showing the Assumed Influence Surface

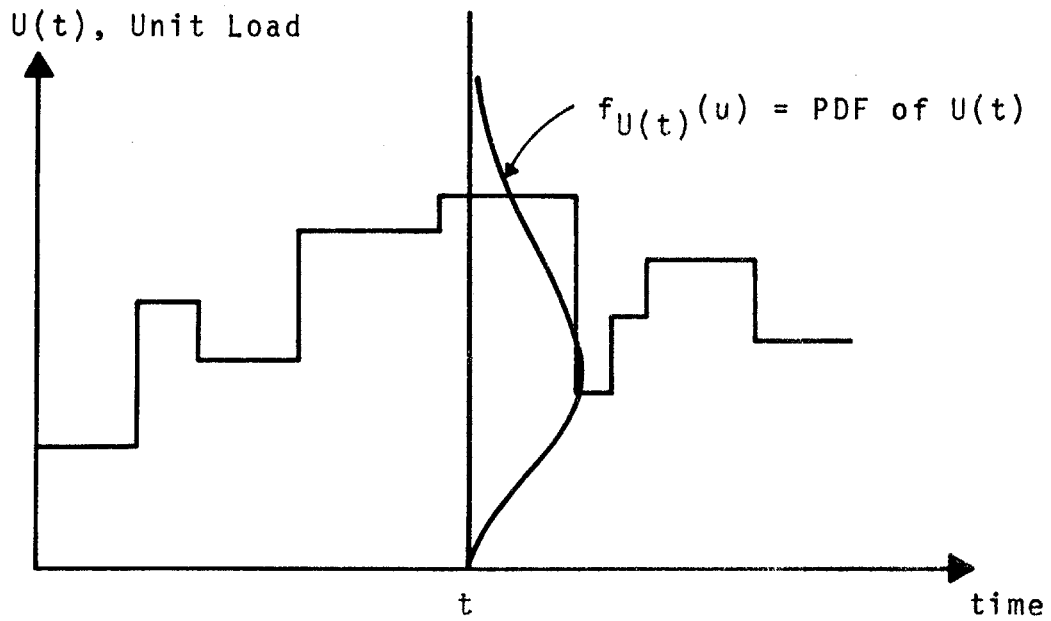


Fig. II-13 Time History and the PDF of a Unit Load

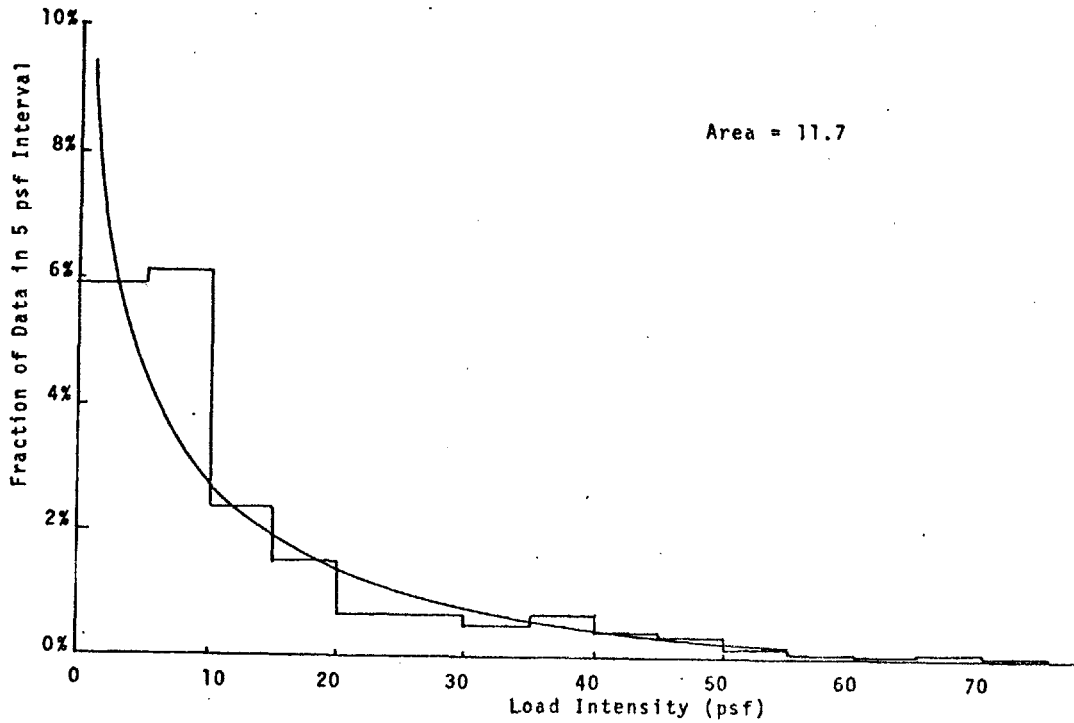


Fig. II-14a Frequency Distribution of Load Intensity and Assumed Gamma Distribution

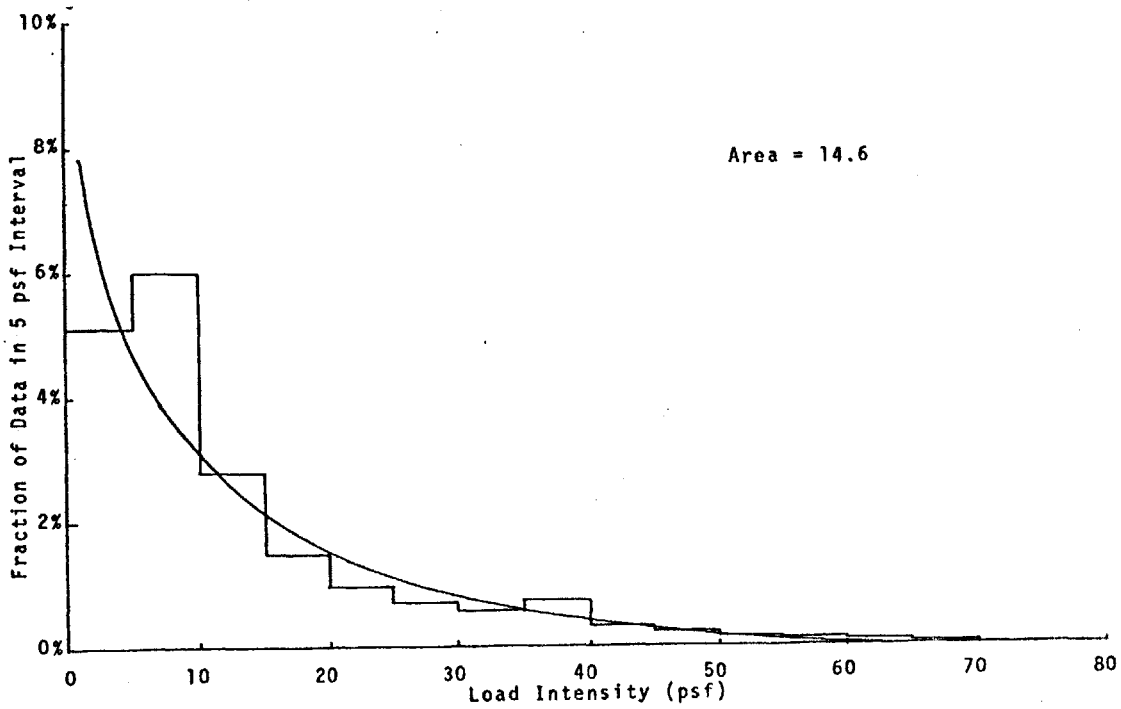


Fig. II-14b Frequency Distribution of Load Intensity and Assumed Gamma Distribution

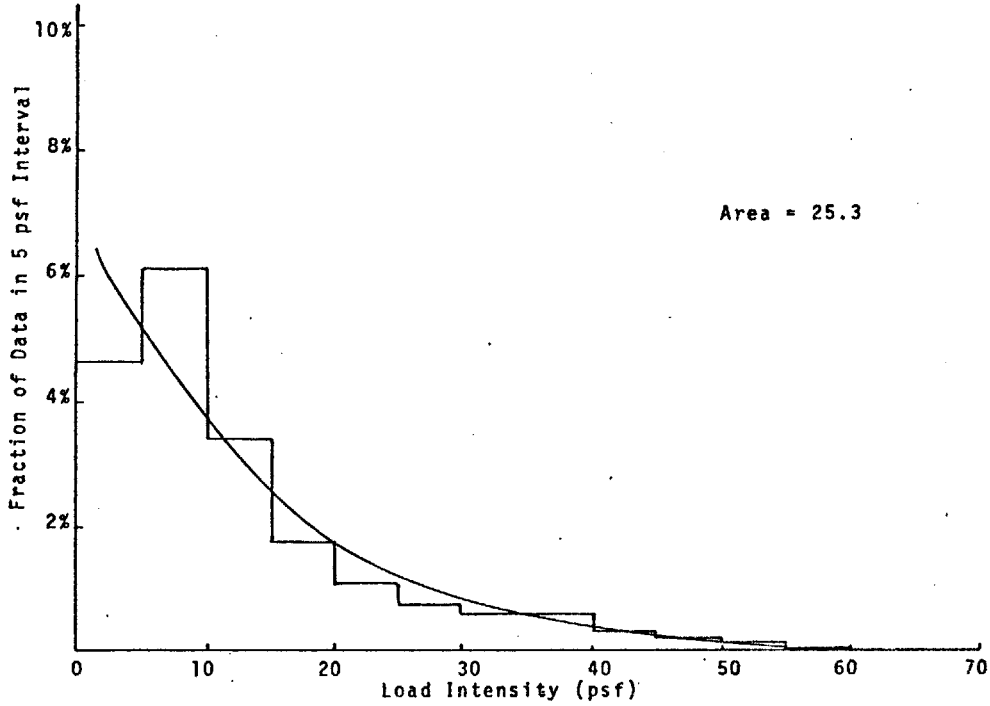


Fig. II-14c Frequency Distribution of Load Intensity and Assumed Gamma Distribution

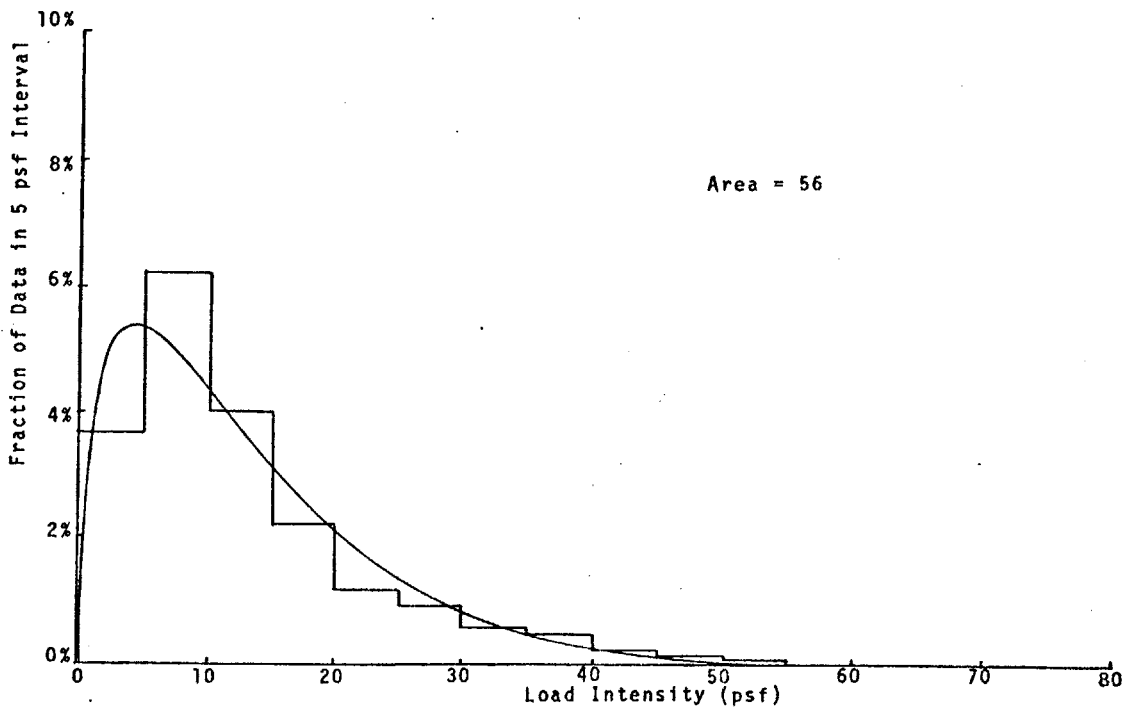


Fig. II-14d Frequency Distribution of Load Intensity and Assumed Gamma Distribution

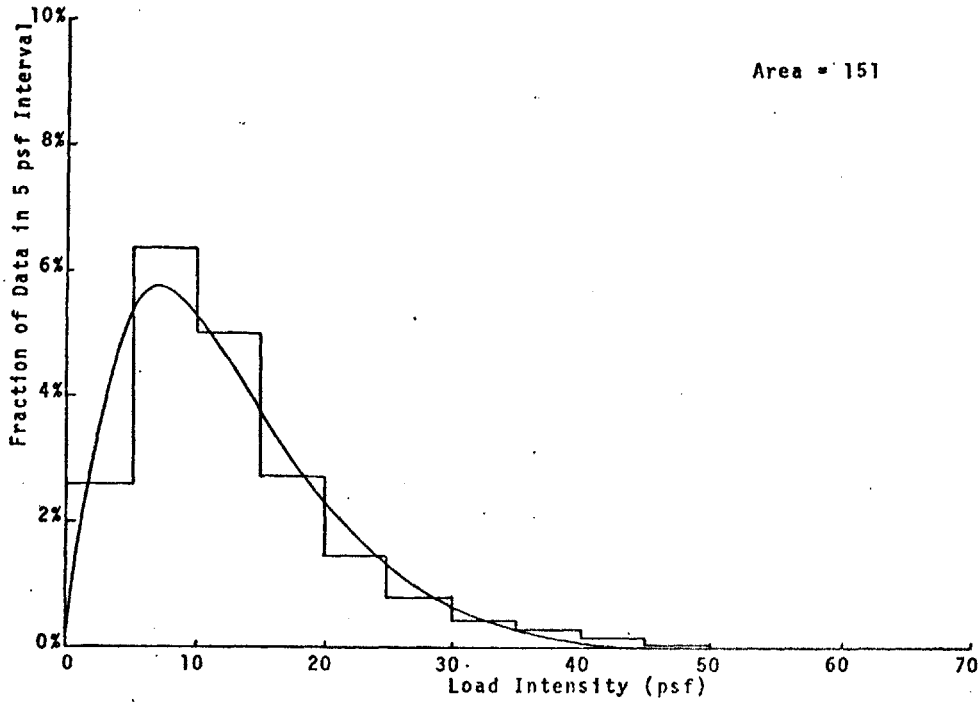


Fig. II-14e Frequency Distribution of Load Intensity and Assumed Gamma Distribution

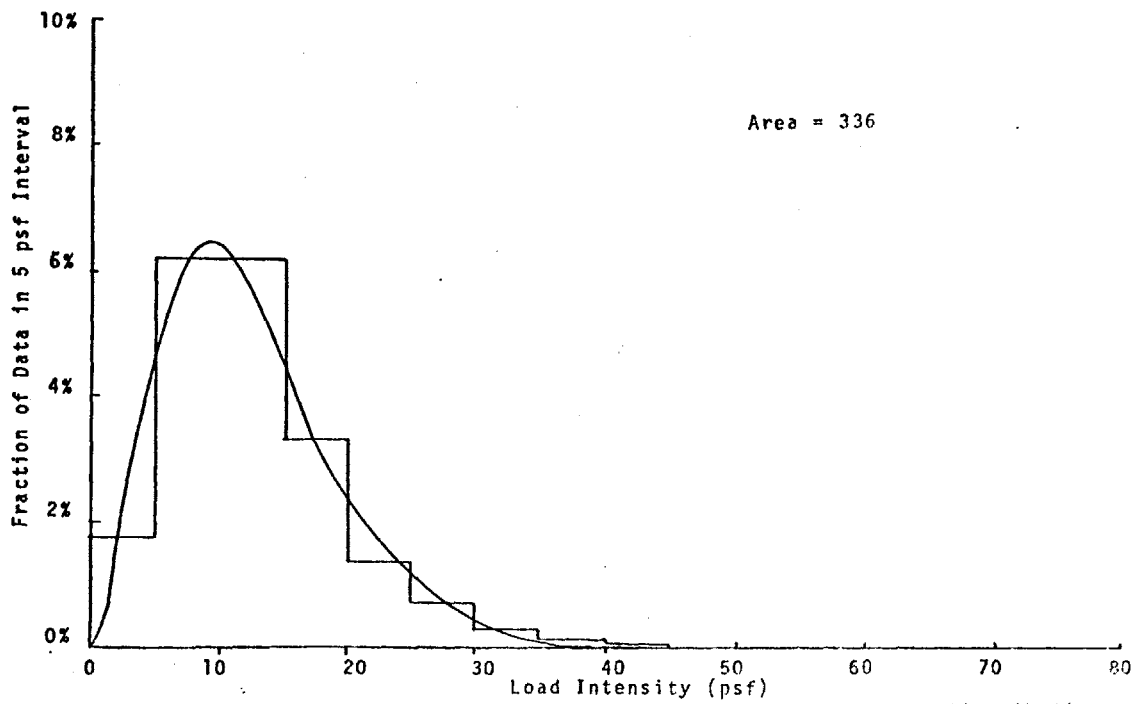


Fig. II-14f Frequency Distribution of Load Intensity and Assumed Gamma Distribution

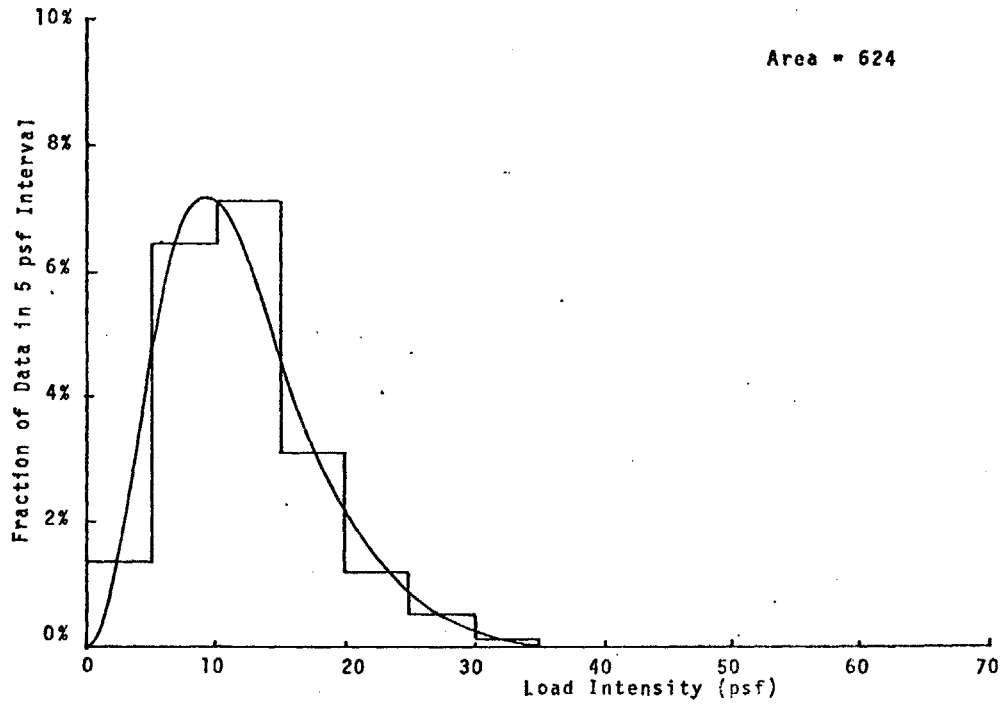


Fig. II-14g Frequency Distribution of Load Intensity and Assumed Gamma Distribution

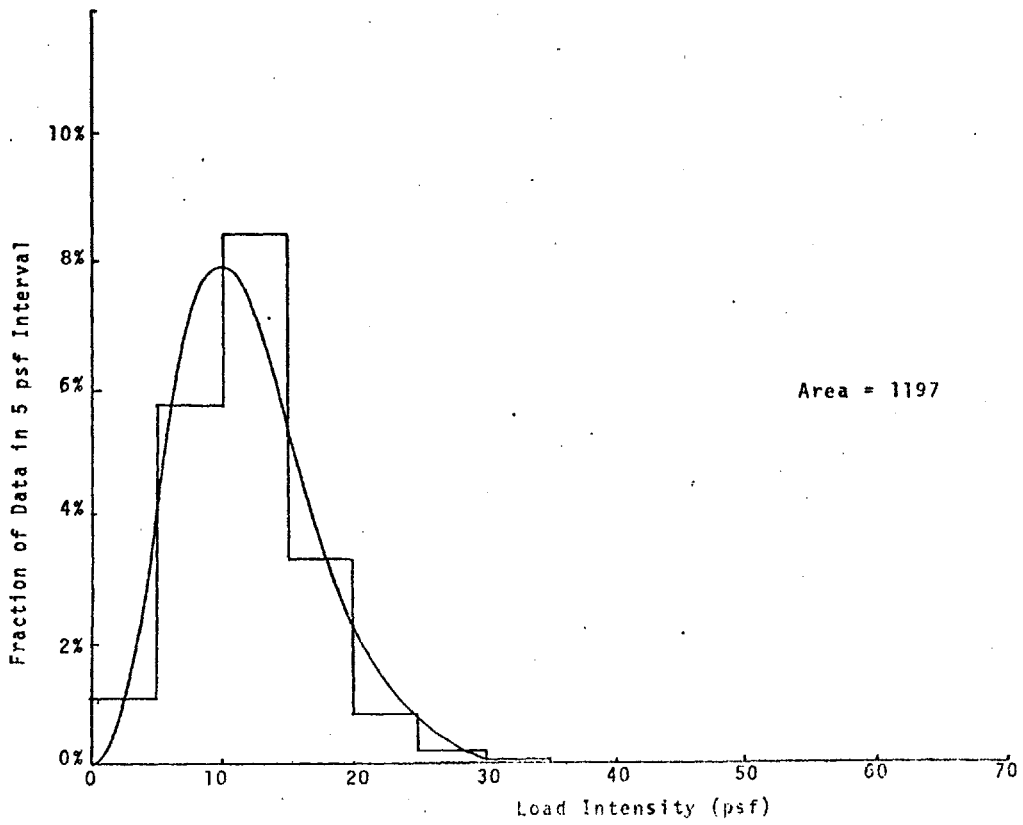


Fig. II-14h Frequency Distribution of Load Intensity and Assumed Gamma Distribution

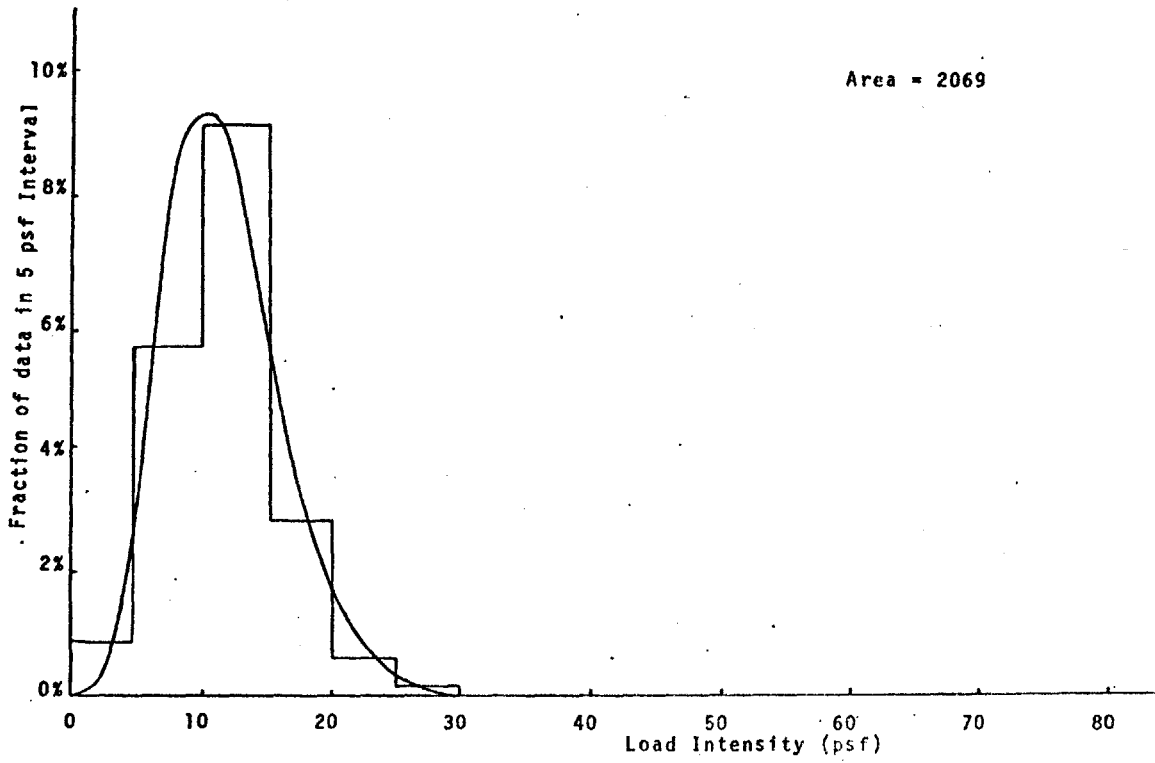


Fig. II-141 Frequency Distribution of Load Intensity and Assumed Gamma Distribution

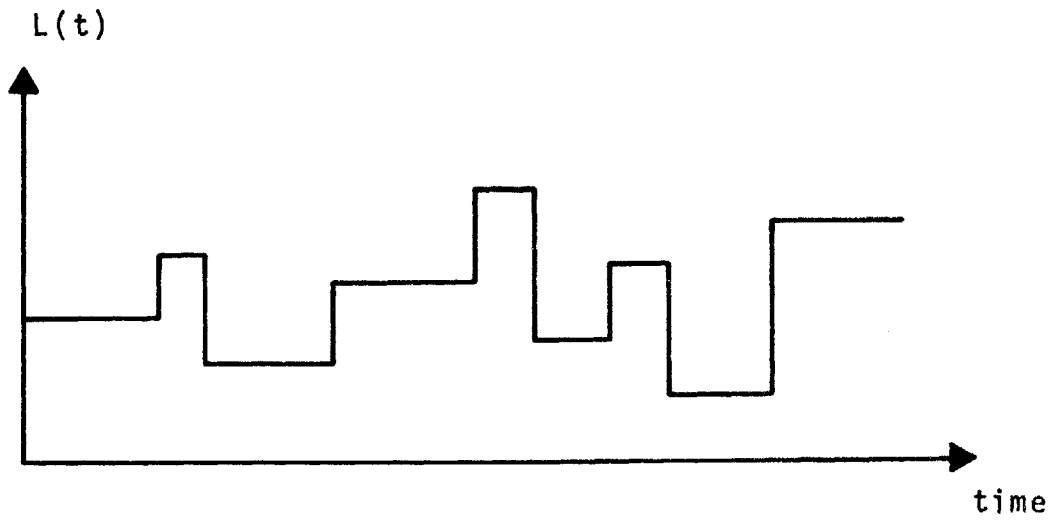


Fig. II-15 Assumed Time History of the Load

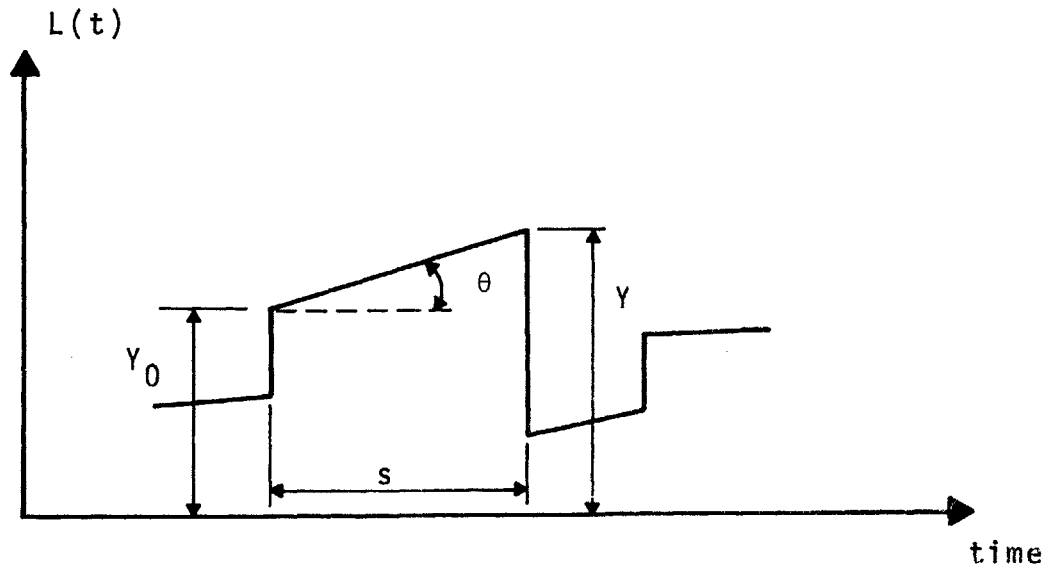


Fig. II-16 Different Time History of the Load
 (The Load Increases Linearly with Time
 between Load Changes)

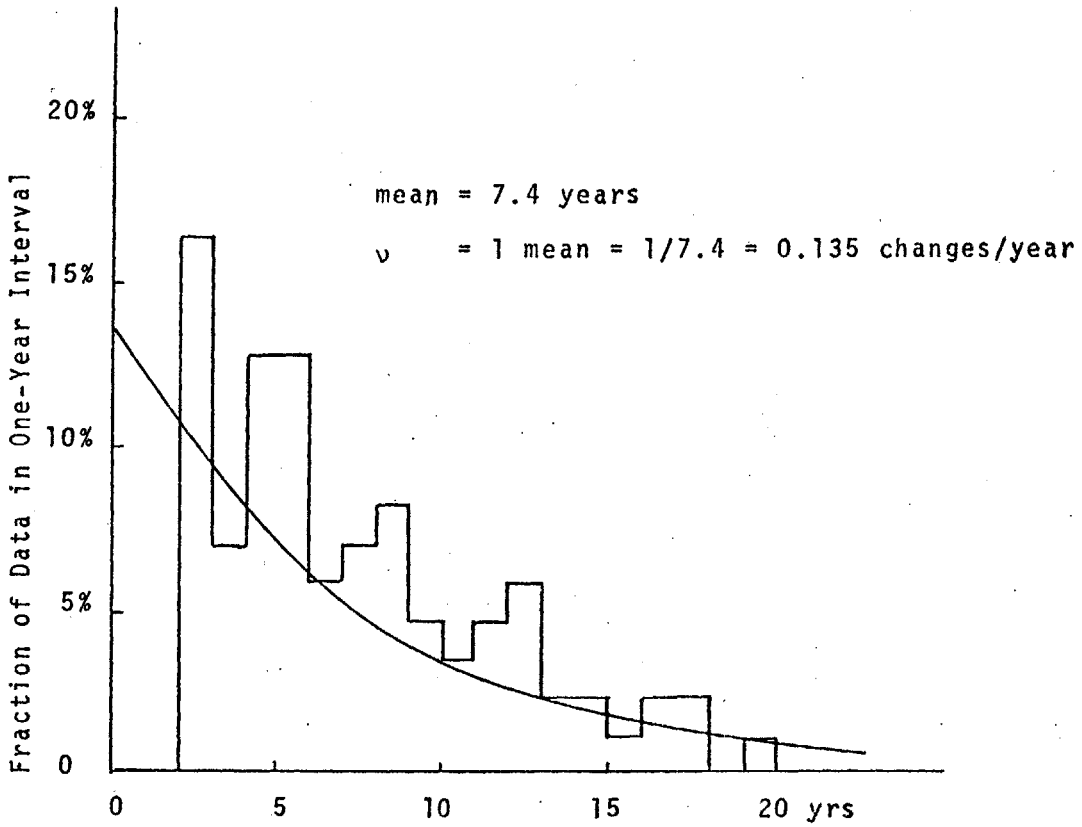


Fig. II-17 Frequency Distribution for the Time between Change in Occupancy and the Assumed Probability Distribution

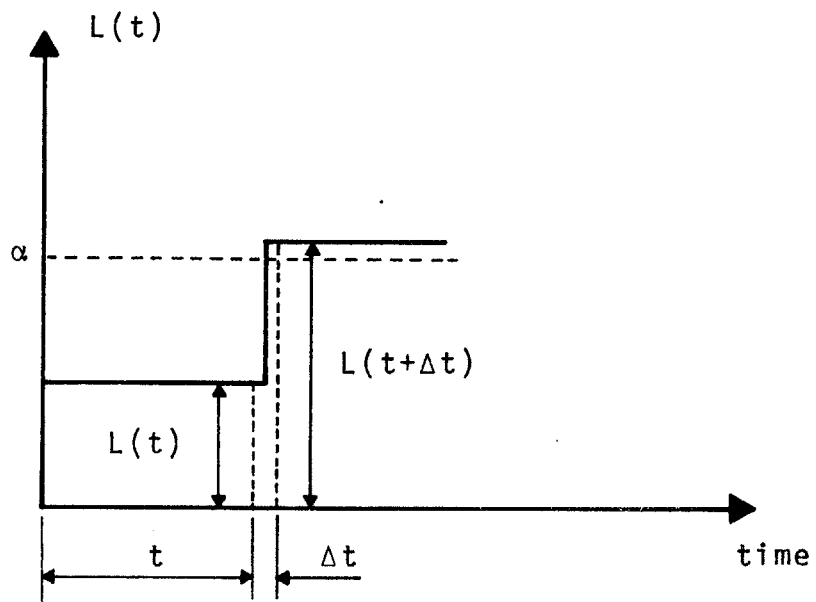
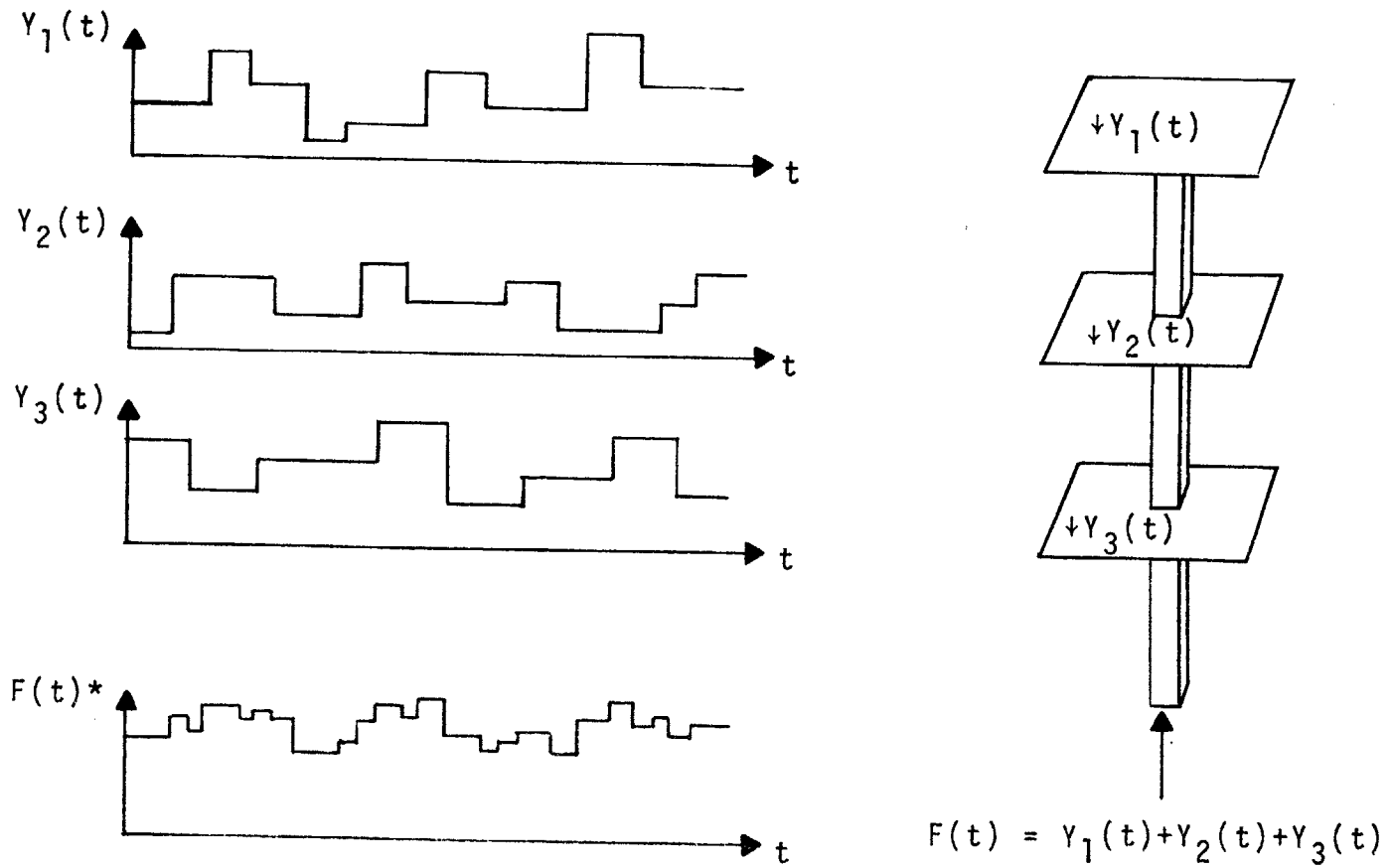


Fig. II-18 Time History of the Load Showing the Up-crossing of α Threshold



* $F(t)$ on different scale

Fig. II-19 Load Histories for Three Individual Loads and Its Summation

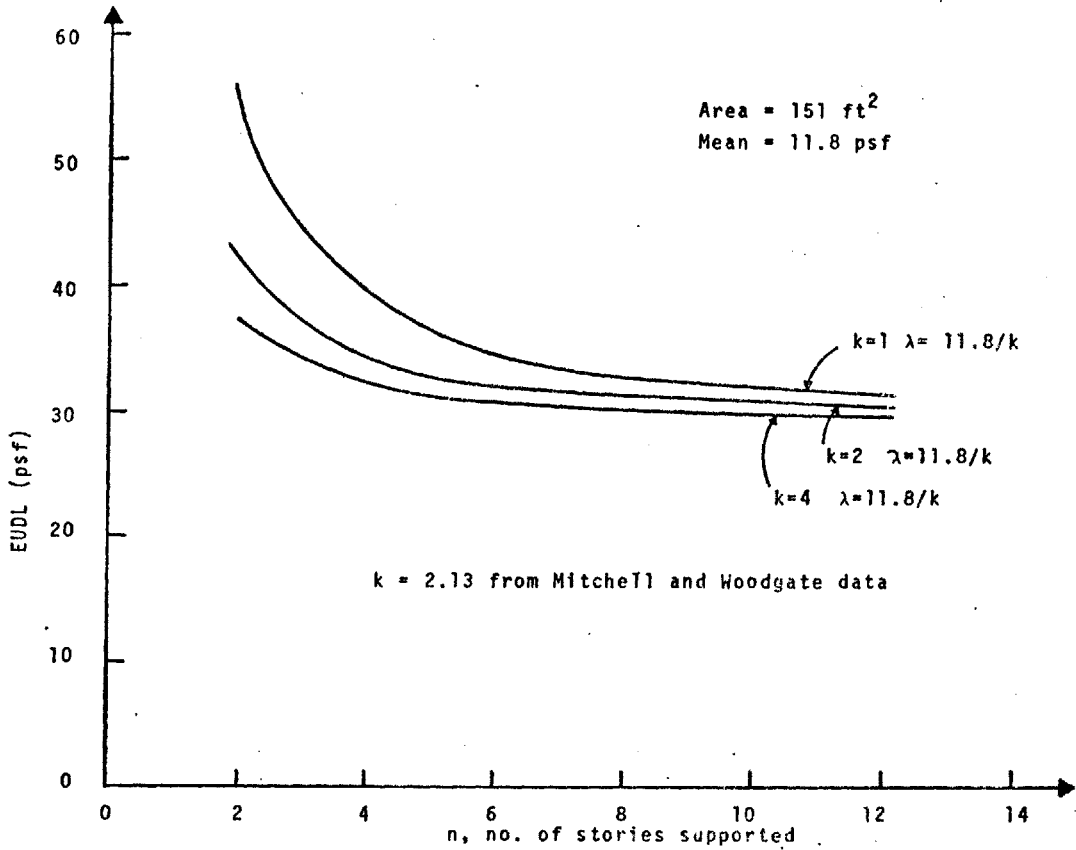


Fig. II-20 99% Maximum Lifetime Sustained Load with Different k Values

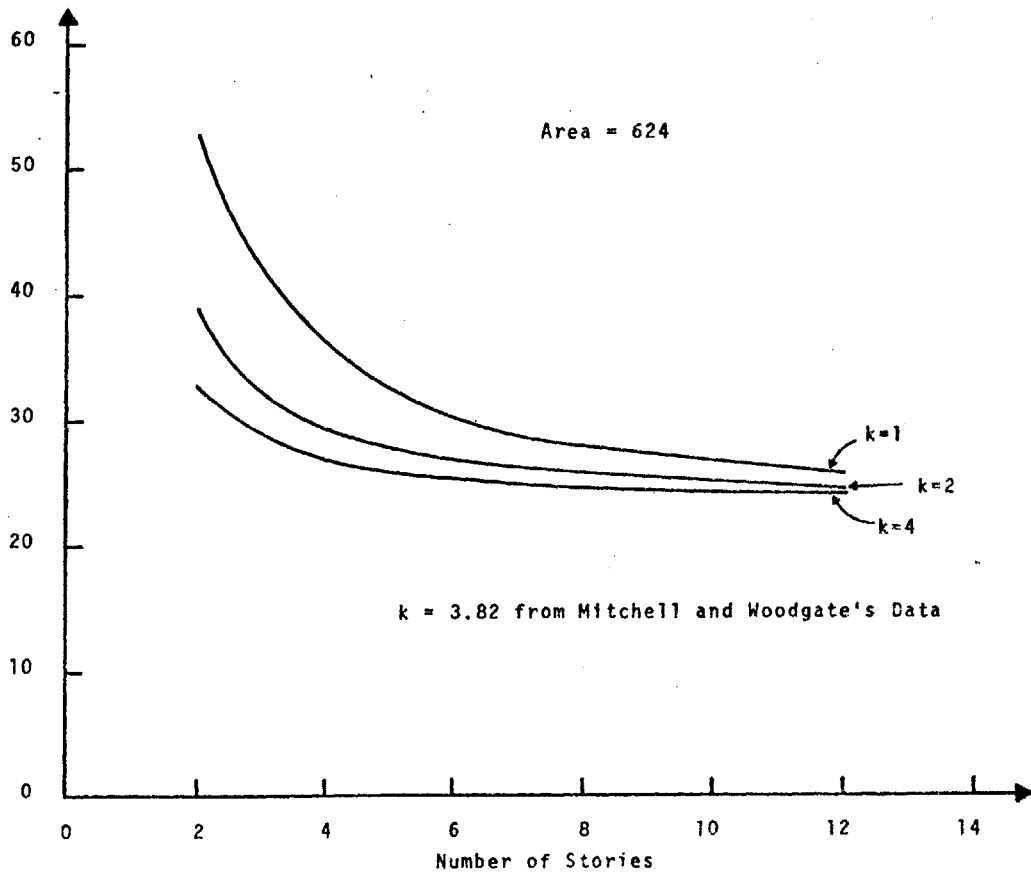


Fig. II-21 99% Maximum Lifetime Sustained Load with Different k Values

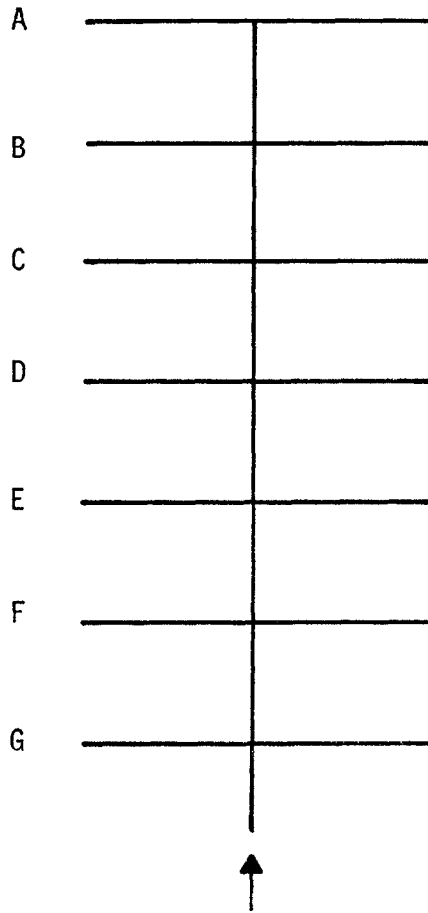


Fig. II-22 Axial Load with Different Occupancies

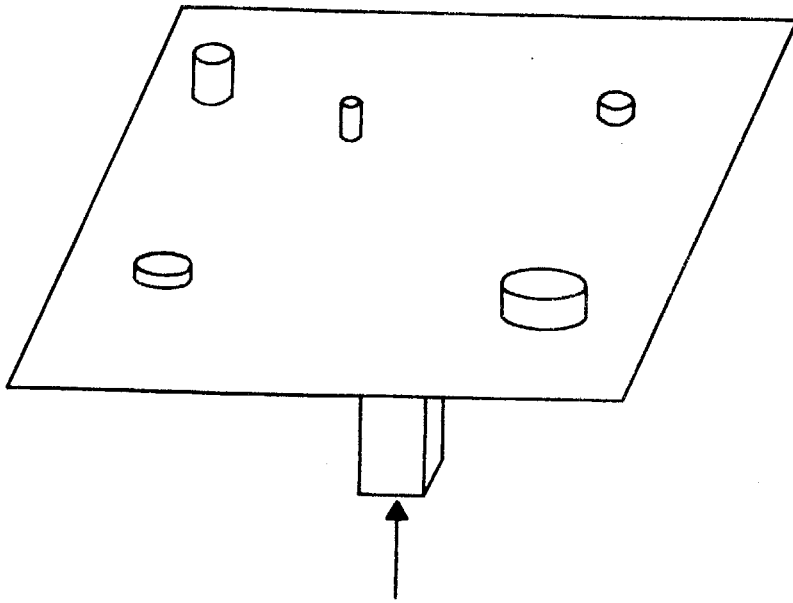


Fig. III-1 Different Load Cells on a Floor

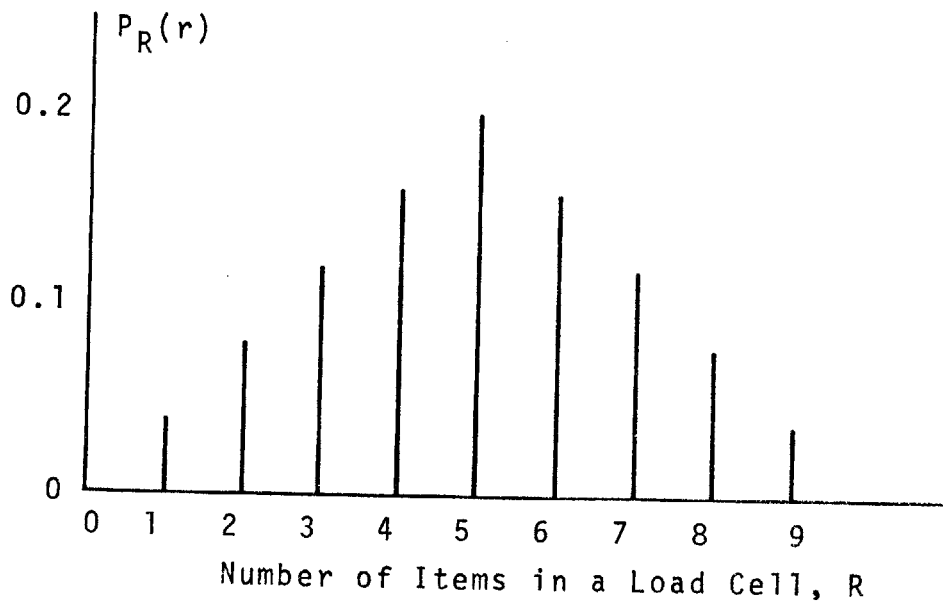


Fig. III-2 PMF of R

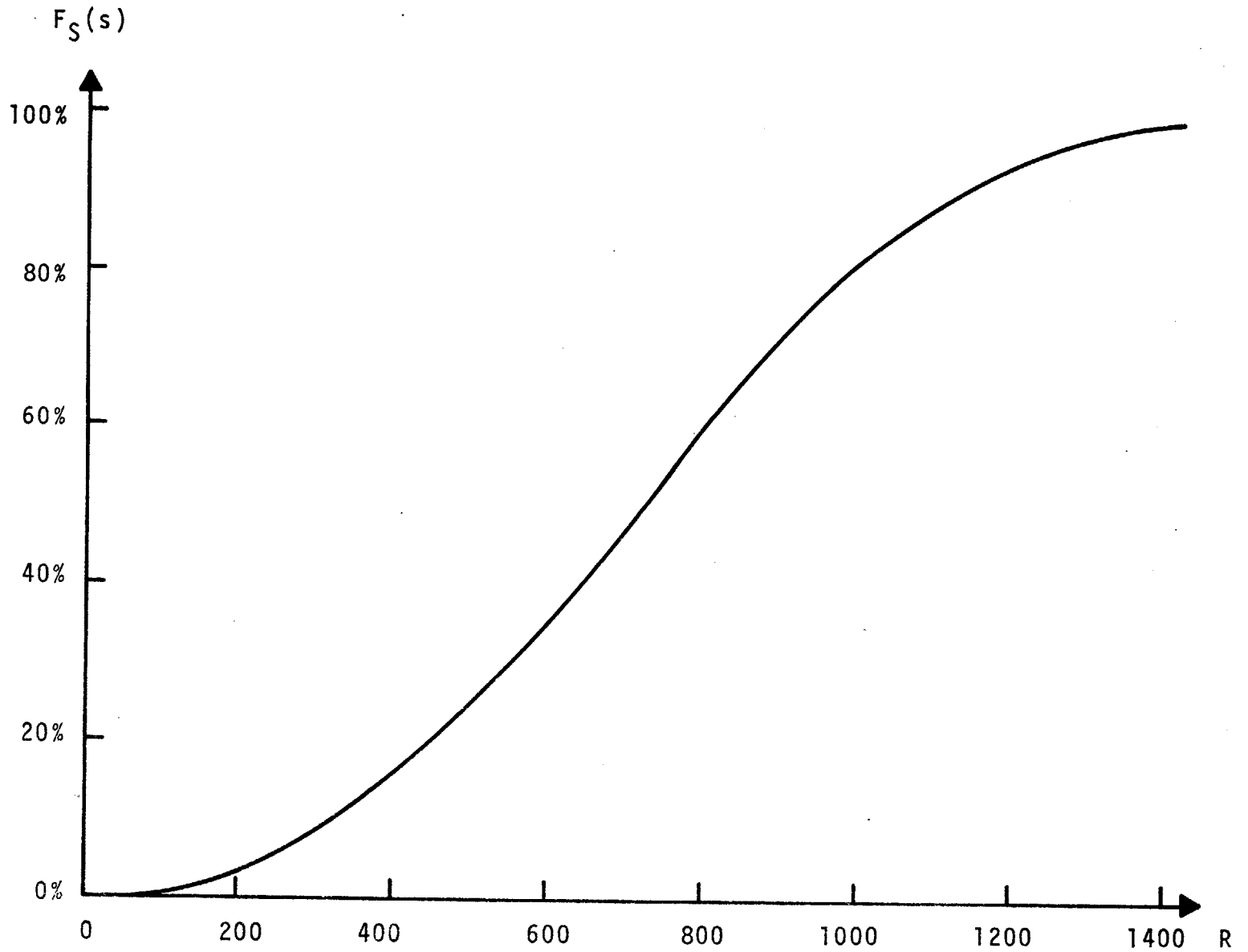


Fig. III-3 CDF of the Total Load of a Load Cell

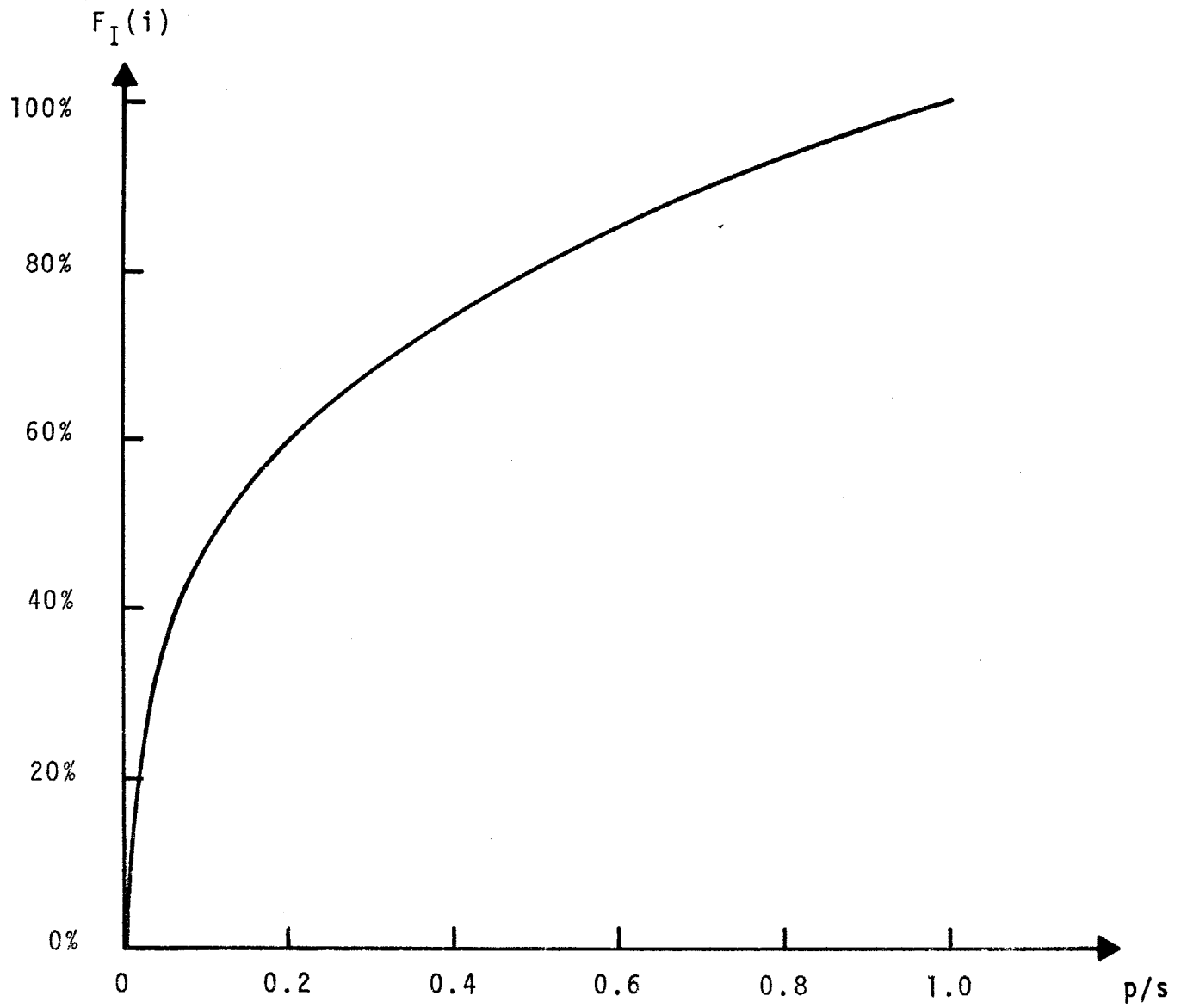


Fig. III-4 CDF of the Influence I

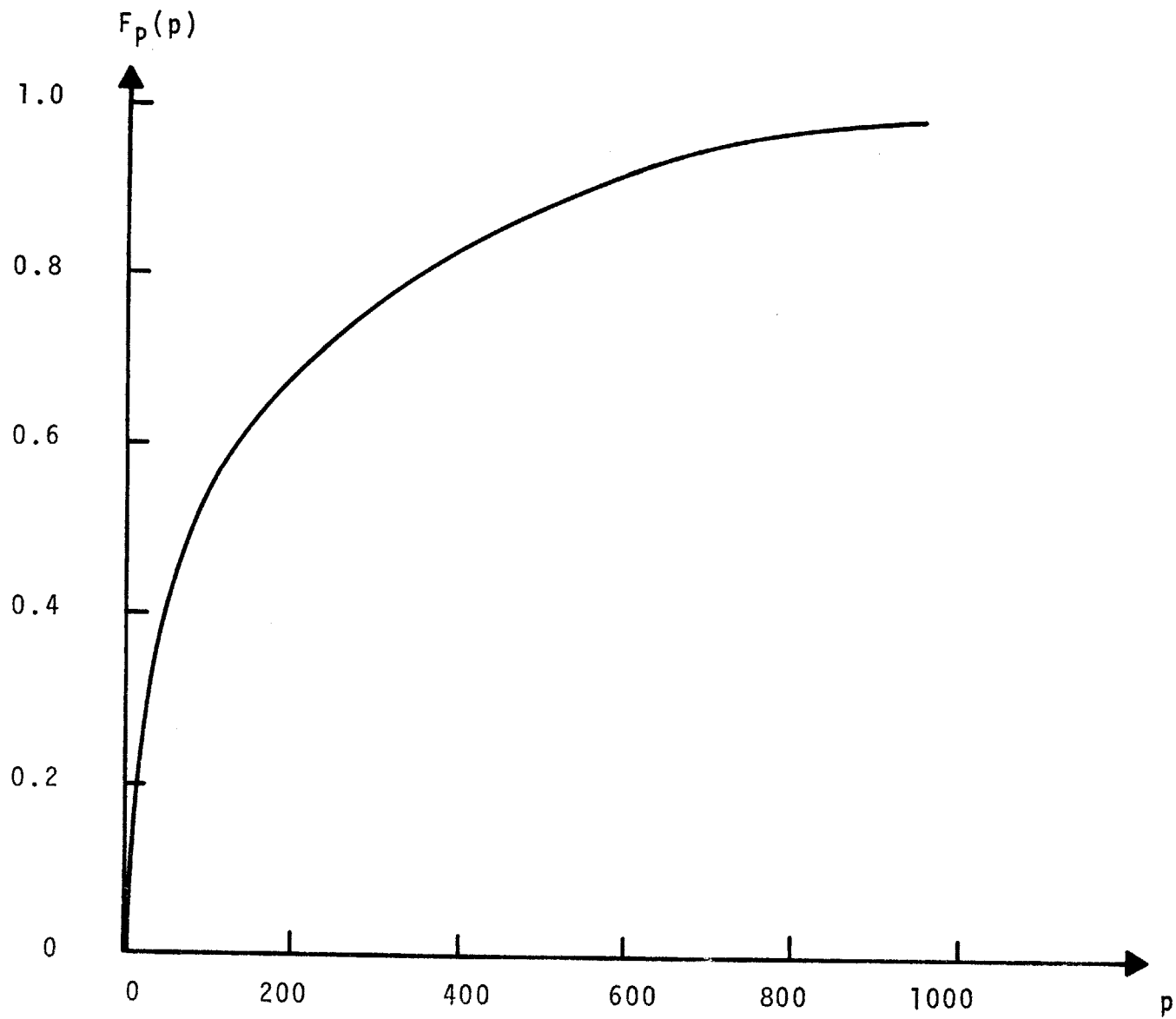


Fig. III-5 CDF of the Load Effect Due to One Load Cell

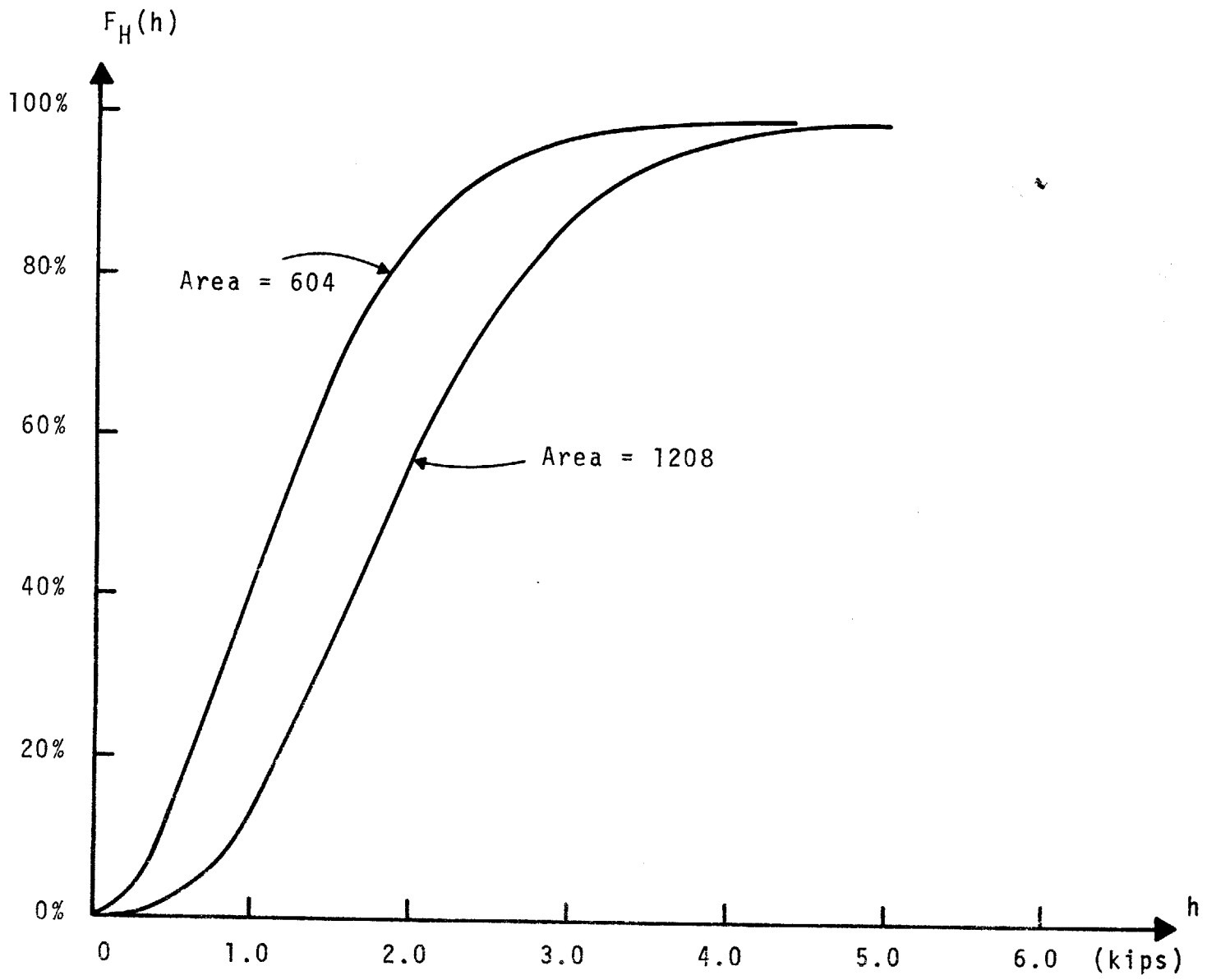


Fig. III-6 CDF of the Total Load Effect, H

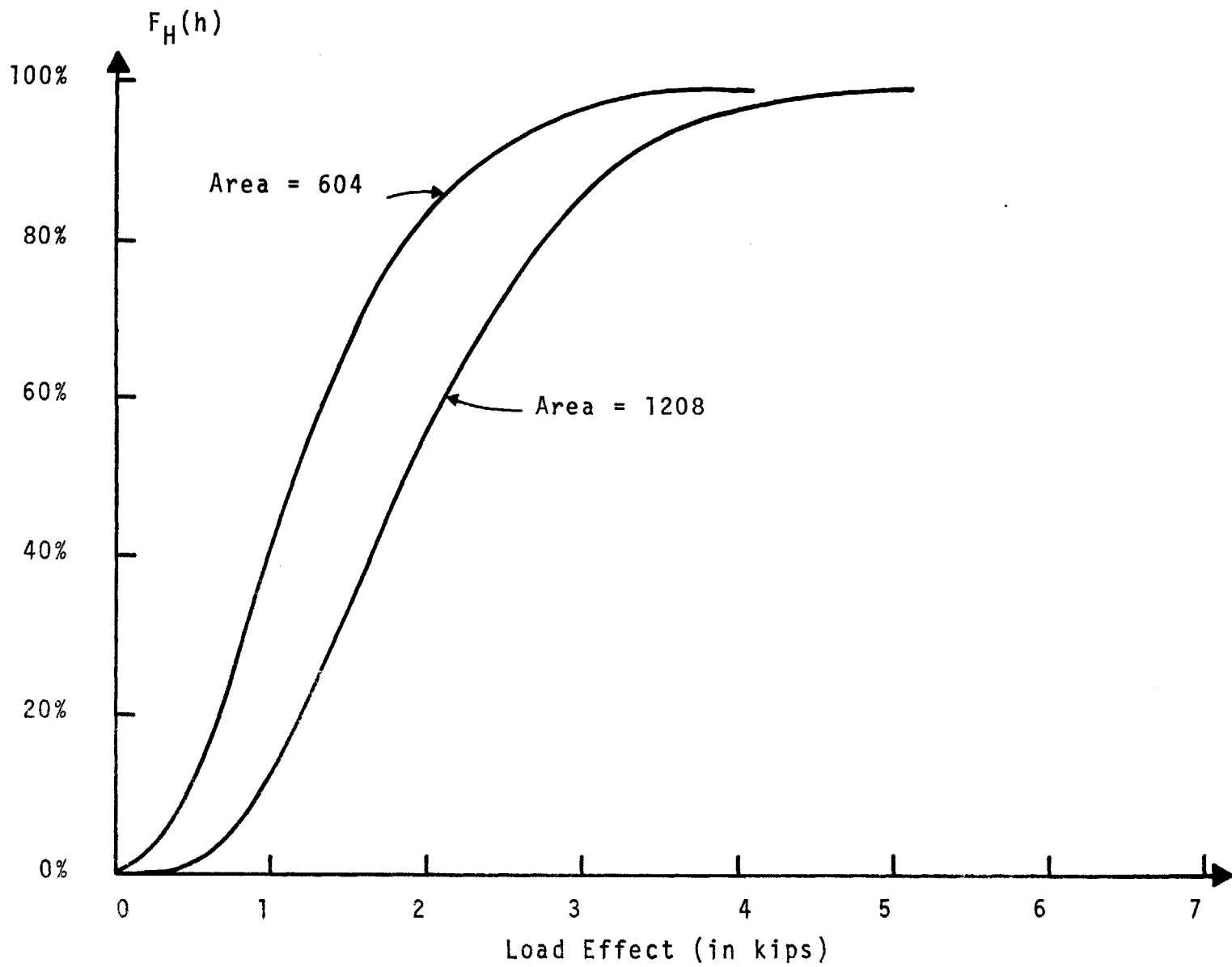


Fig. III-7 Results from Approximate Solution

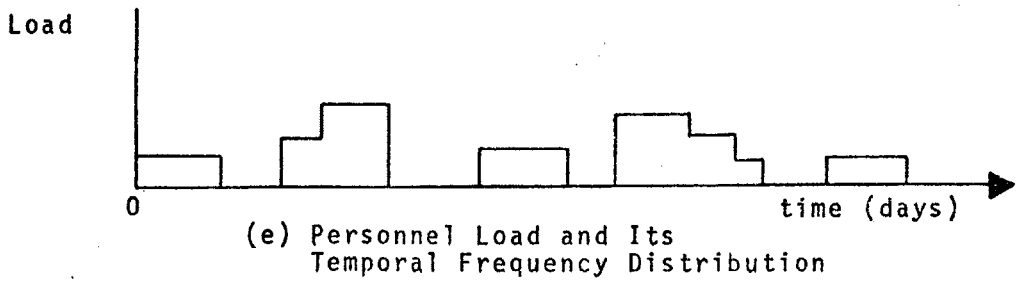
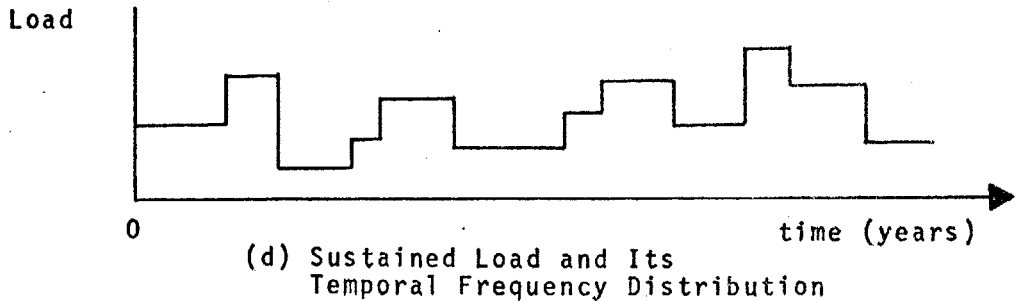
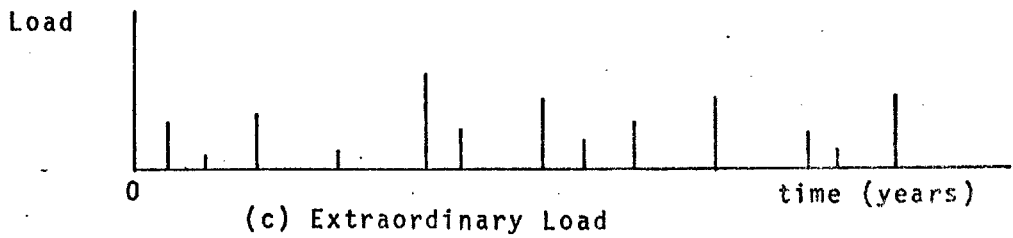
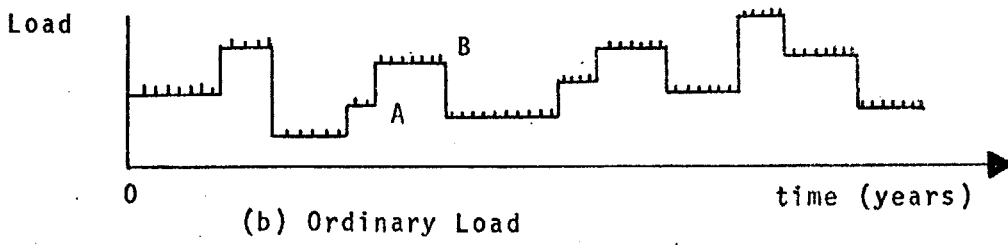
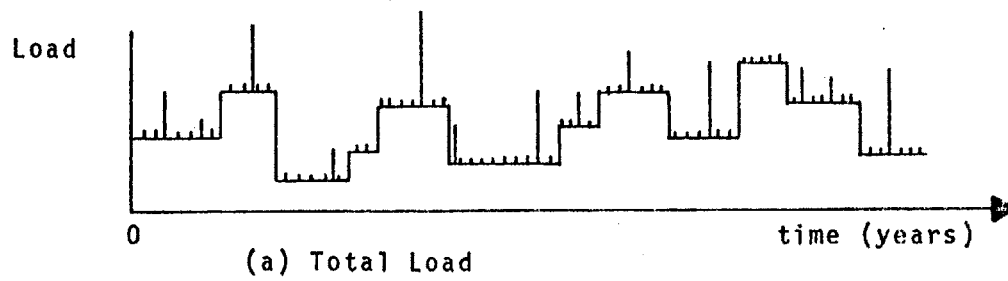


Fig. IV-1 Load Combinations

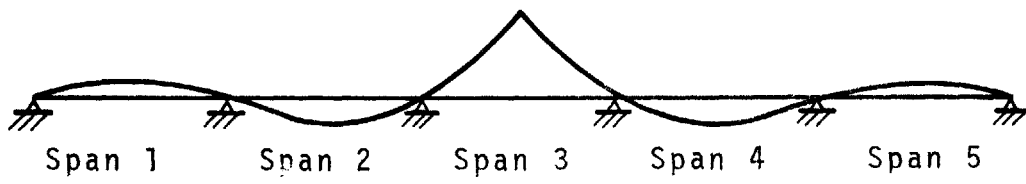


Fig. IV-2 An Influence Line for the Mid-span Moment

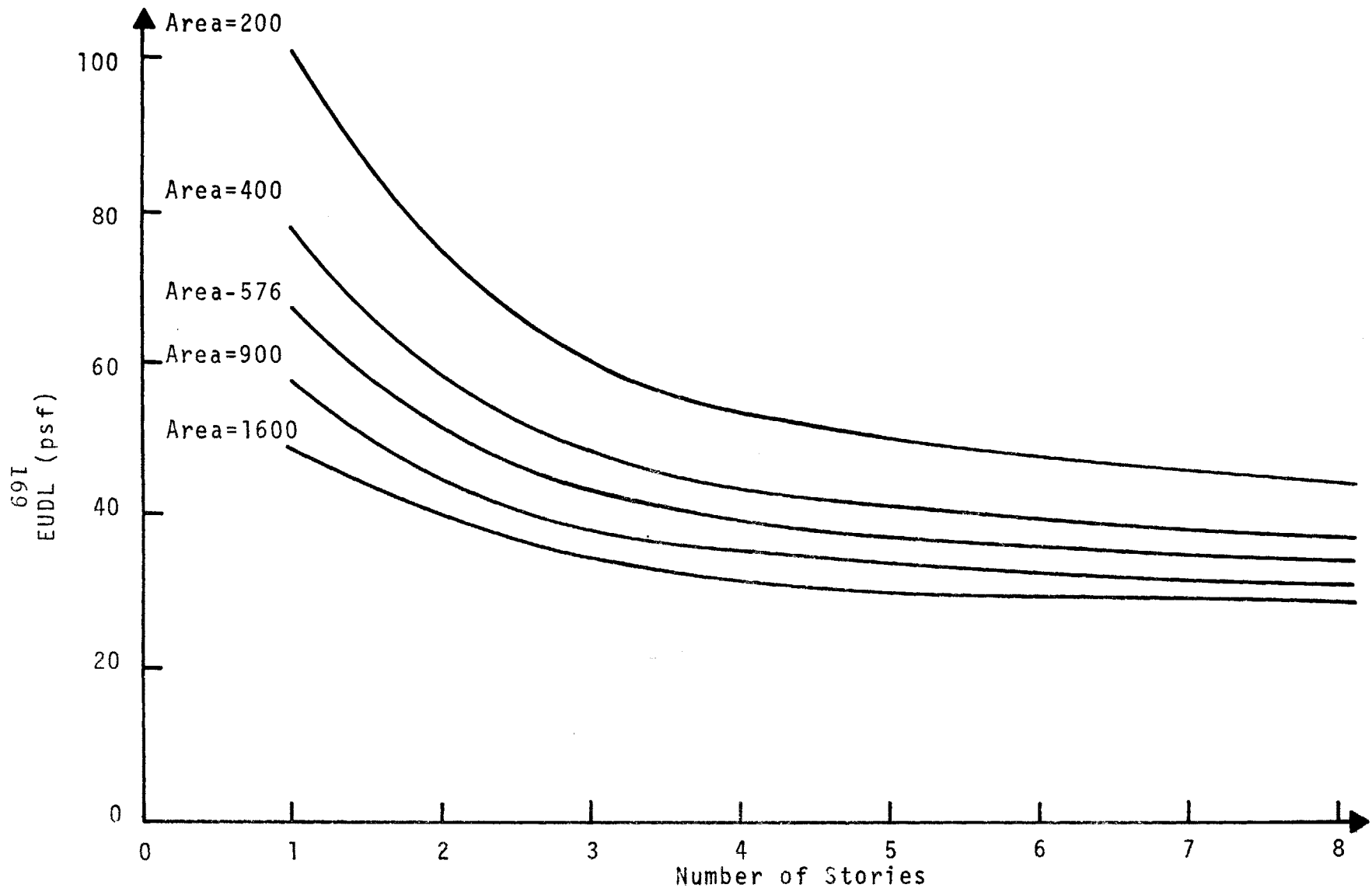


Fig. IV-3 99% Design Load (Combination 1)

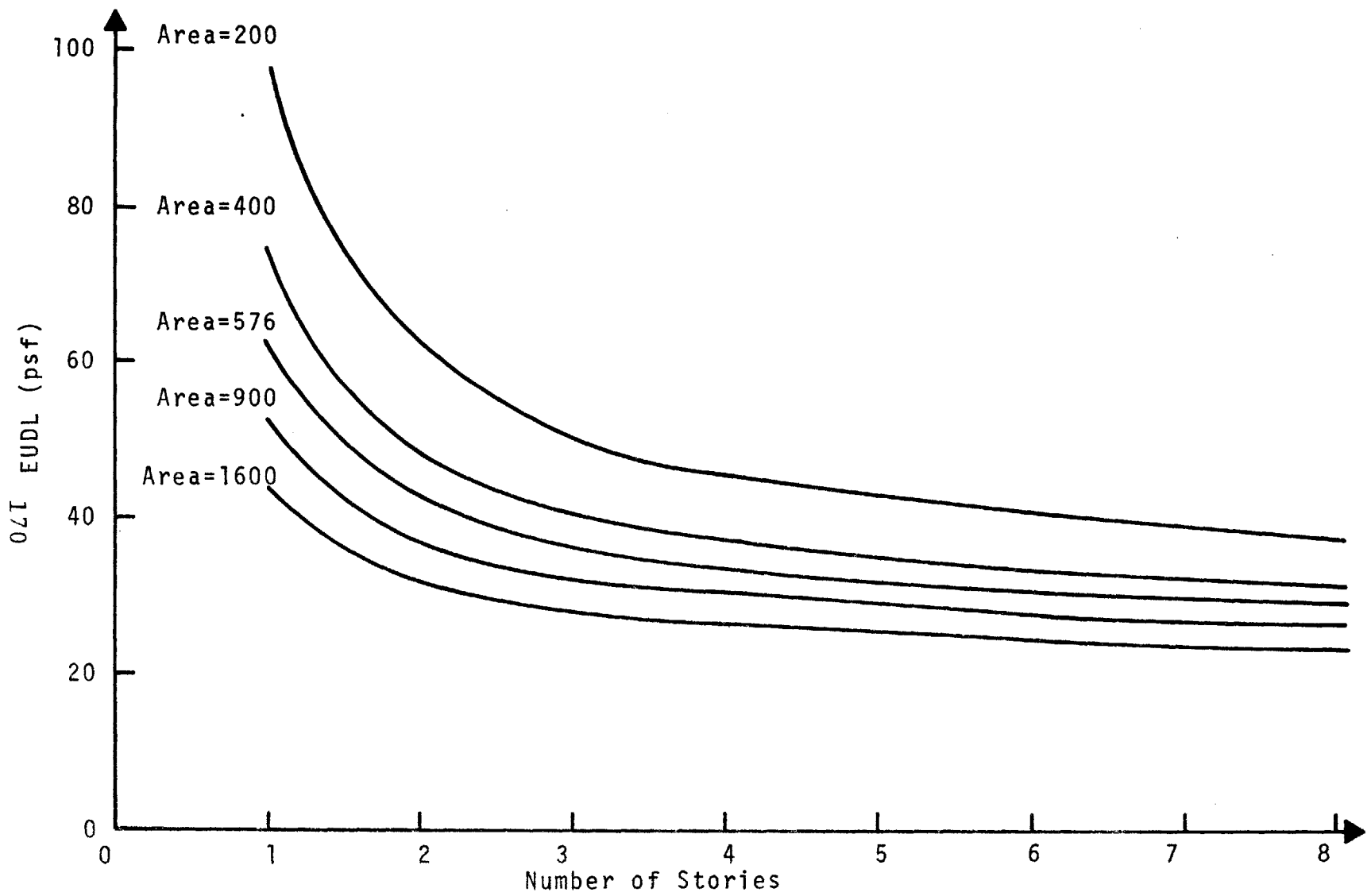


Fig. IV-4 99% Design Load (Combination 2)

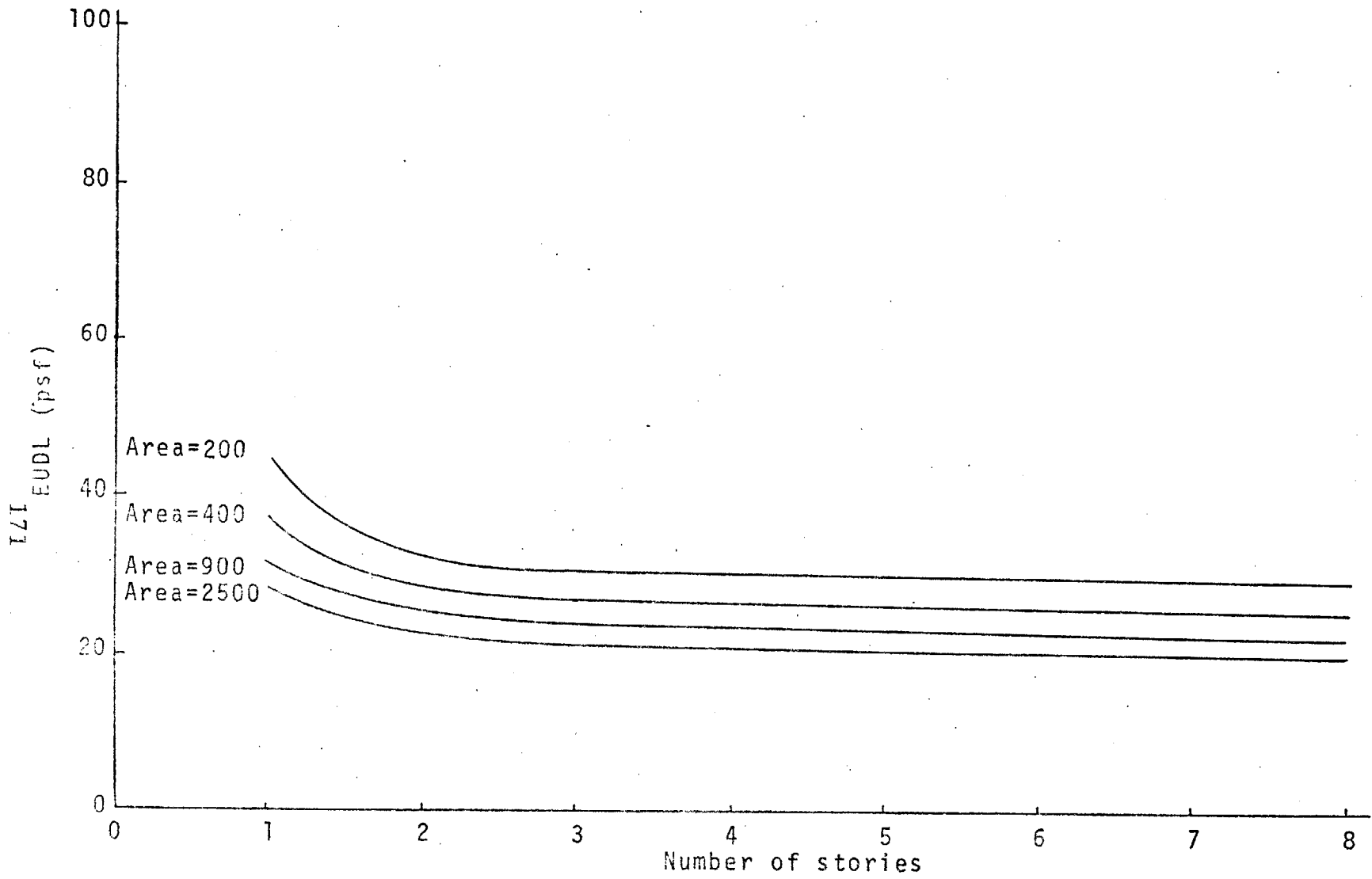


Fig. IV-5 99% Performance Load

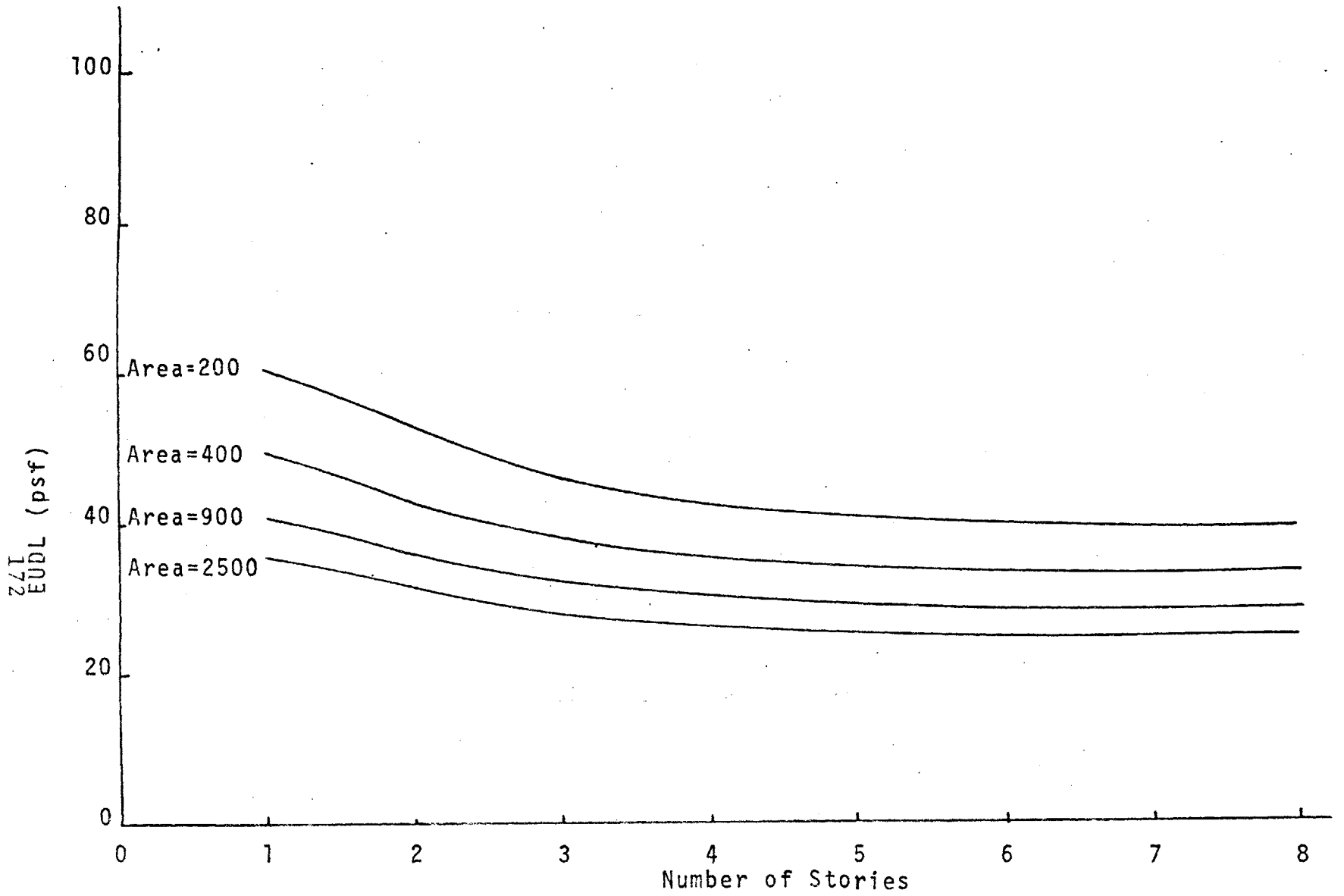


Fig. IV-6 99% Maximum Lifetime Sustained Load

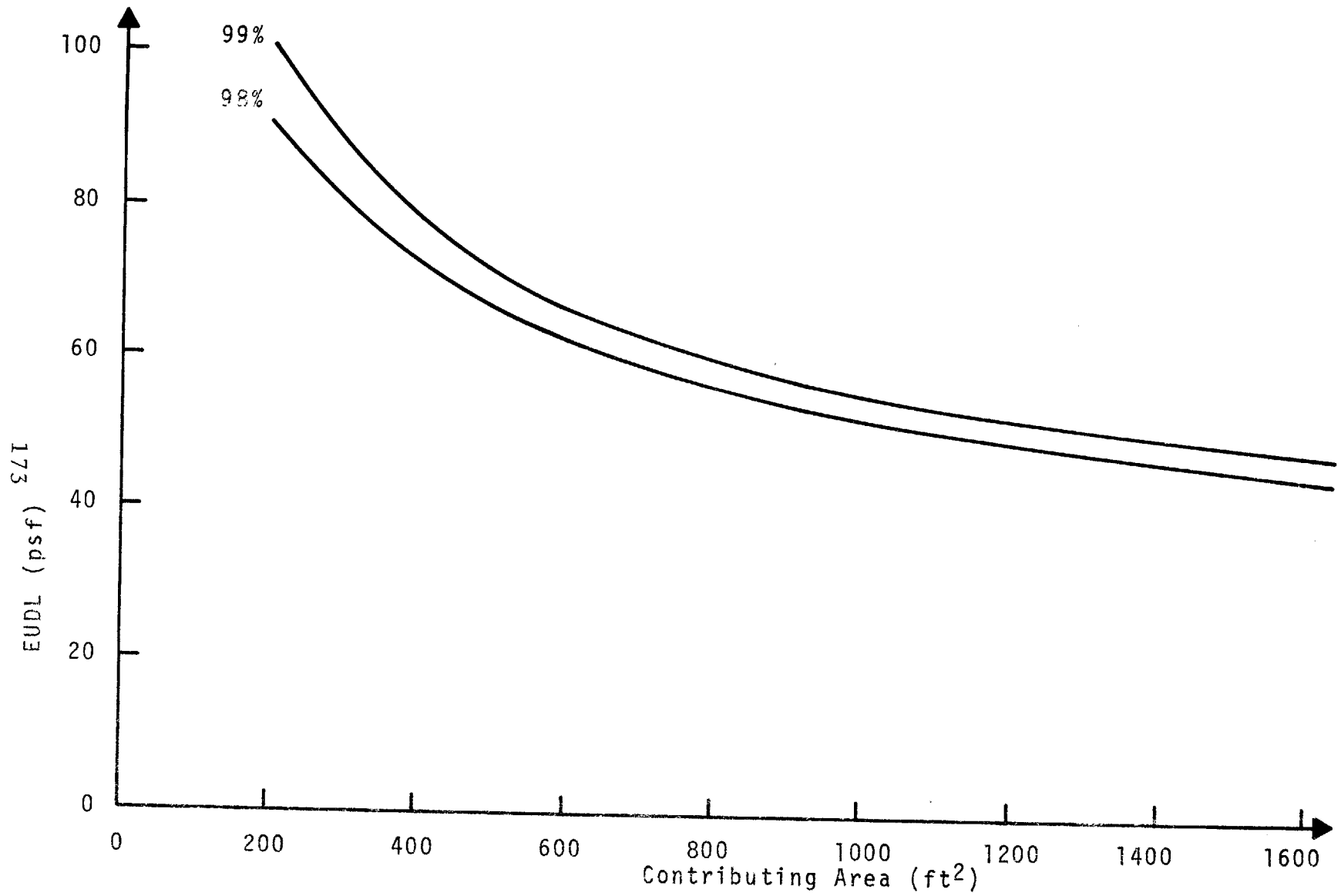


Fig. IV-7 Design Load of Different Probability Levels

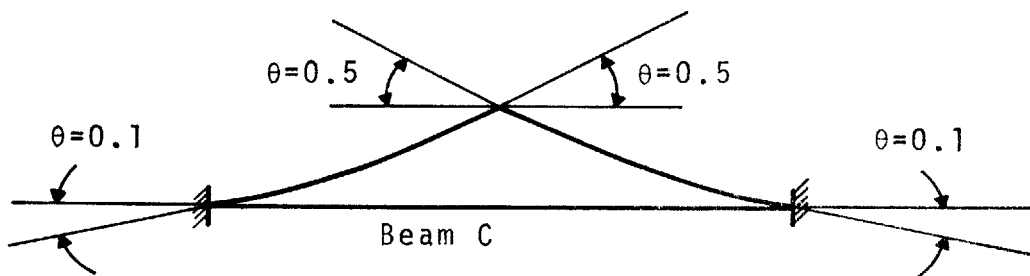
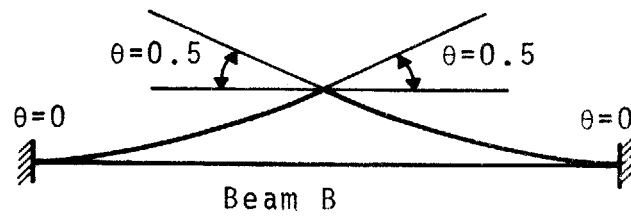
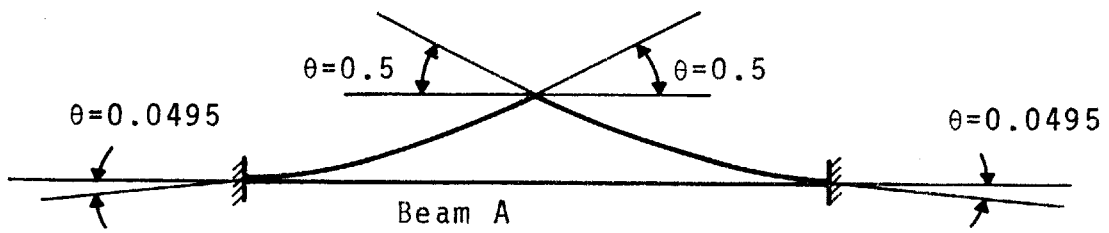


Fig. IV-8 Different Influence Lines for a Single Span Beam

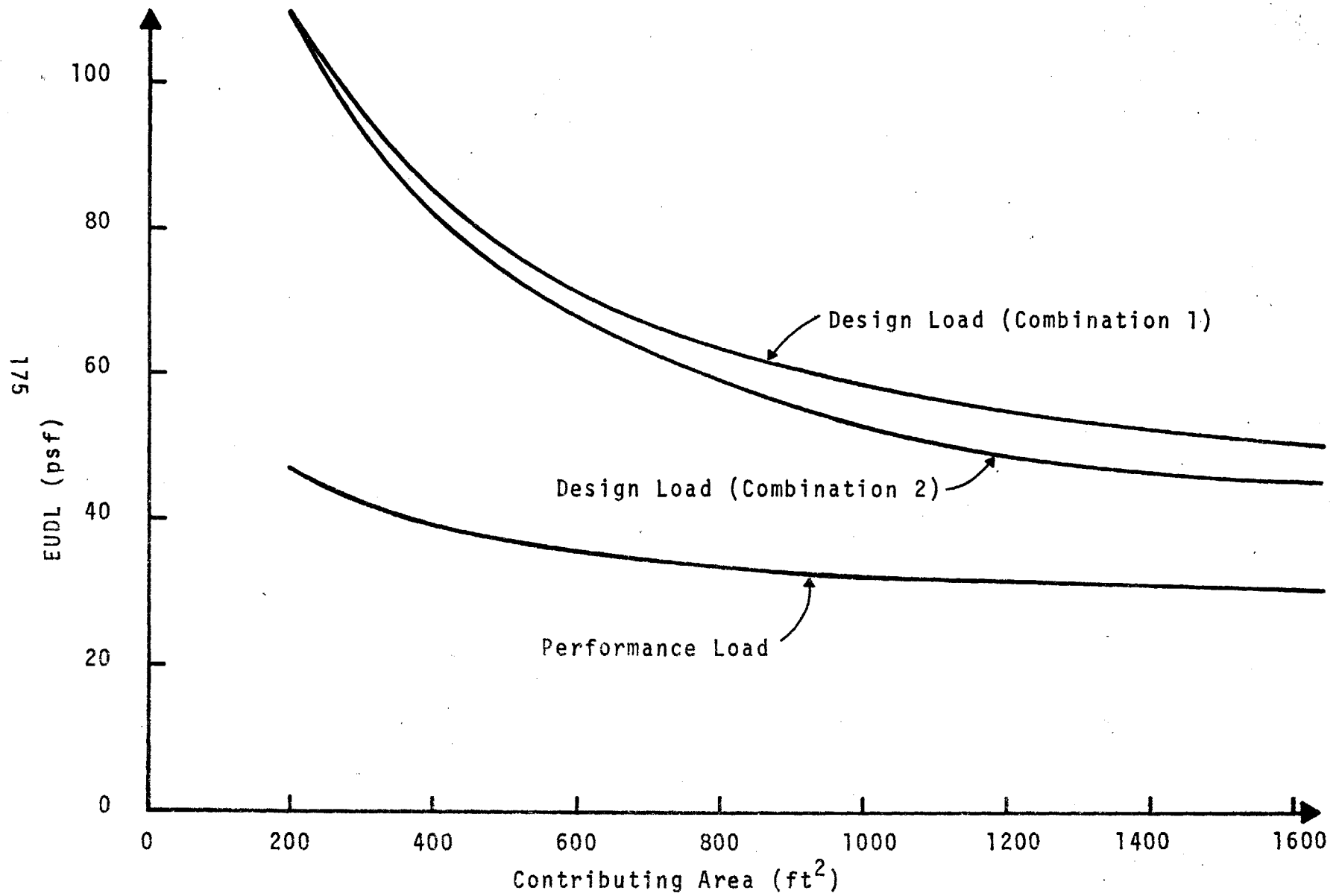


Fig. IV-9 99% Design Load and Performance Load for Mid-Span Moments

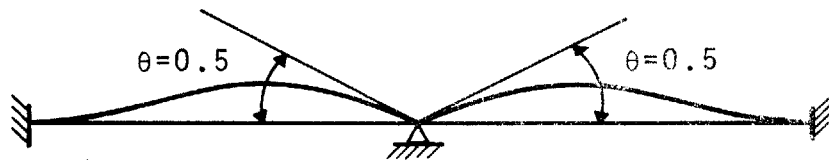


Fig. IV-10 Influence Line for the Negative Moment at the Support

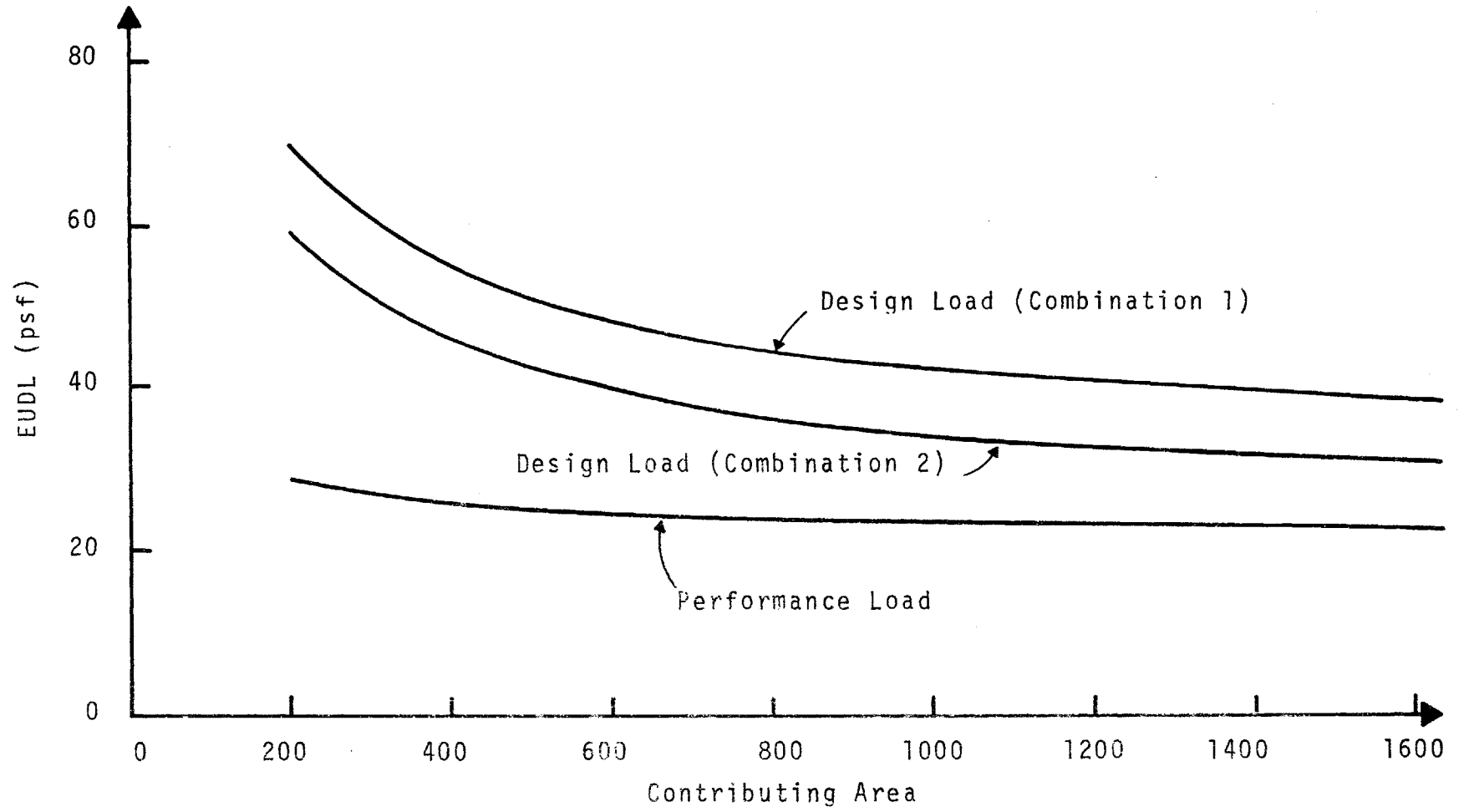
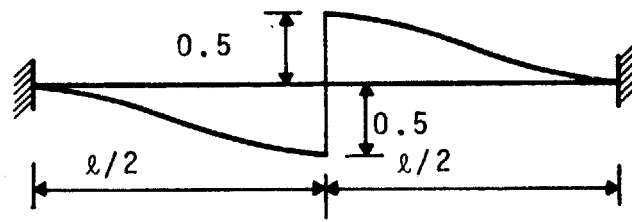
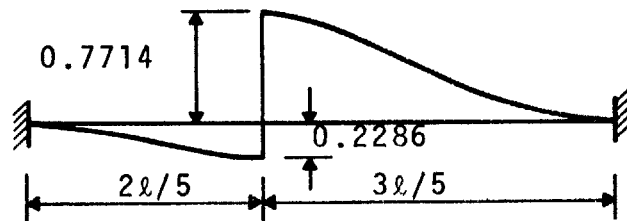


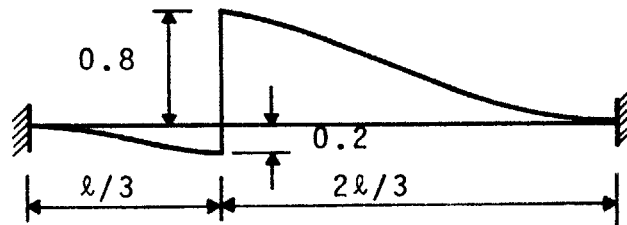
Fig. IV-11. 99% Design Loads and Performance Load for the Negative Moment



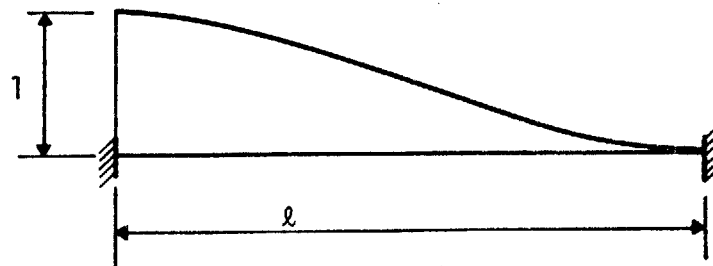
Beam A



Beam B



Beam C



Beam D

Fig. IV-12 Shear Influence Surfaces at Different Locations of a Beam

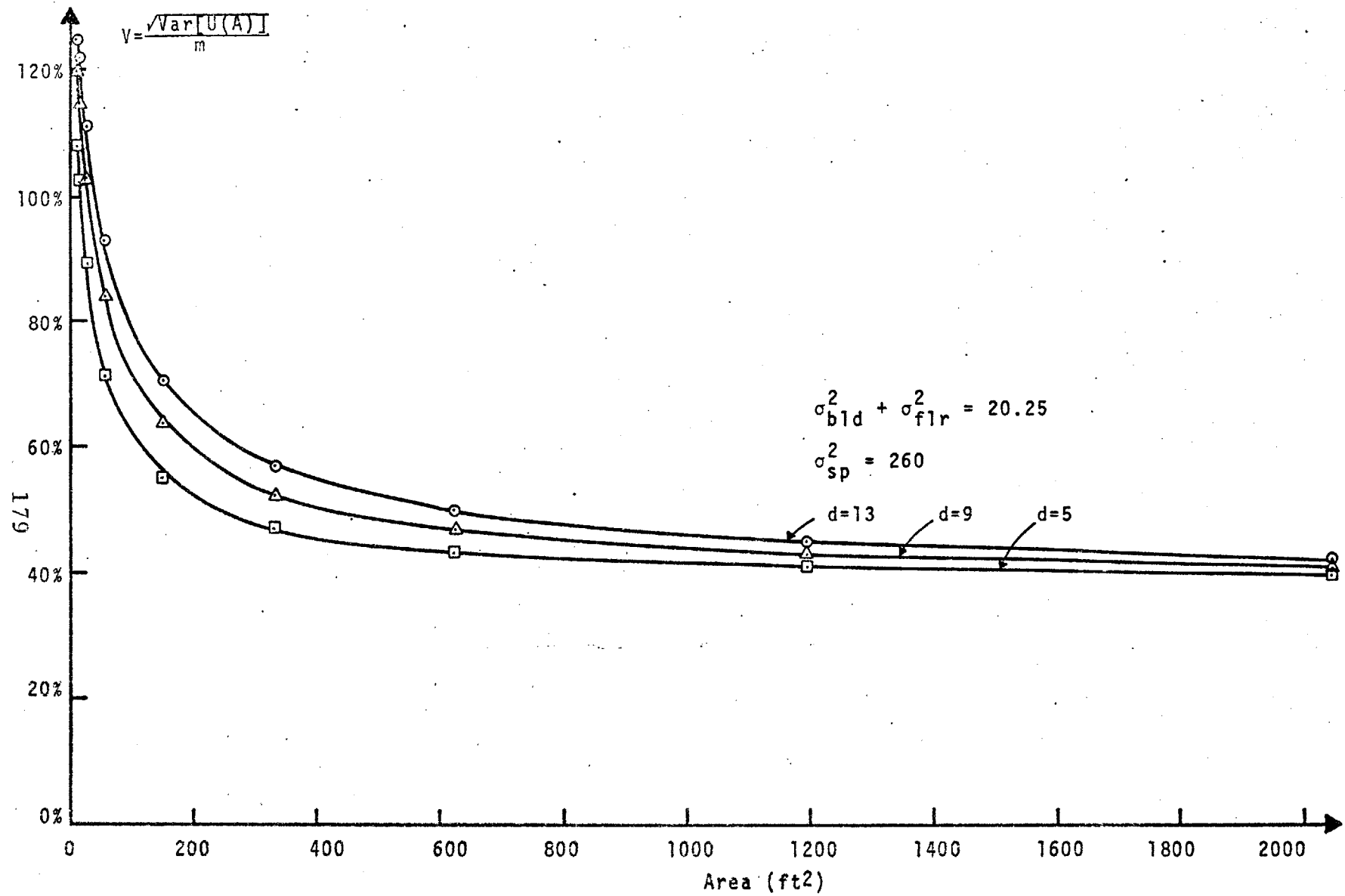


Fig. V-1 The Influence of the Constant d to the Model

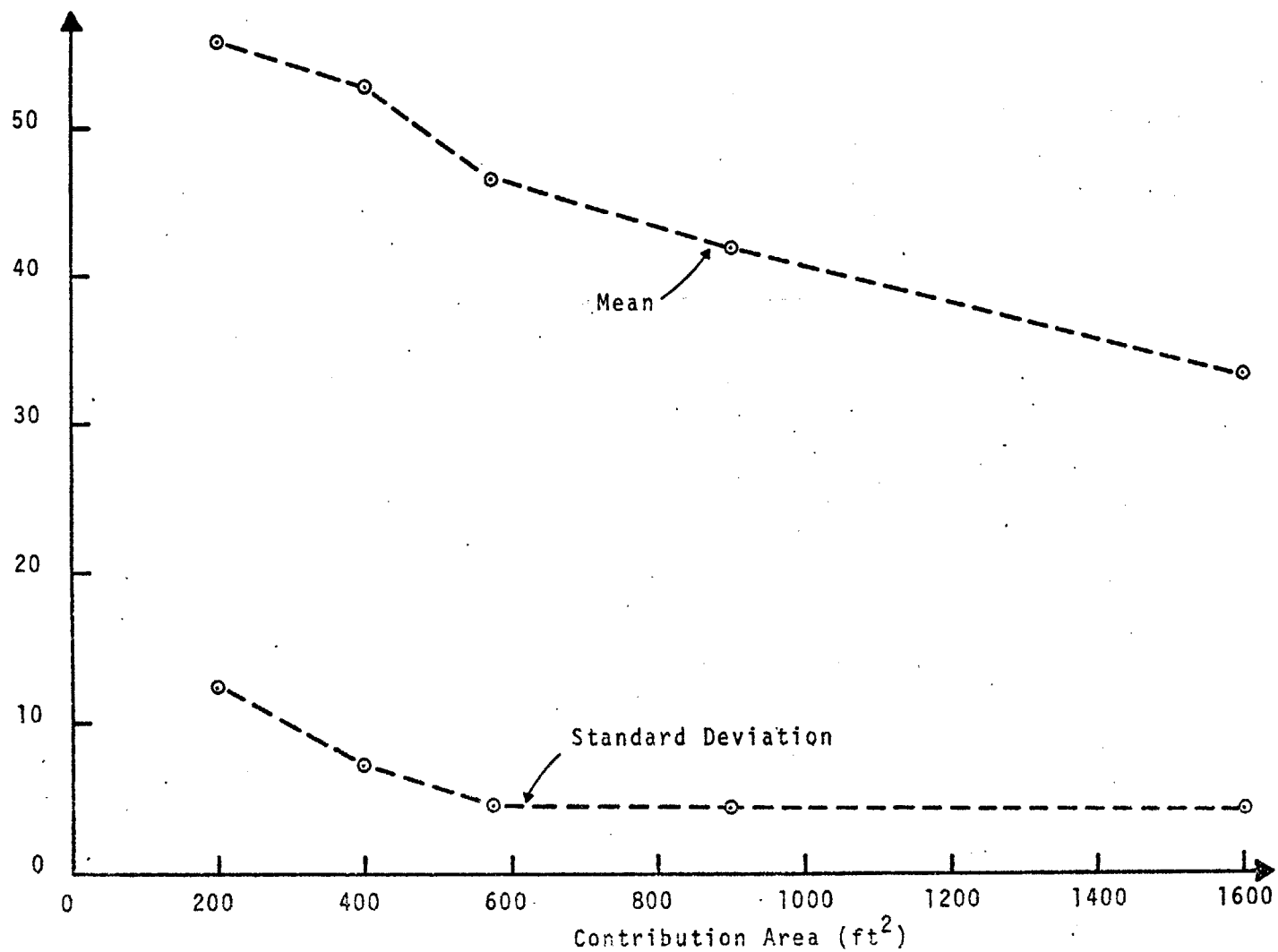


Fig. V-2 Means and Standard Deviations for Design Loads

REFERENCES

1. Cornell, C.A. "Structural Safety Specifications Based on Second-Moment Reliability Analysis", IABSE Symposium on Concepts of Safety of Structures and Methods of Design, 4, Final Report, London, 1969.
2. Cornell, C.A. "Implementing Probability-Based Structural Codes", 1971 Annual Convention, ACI, Denver, March, 1971.
3. Mitchell, G.R. and Woodgate, R.W. "Floor Loadings in Office Building - The Results of a Survey", CP 3/71, Building Research Station, Garston, U.K. Jan. 1971
4. Stoney, B.B. "Theory of Strains II", Ed. of 1869.
5. Dunham, J.W. "Design Live Load in Buildings", Trans. ASCE, 112, 1947
6. Horne, M.R., "The Variation of Mean Floor Loads with Area", Engineering 171, Feb. 16, 1951.
7. Rosenblueth, E., "Theory of Live Loads in Buildings" Ingenieria, Oct. 1959.
8. Jauffred, F.J., "Live Load in Office and Dwelling Units of the Federal District", Ingenieria, Oct. 1960.
9. Fader, D.J., "Rational Considerations for the Design Loading of Office Building Floors", B. Eng. Thesis, Univ. of Western Ontario, London, Ontario, 1963.

10. Karman, T. von., "Untersuchungen uber die Nutzlasten von Decken bei Wohngebauten," ("Investigations of Live Loads on Floors in Residential Buildings"), Osterreichische Ingenieur - Zeitschrift Jg 9, 1966.
11. Bryson, J.O. and Gross, D., "Techniques for the Survey and Evaluation of Live Floor Loads and Fire Loads in Modern Office Buildings", U.S. Dept. Commerce, NBS, Building Science Series, 16, Dec. 1968.
12. Corotis, R.B., "Statistical Measurement and Prediction of Building Design Loads", M.S. Thesis, Department of Civil Engineering, M.I.T. Sept. 1968.
13. Hasofer, A.M., "Statistical Model for Live Floors Loads; J. of Str. Div., ASCE, Oct. 1968.
14. Heaney, A.C., "A Reliability-Based Study Concerning Live Loads and Codified Structural Design", Ph.D. Thesis, Department of Civil Engineering, University of Waterloo, March, 1971.
15. Borges, J.F. and Castanheta, M., "Structural Safety", Lisbon, Nov. 1968.
16. Mitchell, G.R., "Loadings on Buildings" IABSE Symposium on Concepts of Safety of Structures and Methods of Design, London, 1969.
17. Hauser, R., "Load Correlation Models in Structural Reliability", M.S. Thesis, Department of Civil Engineering, M.I.T., Dec. 1970.

18. Cox, D.R. and Miller, H.D., "The Theory of Stochastic Process", John Wiley and Sons, Inc., New York, 1965.
19. Vanmarcke, E.H., "Variance Function", Working Paper, Department of Civil Engineering, M.I.T., 1970.
20. Private Communication with Mr. G.R. Mitchell
21. Timoshenko, S., and Woinowsky-Krieger, S., "Theory of Plates and Shells", 2nd Ed. McGraw-Hill Book Company, 1959.
22. Clough, R.W. and Tocher, J.L., "Finite Element Stiffness Matrices for Analysis of Plate Bending", Conference on Matrix Methods in Structural Mechanics, Wright-Patterson Air Force Base, Ohio, October, 1965.
23. Ayer, F. and Cornell, C.A., "Grid Maximization by Mathematical Programming", J. of Str. Div., ASCE, Feb. 1965.
24. Logcher, R.D. et al., "STRU DL II, The Structural Design Language, Engineering User's Manual, Volume 1, Frame Analysis", Dept. of Civil Engineering, M.I.T. R68-91, Nov. 1968.
25. Benjamin, J.R. and Cornell, C.A. "Probability, Statistics and Decision for Civil Engineering", McGraw-Hill 1970.

BIOGRAPHY

The author was born in China on October 20, 1941. He entered the National Taiwan University and received a Bachelor of Science degree in June, 1963.

After finishing his military duty as a civil Engineer Officer in Chinese Air Force, he received an assistantship from the Ohio State University and came to this country in May 1965. He completed the Master of Science degree in June 1967.

Upon graduation, he worked for one and a half years in a consulting engineer firm as a structural engineer.

In September, 1968 he attended the Massachusetts Institute of Technology for study toward a doctoral degree.

APPENDIX A

As shown in Fig. II-2 the mean and the variance of the sum of the load from two floors will be derived below. Let

$$L(A_2) = \iint \omega(x,y) dx dy + \iint \omega(u,v) du dv$$

Then

$$\begin{aligned} E[L(A_2)] &= E[\iint \omega(x,y) dx dy + \iint \omega(u,v) du dv] \\ &= E\left[\lim_{\substack{\Delta x \rightarrow 0 \\ \Delta y \rightarrow 0}} \sum_x \sum_y \omega(x,y) \Delta x \Delta y + \lim_{\substack{\Delta u \rightarrow 0 \\ \Delta v \rightarrow 0}} \sum_u \sum_v \omega(u,v) \Delta u \Delta v\right] \\ &= E\left[\lim_{\substack{\Delta x \rightarrow 0 \\ \Delta y \rightarrow 0}} \sum_x \sum_y \omega(x,y) \Delta x \Delta y\right] + E\left[\lim_{\substack{\Delta u \rightarrow 0 \\ \Delta v \rightarrow 0}} \sum_u \sum_v \omega(u,v) \Delta u \Delta v\right] \\ &= \lim_{\substack{\Delta x \rightarrow 0 \\ \Delta y \rightarrow 0}} \sum_x \sum_y \{E[\omega(x,y)]\} \Delta x \Delta y + \lim_{\substack{\Delta u \rightarrow 0 \\ \Delta v \rightarrow 0}} \sum_u \sum_v \{E[\omega(u,v)]\} \Delta u \Delta v \\ &= \iint m_{\omega(x,y)} dx dy + \iint m_{\omega(u,v)} du dv \end{aligned}$$

$$\text{Var}[L(A_2)] = E[L^2(A_2)] - E[L(A_2)]^2$$

$$\begin{aligned}
E[L^2(A_2)] &= E\left[\left(\iint \omega(x,y) dx dy + \iint \omega(u,v) du dv\right)^2\right] \\
&= E\left[\lim_{\substack{\Delta x \rightarrow 0 \\ \Delta y \rightarrow 0}} \sum_x \sum_y \omega(x,y) \Delta x \Delta y + \lim_{\substack{\Delta u \rightarrow 0 \\ \Delta v \rightarrow 0}} \sum_u \sum_v \omega(u,v) \Delta u \Delta v\right]^2 \\
&= E\left[\lim_{\substack{\Delta x, \Delta x_1 \rightarrow 0 \\ \Delta y, \Delta y_1 \rightarrow 0}} \sum_x \sum_{x_1} \sum_y \sum_{y_1} \omega(x,y) \omega(x_1,y_1) \Delta x \Delta x_1 \Delta y \Delta y_1\right. \\
&\quad + 2 \lim_{\substack{\Delta x, \Delta y \rightarrow 0 \\ \Delta u, \Delta v \rightarrow 0}} \sum_x \sum_y \sum_u \sum_v \omega(x,y) \omega(u,v) \Delta x \Delta y \Delta u \Delta v \\
&\quad \left. + \lim_{\substack{\Delta u, \Delta u_1 \rightarrow 0 \\ \Delta v, \Delta v_1 \rightarrow 0}} \sum_u \sum_{u_1} \sum_v \sum_{v_1} \omega(u,v) \omega(u_1,v_1) \Delta u \Delta u_1 \Delta v \Delta v_1\right]
\end{aligned}$$

Following the same steps as before, then

$$\begin{aligned}
E[L^2(A_2)] &= \iiint E[\omega(x,y) \omega(x_1,y_1)] dx dx_1 dy dy_1 \\
&\quad + 2 \iiint E[\omega(x,y) \omega(u,v)] dx dy du dv \\
&\quad + \iiint E[\omega(u,v) \omega(u_1,v_1)] du du_1 dv dv_1 \\
&= \iiint \{ \text{cov}[\omega(x,y), \omega(x_1,y_1)] + E[\omega(x,y)] E[\omega(x_1,y_1)] \} \\
&\quad \quad \quad dx dx_1 dy dy_1
\end{aligned}$$

$$\begin{aligned}
& + 2 \iiint\!\!\!\int \{ \text{cov}[\omega(x,y), \omega(u,v)] + E[\omega(x,y)]E[\omega(u,v)] \} \\
& \quad \quad \quad dx dy du dv \\
& + \iiint\!\!\!\int \{ \text{cov}[\omega(u,v), \omega(u_1,v_1)] + E[\omega(u,v)]E[\omega(u_1,v_1)] \} \\
& \quad \quad \quad du du_1 dv dv_1 \\
& = \iiint\!\!\!\int \text{cov}[\omega(x,y), \omega(x_1,y_1)] dx dx_1 dy dy_1 \\
& + 2 \iiint\!\!\!\int \text{cov}[\omega(x,y), \omega(u,v)] dx dy du dv \\
& + \iiint\!\!\!\int \text{cov}[\omega(u,v), \omega(u_1,v_1)] du du_1 dv dv_1 + E[L(A_2)]^2
\end{aligned}$$

Therefore

$$\begin{aligned}
\text{Var}[L(A_2)] & = E[L^2(A_2)] - E[L(A_2)]^2 \\
& = \iiint\!\!\!\int \text{cov}[\omega(x,y), \omega(x_1,y_1)] dx dx_1 dy dy_1 \\
& + 2 \iiint\!\!\!\int \text{cov}[\omega(x,y), \omega(u,v)] dx dy du dv \\
& + \iiint\!\!\!\int \text{cov}[\omega(u,v), \omega(u_1,v_1)] du du_1 dv dv_1
\end{aligned}$$

The formulas can also be extended to include the influence surface. Let

$$H = \iint I(x,y)\omega(x,y) dx dy$$

then

$$E[H] = \iint I(x,y)m_{\omega(x,y)} dx dy$$

$$\text{Var}[H] = \iiint I(x,y)I(x_1,y_1)\text{cov}[\omega(x,y),\omega(x_1,y_1)] dx dx_1 dy dy_1$$

where $I(x,y)$ is the coordinate of the influence surface at location (x,y) .

Appendix B

A brief description of the live load survey conducted by the Building Research Station at Garston, is presented below in order to add to the understanding of the load results used in this work.

During the period of 1965-1967, an extensive office load survey work was carried out by BRS. About thirty modern office buildings involving over 100 occupying organizations and having a total area of $1 \frac{3}{4}$ million square feet, were surveyed, and the positions, magnitudes and character of the loads present were recorded using a rectangular coordinate system. In addition to the load observed directly, a 3 psf people concentration load and 50 psf fire load were added.

Each building floor was then divided into a number of zones. All loads that happened to be on the dividing line were added to both adjacent zones. The coordinates of the zones and the location of the loads were then fed into the computer which made further subdivisions. Histograms were produced for each of a number of bay sizes.

Information about the change of occupancy was obtained by searching through telephone directories.

Appendix C

The mean and the variance from Mitchell and Woodgate⁽³⁾ were reproduced in Table A.

Table A.

| | | | | | | | | | |
|------|-------|-------|-------|-------|-------|-------|-------|-------|-------|
| Area | 11.7 | 14.6 | 25.3 | 56 | 151 | 336 | 624 | 1197 | 2069 |
| Mean | 14.5 | 14.5 | 13.8 | 13.4 | 13.0 | 12.8 | 12.3 | 12.2 | 11.8 |
| Var. | 324.3 | 256.0 | 182.3 | 121.0 | 79.2 | 51.8 | 39.07 | 30.25 | 20.25 |
| cov. | 1.275 | 1.1 | 0.978 | 0.82 | 0.685 | 0.562 | 0.512 | 0.45 | 0.382 |

Since the data come from the same buildings the mean load should be the same for all area groups. However the report shows otherwise. The reason is when they divided the floor into small areas they put the load on dividing line into both adjacent ares. That simply added an imaginary load into the small area. That is why the smaller the area the higher the mean load. There is no way to go back to the original survey data. Table A has to be changed by other methods. One reasonable way to do it is to adjust the mean load and maintain the same coefficient of variation. The results are shown in Table B.

Table B

| | | | | | | | | | |
|------|-------|------|-------|------|-------|-------|-------|------|-------|
| Area | 11.7 | 14.6 | 25.3 | 56 | 151 | 336 | 624 | 1197 | 2069 |
| Mean | 11.8 | 11.8 | 11.8 | 11.8 | 11.8 | 11.8 | 11.8 | 11.8 | 11.8 |
| Var. | 226 | 168 | 133 | 93.5 | 65.2 | 43.9 | 36.5 | 28.1 | 20.25 |
| cov. | 1.275 | 1.1 | 0.978 | 0.82 | 0.685 | 0.562 | 0.512 | 0.45 | 0.382 |

Appendix D

The gamma distribution derived from Eq. (II-3-1) are plotted in Fig. II-14. The curves fit the data generally well except for smaller areas where the curves show more probability in the 0 to 5 psf interval than the data have. However this discrepancy does not influence many results. The smaller areas seldom participate in a multiple loading case. It is very unlikely that a column has several 20 ft² or 40 ft² contributing occupants or floors or that a beam has several small contributing spans. Smaller areas will be used only in the local load effect cases such as shears or moments in the slab. In these cases Eq. (II-5-8) applies.

$$F_Z(\alpha) = F_{L(t)}(\alpha) \exp\{-vt[1-F_{L(t)}(\alpha)]F_{L(t)}(\alpha)\}$$

It is apparent from this equation that only the upper tail part will be used instead of the whole distribution, when we want to find the load of the high probability level. Since the assumed gamma distributions fit the upper tails very well, it follows that the gamma distribution is suitable for smaller areas also.

Appendix E

As mentioned in Section II-5c an exact method to evaluate the probability of up-crossing of a certain threshold is derived below. The use of this method is limited to the independent loading case which is not really true for buildings because as the load model described in Section II-1 suggests, all loadings in a building are correlated. However this method can still be used to check the approximation adopted during the derivation in Section II-5c for the extreme case, i.e. when all loadings are assumed independent. Let

$$F(t) = \sum_{i=1}^n L_i(t)$$

Starting with Eq. (II-5-14) and following a derivation similar to that presented in Section II-5c, one obtains:

$$(v_{\alpha})_j \Delta t = P[\text{There is a change of the } j\text{th occupant in } \Delta t]^*$$

$$P[\{F(t+\Delta t) \geq \alpha \cap F(t) < \alpha\} \mid (\text{There is a change of$$

$$\text{the } j\text{th occupant in } \Delta t)] \quad (\text{II-5-14})$$

Assume a simple case, with $i = 3$ and $j = 2$, then

$$\begin{aligned}
& P[\{F(t+\Delta t) \geq \alpha \cap F(t) < \alpha\} | (\text{There is a change of the 2nd} \\
& \quad \text{occupant in } \Delta t)] \\
& = P[\{L_1(t) + L_2(t+\Delta t) + L_3(t)\} \geq \alpha \cap \{L_1(t) + L_2(t) + L_3(t)\} < \alpha] \\
& = \int_0^\alpha P[\{L_1(t) + L_2(t+\Delta t) \geq \alpha - x_3\} \cap \{L_1(t) + L_2(t) < \alpha - x_3\} | L_3(t) = x_3] \\
& \quad f_{L_3}(x) (x_3) dx_3 \\
& = \int_0^\alpha P[\{L_1(t) + L_2(t+\Delta t) \geq \alpha - x_3\} \cap \{L_1(t) + L_2(t) < \alpha - x_3\}] f_{L_3}(t) (x_3) \\
& \quad dx_3 \tag{E-1}
\end{aligned}$$

Since $L_3(t)$ is independent of $L_1(t)$ and $L_2(t)$, the conditional probability can be replaced by a marginal probability. Substitution of Eq. (II-5-15) and Eq. (E-1) into Eq. (II-5-14) yields:

$$\begin{aligned}
(v_\alpha)_3 \Delta t & = v_3 \Delta t \int_0^\alpha P[\{L_1(t) + L_2(t+\Delta t) \geq \alpha - x_3\} \cap \{L_1(t) + L_2(t) < \alpha - x_3\}] \\
& \quad f_{L_3}(t) (x_3) dx_3 \tag{E-2}
\end{aligned}$$

Now,

$$\begin{aligned}
& P[\{L_1(t) + L_2(t + \Delta t) \geq \alpha - x_3\} \cap \{L_1(t) + L_2(t) < \alpha - x_3\}] \\
&= \int_0^{\alpha - x_3} P[L_2(t + \Delta t) \geq \alpha - x_3 - x_1 \cap L_2(t) < \alpha - x_3 - x_1 | L_1(t) = x_1] \\
&\quad f_{L_1(t)}(x_1) dx_1 \\
&= \int_0^{\alpha - x_3} P[L_2(t + \Delta t) \geq \alpha - x_3 - x_1 \cap L_2(t) < \alpha - x_3 - x_1] f_{L_1(t)}(x_1) dx_1
\end{aligned}
\tag{E-3}$$

and

$$\begin{aligned}
& P[L_2(t + \Delta t) \geq \alpha - x_3 - x_1 \cap L_2(t) < \alpha - x_3 - x_1] \\
&= \int_0^{\alpha - x_3 - x_1} P[L_2(t + \Delta t) \geq \alpha - x_3 - x_1 | L_2(t) = x_2] f_{L_2(t)}(x_2) dx_2 \\
&= \int_0^{\alpha - x_3 - x_1} P[L_2(t + \Delta t) \geq \alpha - x_3 - x_1] f_{L_2(t)}(x_2) dx_2 \\
&= \int_0^{\alpha - x_3 - x_1} [1 - F_{L_2(t)}(\alpha - x_3 - x_1)] f_{L_2(t)}(x_2) dx_2 \\
&= [1 - F_{L_2}(\alpha - x_3 - x_1)] F_{L_2(t)}(\alpha - x_3 - x_1)
\end{aligned}
\tag{E-4}$$

This follows from the fact that the load after the change is assumed to be independent of that before the change. Substituting Eq. (E-4) into Eq. (E-3) and then into Eq. (E-2):

$$(v_{\alpha})_3 \Delta t = v_3 \Delta t \int_0^{\alpha} f_{L_3}(t)(x_3) \left\{ \int_0^{\alpha-x_3} [1-F_{L_2}(t)(\alpha-x_3-x_1)] F_{L_2}(t)(\alpha-x_3-x_1) f_{L_1}(t)(x_1) dx_1 \right\} dx_3$$

Following the same argument as in Section II-5c:

$$(v_{\alpha})_3^t = v_3^t \int_0^{\alpha} f_{L_3}(t)(x_3) \left\{ \int_0^{\alpha-x_3} [1-F_{L_2}(t)(\alpha-x_3-x_1)] F_{L_2}(t)(\alpha-x_3-x_1) f_{L_1}(t)(x_1) dx_1 \right\} dx_3 \quad (E-5)$$

The above equation can be extended to the case when there are n loadings.

$$(v_{\alpha})_n^t = v_n^t \int_0^{\alpha} f_{L_1}(t)(x_1) \int_0^{\alpha-x_1} f_{L_2}(t)(x_2) \dots \int_0^{\alpha-x_1-x_2-\dots-x_{n-2}} f_{L_{n-1}}(t)(x_{n-1})^* F_{L_n}(t)(\alpha-x_1-x_2-\dots-x_{n-1})^*$$

$$[1 - F_{L_n(t)}(\alpha - x_1 - x_2 \dots - x_{n-1})] dx_1 dx_2 \dots dx_{n-1} \quad (E-6)$$

The CDF of the maximum lifetime load can be found by using Eq. (II-5-13) and Eq. (II-5-1), i.e.

$$v_\alpha = \sum_{i=1}^n (v_\alpha)_i$$

and

$$F_z(\alpha) = F_{F(t)}(\alpha) \exp[-v_\alpha t]$$

All $L_i(t)$'s are assumed to be gamma distributed. If the parameter k of the gamma distribution is an integer, then the Eq. (E-6) can be integrated exactly. A special case, studied below, is that when all $L_i(t)$'s are assumed to be independent to each other, and have a value $k = 4$ (Note that $k = 4$ corresponding to $A \approx 700 \text{ ft}^2$, from the Mitchell and Woodgate⁽³⁾ data). The results are tabulated in Table E-1. Since the two sets of results are so close, the independence and normality assumptions made before seem justified for this special case.

Table E-1 Comparison of the Exact and the Approximate Analysis

| Number of Stories | 2 | 3 | 4 | 5 | 6 | 7 | 8 | 9 | 10 | 11 |
|-----------------------------------|------|------|------|------|------|------|------|------|------|------|
| Results from Exact Analysis | 29.9 | 26.5 | 24.6 | 23.2 | 22.2 | 21.3 | 20.8 | 20.3 | 19.8 | 19.4 |
| Results from Approximate Analysis | 31.0 | 27.6 | 24.5 | 22.9 | 21.9 | 20.9 | 20.3 | 19.7 | 19.3 | 18.9 |

Appendix F

As mentioned in Section II-5c the unit load can be used to replace the total load in evaluating Eq. (II-5-21).

$$(v_{\alpha})_j t = \int_0^{\alpha} v_j t [1 - F_{W_j}(\alpha - x)] \frac{1}{\sigma_{F(t)} \sqrt{2\pi}} \exp\left[-\frac{1}{2} \left(\frac{x - m_{F(t)}}{\sigma_{F(t)}}\right)^2\right] dx \quad (\text{II-5-21})$$

even though all the variables in the original derivation represent the total load (or load effect). If the real value of these variables were used in the calculation, there would be quite a wide range of numbers. Special attention has to be paid to the accuracy of the numerical integration. It would be much preferred to use the unit load instead of the total load. The validity of the procedure is proved below. Recall (Section II-5c) that: $[1 - F_W(\alpha - x)]$ is a function of $\lambda(\alpha - x)$. For unit load, we have

$$\text{mean} = m_U$$

$$\text{standard deviation} = \sigma_U$$

$$k_U = \frac{m_U^2}{\sigma_U^2}$$

$$\lambda_U = \frac{m_U}{\sigma_U^2}$$

And for the total load $L = U \cdot A$

$$\text{mean} = m_L = m_U \cdot A$$

$$\text{Standard deviation} = \sigma_L = \sigma_U A$$

$$k_L = m_L^2 / \sigma_L^2 = k_U$$

$$\lambda_L = m_L / \sigma_L^2 = \lambda_U / A$$

Let Y represent the unit load, then

$$Y = \frac{X}{A}$$

Changing the variable in Eq. (II-5-21) from X to Y , one can write:

$$\begin{aligned}
(v_\alpha)_j t &= \int_0^{\alpha/A} v_j t [f(\lambda_L(\alpha - y \cdot A))] \exp[-\frac{1}{2} (\frac{yA - m_L}{\sigma_L})^2] dy \\
&= \int_0^{\alpha/A} v_j t [f(\lambda_L A (\frac{\alpha}{A} - y))] \exp[-\frac{1}{2} (\frac{y - \frac{m_L}{A}}{\sigma_L/A})^2] dy \\
&= \int_0^{\alpha/A} v_j t [f(\lambda_U (\frac{\alpha}{A} - y))] \exp[-\frac{1}{2} (\frac{y - m_U}{\sigma_U})^2] dy
\end{aligned}$$

This result is identical to that one would obtain if the unit load were used to compute $(v_\alpha)_j t$.

Appendix G

A closed form solution for Eq. (II-5-23) is derived below for the integer value of the parameter k . Rewrite the equation below:

$$v_{\alpha t} = \int_0^{\alpha} nvt [1 - F_{W_j}(\alpha - x)] \frac{1}{\sigma_{F(t)} \sqrt{2\pi}} \exp\left[-\frac{1}{2} \left(\frac{x - m_{F(t)}}{\sigma_{F(t)}}\right)^2\right] dx$$

(II-5-23)

For integer k , there is a closed form solution for $[1 - F_{W_j}(\alpha - x)]$ (Eq. II-5-24). For illustrative purposes assume $k = 4$.

$$1 - F_{W_j}(\alpha - x) = e^{-\lambda(\alpha - x)} \left[\frac{1}{2} + \frac{11}{32} \lambda(\alpha - x) + \frac{3}{32} \lambda^2(\alpha - x)^2 + \frac{1}{96} \lambda^3(\alpha - x)^3 \right]$$

(G-1)

Substituting Eq. (G-1) into Eq. (II-5-23)

$$v_{\alpha t} = \int_0^{\alpha} nvt \left[\frac{1}{2} + \frac{11}{32} \lambda(\alpha - x) + \frac{3}{32} \lambda^2(\alpha - x)^2 + \frac{1}{96} \lambda^3(\alpha - x)^3 \right] e^{-\lambda(\alpha - x)} \frac{1}{\sigma_{F(t)} \sqrt{2\pi}} \exp\left[-\frac{1}{2} \left(\frac{x - m_{F(t)}}{\sigma_{F(t)}}\right)^2\right] dx$$

(G-2)

Combine the two exponential terms in the above equation

$$v_{\alpha} t = \frac{nvt}{\sqrt{2\pi} \sigma_F(t)} \exp[-(\lambda\alpha - \frac{\lambda^2}{2} \sigma_F^2(t) - \lambda m_F(t))]^*$$

$$\int_0^{\alpha} [\frac{1}{2} + \frac{11}{32} \lambda (\alpha - x) + \frac{3}{32} \lambda^2 (\alpha - x)^2 + \frac{1}{96} \lambda^3 (\alpha - x)^3] \exp[-\frac{1}{2\sigma_F^2(t)} (x - m_F(t) - \lambda\sigma_F^2(t))^2] dx$$

Let

$$u = x - m_F(t) - \lambda\sigma_F^2(t)$$

and change the variable in the above equation.

$$v_{\alpha} t = \frac{nvt}{\sqrt{2\pi} \sigma_F(t)} \exp[-(\lambda\alpha - \frac{\lambda^2}{2} \sigma_F^2(t) - \lambda m_F(t))]^*$$

$$\int_{-(m_F(t) + \lambda\sigma_F^2(t))}^{\alpha'} [\frac{1}{2} + \frac{11}{32} \lambda (\alpha' - u) + \frac{3}{32} \lambda^2 (\alpha' - u)^2$$

$$+ \frac{1}{96} \lambda^3 (\alpha' - u)^3] \exp[-\frac{1}{2\sigma_F^2(t)} u^2] du \quad (G-3)$$

where

$$\alpha' = \alpha - m_{F(t)} - \lambda \sigma_{F(t)}^2$$

If $(m_{F(t)} + \lambda \sigma_{F(t)}^2)$ is very large and close to α , then we can make the following approximation:

$$\alpha' \cong 0$$

$$m_{F(t)} + \lambda \sigma_{F(t)}^2 \cong \infty \quad (G-4)$$

The integration limits of Eq. (G-3) can be changed from $-\infty$ to 0. Since

$$\int_{-\infty}^0 u^{2n} e^{-au^2} du = \frac{1 \cdot 3 \cdot 5 \cdot \dots \cdot (2n-1)}{2^{n+1} a^n} \sqrt{\frac{\pi}{a}}$$

$$\int_{-\infty}^0 u^{2n+1} e^{-au^2} du = - \frac{n!}{2a^{n+1}} \quad (G-5)$$

Using Eq. (G-5) we can find a closed form solution for Eq. (G-3).

$$\begin{aligned}
v_{\alpha} t = & \frac{nvt}{\sqrt{2\pi}} \exp\left[-\lambda\alpha' - \frac{\lambda^2}{2} \sigma_{F(t)}^2\right] \left[\frac{\sqrt{2\pi}}{2} L_1 + \sigma_{F(t)} L_2 \right. \\
& + \sqrt{2\pi} \sigma_{F(t)}^2 L_3 + 2\sigma_{F(t)}^3 L_4 + \left. \left(\frac{\sqrt{2\pi}}{2} L_2 + 2\sigma_{F(t)} L_3 \right) \alpha' \right. \\
& + \left. 3\sqrt{2\pi} \sigma_{F(t)}^2 L_4 \right] \alpha'^2 + \left(\frac{\sqrt{2\pi}}{2} L_3 + 3\sigma_{F(t)} L_4 \right) \alpha'^3 \\
& + \frac{\sqrt{2\pi}}{2} L_4 \alpha'^4 \quad (G-6)
\end{aligned}$$

where

$$L_1 = \frac{1}{2}$$

$$L_2 = \frac{11}{32} \lambda$$

$$L_3 = \frac{3}{32} \lambda^2$$

$$L_4 = \frac{1}{96} \lambda^3$$

Eq. (G-6) gives good results when α is close to $(m_{F(t)} + \lambda\sigma_{F(t)}^2)$. Otherwise the results are not good because the solution for $[1 - F_{W_j}(\alpha - x)]$ can not be used when $\alpha - x$ is negative. Therefore the use of Eq. (G-6) is limited.